

# Understanding the Impacts of Work Zone Activities on Traffic Flow Characteristics

**Final Report  
January 2018**



---

**Sponsored by**

Smart Work Zone Deployment Initiative  
Federal Highway Administration  
(TPF-5(295) and InTrans Project 15-535)  
Midwest Transportation Center  
U.S. Department of Transportation  
Office of the Assistant Secretary for  
Research and Technology



IOWA STATE UNIVERSITY  
Institute for Transportation

## **About SWZDI**

Iowa, Kansas, Missouri, and Nebraska created the Midwest States Smart Work Zone Deployment Initiative (SWZDI) in 1999 and Wisconsin joined in 2001. Through this pooled-fund study, researchers investigate better ways of controlling traffic through work zones. Their goal is to improve the safety and efficiency of traffic operations and highway work.

## **About MTC**

The Midwest Transportation Center (MTC) is a regional University Transportation Center (UTC) sponsored by the U.S. Department of Transportation Office of the Assistant Secretary for Research and Technology (USDOT/OST-R). The mission of the UTC program is to advance U.S. technology and expertise in the many disciplines comprising transportation through the mechanisms of education, research, and technology transfer at university-based centers of excellence. Iowa State University, through its Institute for Transportation (InTrans), is the MTC lead institution.

## **About InTrans**

The mission of the Institute for Transportation (InTrans) at Iowa State University is to develop and implement innovative methods, materials, and technologies for improving transportation efficiency, safety, reliability, and sustainability while improving the learning environment of students, faculty, and staff in transportation-related fields.

## **ISU Non-Discrimination Statement**

Iowa State University does not discriminate on the basis of race, color, age, ethnicity, religion, national origin, pregnancy, sexual orientation, gender identity, genetic information, sex, marital status, disability, or status as a U.S. veteran. Inquiries regarding non-discrimination policies may be directed to Office of Equal Opportunity, 3410 Beardshear Hall, 515 Morrill Road, Ames, Iowa 50011, Tel. 515-294-7612, Hotline: 515-294-1222, email [eooffice@iastate.edu](mailto:eooffice@iastate.edu).

## **Notice**

The contents of this report reflect the views of the authors, who are responsible for the facts and the accuracy of the information presented herein. The opinions, findings and conclusions expressed in this publication are those of the authors and not necessarily those of the sponsors.

This document is disseminated under the sponsorship of the U.S. DOT UTC program in the interest of information exchange. The U.S. Government assumes no liability for the use of the information contained in this document. This report does not constitute a standard, specification, or regulation.

The U.S. Government does not endorse products or manufacturers. If trademarks or manufacturers' names appear in this report, it is only because they are considered essential to the objective of the document.

## **Quality Assurance Statement**

The Federal Highway Administration (FHWA) provides high-quality information to serve Government, industry, and the public in a manner that promotes public understanding. Standards and policies are used to ensure and maximize the quality, objectivity, utility, and integrity of its information. The FHWA periodically reviews quality issues and adjusts its programs and processes to ensure continuous quality improvement.

**Technical Report Documentation Page**

<b>1. Report No.</b>		<b>2. Government Accession No.</b>		<b>3. Recipient's Catalog No.</b>	
<b>4. Title</b> Understanding the Impacts of Work Zone Activities on Traffic Flow Characteristics				<b>5. Report Date</b> January 2018	
				<b>6. Performing Organization Code</b>	
<b>7. Author(s)</b> Praveen Edara, Nipjyoti Bharadwaj, Carlos Sun, Yohan Chang, and Henry Brown				<b>8. Performing Organization Report No.</b>	
<b>9. Performing Organization Name and Address</b> University of Missouri-Columbia Department of Civil and Environmental Engineering E 2509 Lafferre Hall Columbia, MO 65211				<b>10. Work Unit No. (TRAIS)</b>	
				<b>11. Contract or Grant No.</b> Part of USDOT DTRT13-G-UTC37	
<b>12. Sponsoring Organization Name and Address</b> Smart Work Zone Deployment Initiative Iowa Department of Transportation 800 Lincoln Way Ames, Iowa 50010 Midwest Transportation Center 2711 S. Loop Drive, Suite 4700 Ames, IA 50010-8664				<b>13. Type of Report and Period Covered</b> Final Report	
				<b>14. Sponsoring Agency Code</b> Part of TPF-5(295) and Part of InTrans Project 15-535	
<b>15. Supplementary Notes</b> Visit <a href="http://www.intrans.iastate.edu/smartwz/">http://www.intrans.iastate.edu/smartwz/</a> for color pdfs of this and other Smart Work Zone Deployment Initiative research reports and <a href="http://www.intrans.iastate.edu">http://www.intrans.iastate.edu</a> for color pdfs of this and other research reports from InTrans.					
<b>16. Abstract</b> <p>What effect does work activity have on traffic conditions in a work zone? This question has still not been answered satisfactorily in practice. Without knowing the true effect a work activity has on traffic, practitioners are forced to make assumptions while scheduling work. This report attempts to answer this question by studying the traffic flow characteristics for various work activities, i.e., traffic speed versus flow curves, capacity reduction factors, and free-flow speed reduction factors.</p> <p>The importance of the speed-flow curves and reduction factors for work zone planning is also stressed in the latest edition of the Highway Capacity Manual (HCM). The HCM recommends capacity and speed reduction factors for work zones yet does not include specific guidance for including the impact of work activities.</p> <p>Three traffic stream models, Gipps, Newell-Franklin, and Van Aerde, were calibrated using field data from St. Louis, Missouri. The Van Aerde model offered the best fit with the field data compared to the other two models. Using the Van Aerde model-generated speed-flow curves, it was found that the capacity for bridge-related activities varied from 1,416 vehicles per hour per lane (vphpl) to 1,656 vphpl and for pavement-related activities from 1,120 vphpl to 1,728 vphpl.</p> <p>The capacity reduction factor for different work activities was found to be in the range of 0.68 to 0.95, while the free-flow speed reduction factor was found to be in the range of 0.78 to 1.0. The methodology proposed in this report allows the incorporation of work activity effects into traffic impact assessment tools and results in quantitative guidance for work zone planning and design.</p>					
<b>17. Key Words</b> free-flow speed—lane closure configurations—model calibration—traffic stream models—work zone activities—work zone planning				<b>18. Distribution Statement</b> No restrictions.	
<b>19. Security Classification (of this report)</b> Unclassified.		<b>20. Security Classification (of this page)</b> Unclassified.		<b>21. No. of Pages</b> 96	<b>22. Price</b> NA



# **UNDERSTANDING THE IMPACTS OF WORK ZONE ACTIVITIES ON TRAFFIC FLOW CHARACTERISTICS**

**Final Report  
January 2018**

**Principal Investigator**  
Praveen Edara, Professor  
University of Missouri-Columbia

**Co-Principal Investigators**  
Carlos Sun, Professor  
Henry Brown, Research Engineer  
University of Missouri-Columbia

**Research Assistants**  
Nipjyoti Bharadwaj and Yohan Chang

**Authors**  
Praveen Edara, Nipjyoti Bharadwaj, Carlos Sun, Yohan Chang, and Henry Brown

Sponsored by Midwest Transportation Center,  
U.S. Department of Transportation  
Office of the Assistant Secretary for Research and Technology, and  
FHWA Smart Work Zone Deployment Initiative  
Pooled Fund Study (TPF-5(295))

Preparation of this report was financed in part  
through funds provided by the Iowa Department of Transportation  
through its Research Management Agreement  
with the Institute for Transportation  
(InTrans Project 15-535)

A report from  
**Institute for Transportation**  
**Iowa State University**  
2711 South Loop Drive, Suite 4700  
Ames, IA 50010-8664  
Phone: 515-294-8103 / Fax: 515-294-0467  
<http://www.intrans.iastate.edu>



## TABLE OF CONTENTS

ACKNOWLEDGMENTS .....	ix
EXECUTIVE SUMMARY .....	xi
1. INTRODUCTION .....	1
2. LITERATURE REVIEW .....	2
2.1 Research Studies on Work Zone Capacity.....	2
2.2 Current Practice of Work Zone Capacity Estimation (2010 HCM) .....	12
2.3 2016 HCM Method for Work Zone Capacity Calculations.....	16
2.4 Other Existing Guidance.....	19
3. STUDY AREA AND DATA COLLECTION .....	21
3.1. Identification of Work Zone Locations.....	22
3.2. Identification of Work Zone Segments.....	25
3.3. Traffic Data Collection .....	25
4. METHODOLOGY .....	27
4.1. Identification of Work Zone Time.....	27
4.2. Aggregation of Speed-Flow Data .....	28
4.3. Estimation of Traffic Flow Characteristics.....	29
4.4 Calibration of Traffic Stream Models with Macroscopic Sensor Data.....	31
4.5 Goodness of Fit.....	34
5. DEVELOPMENT OF SPEED-FLOW CURVES .....	36
5.1. Speed-Flow Relationship by Direction.....	36
5.2. Speed-Flow Relationship by Lane .....	59
6. CONCLUSIONS.....	74
REFERENCES .....	77

## LIST OF FIGURES

Figure ES.1. Locations of study work zones from the St. Louis region .....	xi
Figure ES.2. Speed-flow plot in order of time for capacity identification .....	xii
Figure ES.3. Comparison of speed-flow plots for bridge- and pavement-related activities for (3,2), (2,1), and (4,2) lane drop configurations .....	xvi
Figure 2.1. Short-term freeway work zone lane closure capacity.....	13
Figure 2.2. Representative work zone speed-flow model.....	19
Figure 3.1. Geographical distribution of fixed traffic sensors for all Interstate highways in the St. Louis District .....	21
Figure 3.2. Information related to route, location, date, and type of work for the work zones .....	23
Figure 3.3. Geographical distribution of work zone locations for all Interstate highways in the St. Louis District .....	24
Figure 3.4. Identification of work zone segment at I-64 Boone Bridge .....	25
Figure 3.5. Traffic sensor information (left) and XML feed detector information (right) .....	26
Figure 4.1. Study methodology.....	27
Figure 4.2. Identification of work zone time at I-70 near Foristell.....	28
Figure 4.3.1. Speed-flow plot in order of time for capacity identification when breakdown flow is higher than recovery flow .....	30
Figure 4.3.2. Speed-flow plot in order of time for capacity identification when breakdown flow is lower than recovery flow .....	30
Figure 4.4. Creating flow-density diagram for work zone at I-64 Boone Bridge.....	31
Figure 5.1. Sample of speed-flow plots for non-work zone days in a work zone location.....	36
Figure 5.2.1. Fitting traffic stream models for Eastbound I-64 at Boone Bridge (restriping, 3,2) .....	38
Figure 5.2.2. Fitting traffic stream models for Eastbound I-64 at Boone Bridge (bridge work, 3,2) .....	39
Figure 5.2.3. Fitting traffic stream models for Westbound I-64 at Boone Bridge (bridge demolition preparation, 3,2).....	40
Figure 5.2.4. Fitting traffic stream models for Eastbound I-64 from Chesterfield Parkway to I-270 (paving operations, 3,2).....	41
Figure 5.2.5. Fitting traffic stream models for Eastbound I-70 at Foristell (pavement repair, 2,1) .....	42
Figure 5.2.6. Fitting traffic stream models for Westbound I-70 at Foristell (paving operations, 2,1).....	43
Figure 5.2.7. Fitting traffic stream models for Eastbound I-270 from McDonnell Boulevard to Route 367 (bridge work, 4,2).....	44
Figure 5.2.8. Fitting traffic stream models for Westbound I-270 from I-170 to Route 367 (pavement work, 3,2) .....	45
Figure 5.2.9. Fitting traffic stream models for Eastbound I-44 at I-270 (Meramec Bridge) (bridge work, 3,2) .....	46
Figure 5.2.10 Fitting traffic stream models for Westbound I-44 (resurfacing, 3,2) .....	47
Figure 5.2.11. Fitting traffic stream models for Eastbound I-44 at Hampton (bridge rehabilitation, 4,2).....	48

Figure 5.3.1. Comparison of work zone versus non-work zone day speed-flow plots for Eastbound I-64 at Boone Bridge (restriping, 3,2).....	51
Figure 5.3.2. Comparison of work zone versus non-work zone day speed-flow plots for Eastbound I-64 at Boone Bridge (bridge work, 3,2).....	52
Figure 5.3.3. Comparison of work zone versus non-work zone day speed-flow plots for Westbound I-64 at Boone Bridge (bridge demolition preparation, 3,2).....	52
Figure 5.3.4. Comparison of work zone versus non-work zone day speed-flow plots for Eastbound I-64 from Chesterfield Parkway to I-270 (paving operations, 3,2).....	53
Figure 5.3.5. Comparison of work zone versus non-work zone day speed-flow plots for Eastbound I-70 at Foristell (pavement repair, 2,1) .....	53
Figure 5.3.6. Comparison of work zone versus non-work zone day speed-flow plots for Westbound I-70 at Foristell (paving operations, 2,1) .....	54
Figure 5.3.7. Comparison of work zone versus non-work zone day speed-flow plots for Eastbound I-270 from McDonnell Boulevard to Route 36 (bridge work, 4,2).....	54
Figure 5.3.8. Comparison of work zone versus non-work zone day speed-flow plots for Westbound I-270 from I-170 to 367 (pavement work, 3,2).....	55
Figure 5.3.9. Comparison of work zone versus non-work zone day speed-flow plots for Eastbound I-44 at I-270 (Meramec Bridge) (bridge work, 3,2).....	55
Figure 5.3.10. Comparison of work zone versus non-work zone day speed-flow plots for Westbound I-44 (resurfacing, 3,2) .....	56
Figure 5.3.11. Comparison of work zone versus non-work zone day speed-flow plots for Eastbound I-44 at Hampton (bridge rehabilitation, 4,2) .....	56
Figure 5.4.1. Speed-flow plot for Eastbound I-64 at Boone Bridge (restriping, 3,2).....	59
Figure 5.4.2. Speed-flow plot for Eastbound I-64 at Boone Bridge (bridge work, 3,2).....	59
Figure 5.4.3. Speed-flow plot for Westbound I-64 at Boone Bridge (bridge demolition preparation, 3,2) .....	60
Figure 5.4.4. Speed-flow plot for Eastbound I-64 from Chesterfield Parkway to I-270 (paving operations, 3,2) .....	60
Figure 5.4.5. Speed-flow plot for Eastbound I-70 at Foristell (pavement repair, 2,1) .....	61
Figure 5.4.6. Speed-flow plot for Westbound I-70 at Foristell (paving operations, 2,1) .....	61
Figure 5.4.7. Speed-flow plot for Eastbound I-270 from McDonnell Boulevard to Route 367 (bridge work, 4,2) .....	62
Figure 5.4.8. Speed-flow plot for Westbound I-270 from I-170 to Route 367 (pavement work, 3,2) .....	62
Figure 5.4.9. Speed-flow plot for Eastbound I-44 at I-270 (Meramec Bridge) (bridge work, 3,2) .....	63
Figure 5.4.10. Speed-flow plot for Westbound I-44 (resurfacing, 3,2) .....	63
Figure 5.4.11. Speed-flow plot for Eastbound I-44 at Hampton (bridge rehabilitation, 4,2) .....	64
Figure 5.5.1. Speed-flow plot for pavement-related activities.....	65
Figure 5.5.2. Speed-flow plot for bridge-related activities.....	66
Figure 5.6.1. Speed-flow plot for bridge-related activities for (3,2) configuration .....	67
Figure 5.6.2. Speed-flow plot for pavement-related activities for (3,2) configuration.....	67
Figure 5.7. Comparison of speed-flow plots for bridge- and pavement-related activities for (3,2) configuration .....	68
Figure 5.8. Speed-flow plot for pavement-related activities for (2,1) configuration.....	69
Figure 5.9. Speed-flow plot for bridge-related activities for (4,2) configuration.....	70

Figure 5.10. Comparison of speed-flow plots for bridge- and pavement-related activities for (2,1) configuration.....	71
Figure 5.11. Comparison of speed-flow plots for bridge- and pavement-related activities for (4,2) configuration.....	71
Figure 5.12. Comparison of speed-flow plots for different lane closure configurations .....	73

## LIST OF TABLES

Table ES.1. Capacity and free-flow speed reduction factors .....	xiv
Table 2.1 Summary of key findings from literature .....	6
Table 2.2. Work zone capacity (vphpl) variation by lane closure configuration and type of work .....	13
Table 2.3. Capacity of long-term work zones (vphpl) .....	15
Table 2.4. Work zone capacity and minimum free-flow speed adjustment factors for freeway work zones .....	16
Table 2.5. Lane closure severity index .....	17
Table 2.6. Work zone capacities from MassDOT design guide .....	19
Table 2.7. Work zone capacities from MoDOT design guide .....	20
Table 3.1. Classification of work zones observed in two months .....	22
Table 3.2. Details of the work zone locations.....	24
Table 5.1. Goodness of fit statistics .....	50
Table 5.2. Capacity and free-flow speed reduction factors .....	58
Table 5.3. Work activities related to bridges and pavements .....	65
Table 5.4. Work zone capacity (vphpl) by lane closure configuration and type of work.....	72
Table 5.5. Work zone FFS (mph) by lane closure configuration and type of work .....	72

## **ACKNOWLEDGMENTS**

This project was funded by the Midwest Transportation Center, the U.S. Department of Transportation (DOT) Office of the Assistant Secretary for Research and Technology, and the Smart Work Zone Deployment Initiative (SWZDI) and Federal Highway Administration (FHWA) Pooled Fund Study TPF-5(295), involving the following state departments of transportation:

- Iowa (lead state)
- Kansas
- Missouri
- Nebraska
- Wisconsin

The authors would like to thank all of the sponsors and the pooled fund state partners for their financial support and technical assistance.

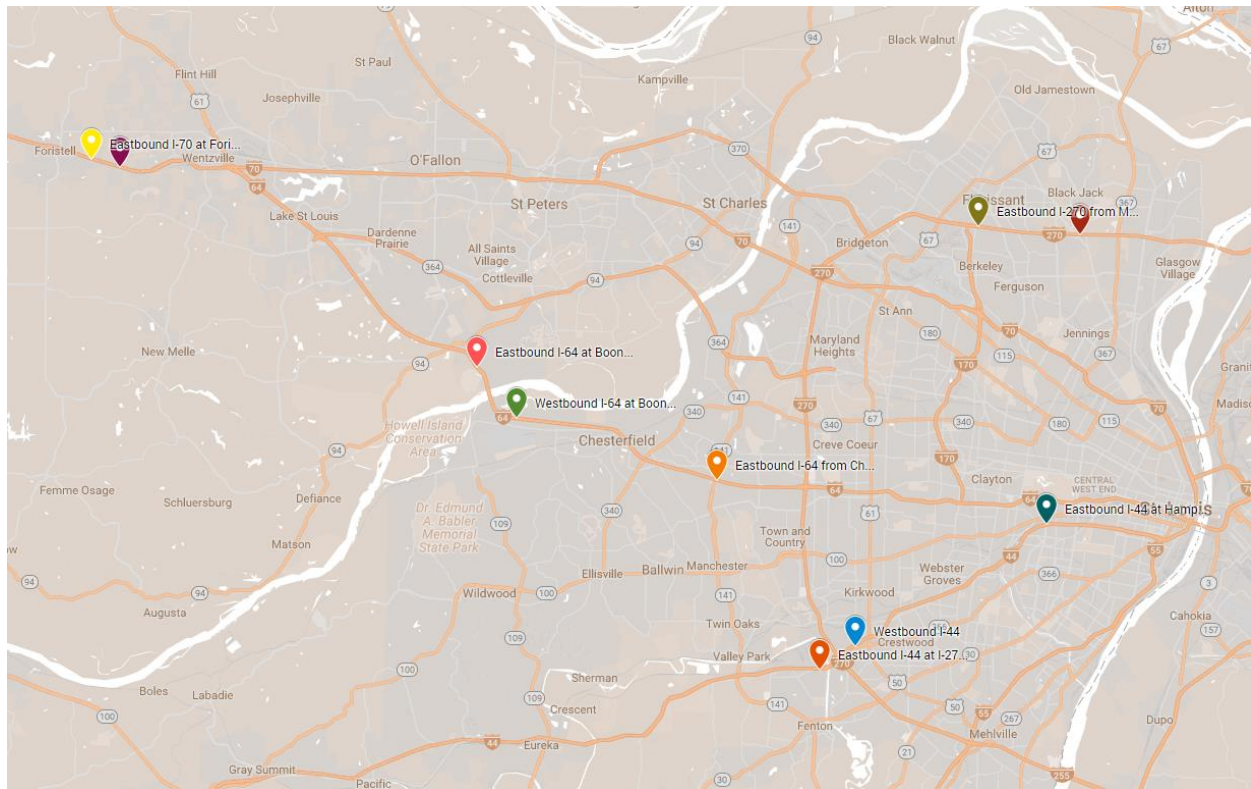
The authors would also like to thank Dan Smith from the Missouri DOT (MoDOT) for being the project manager and serving on the technical advisory committee (TAC). The authors also extend their gratitude to Jim Connell from MoDOT and Dan Sprengeler from the Iowa DOT for serving on the TAC.



## EXECUTIVE SUMMARY

Aging freeways in North America require increasing amounts of construction and maintenance activities. These work activities adversely impact mobility for motorists. A review of existing literature found that studies have estimated work zone capacity using different traffic, geometric, and work zone characteristics such as lane width, presence of heavy vehicles, driver population, weather, and number of closed lanes. However, there is little understanding of how different work activities impact traffic. The main goals of this project were to study the cause and effect relationship between type of work activity and traffic mobility through a work zone and to develop traffic flow characteristic curves using real-world traffic flow and work activity data. The use of data-driven tools enables practitioners to incorporate work zone activity impacts in their planning, design, and operation of work zones.

The work zone locations selected for this study were identified from the Regional Mobility Report published by the Missouri Department of Transportation (MoDOT). The bimonthly report for the St. Louis District chronicles events that significantly affect traffic mobility in the region such as work zone activity and other incidents. Eleven work zone locations were identified with major and moderate travel time impacts. The selected work zones included a variety of work activities related to bridges and pavements. The distribution of work zone locations for Interstate highways in the St. Louis District is illustrated in Figure ES.1.



© 2016 Google

**Figure ES.1. Locations of study work zones from the St. Louis region**

Data on traffic characteristics were collected from fixed traffic sensors distributed over Interstate highways in the St. Louis District. Three major types of traffic information were collected for individual lanes from each traffic sensor in 30-second windows: traffic volume, speed, and occupancy.

Traffic parameters such as free-flow speed, capacity, speed at capacity, and jam density were estimated for the work zone locations. The 85th percentile speed of the traffic stream under low-flow conditions was used as free-flow speed. Jam density was estimated from flow versus density plots, and linear regression was used to create best fit lines for both uncongested and congested states. Jam density was estimated as the density at which the regression line for the congested state meets the x-axis. Capacity was identified as the higher value of either the breakdown flow or pre-recovery discharge flow using the time series plots of speed and flow (see Figure ES.2).

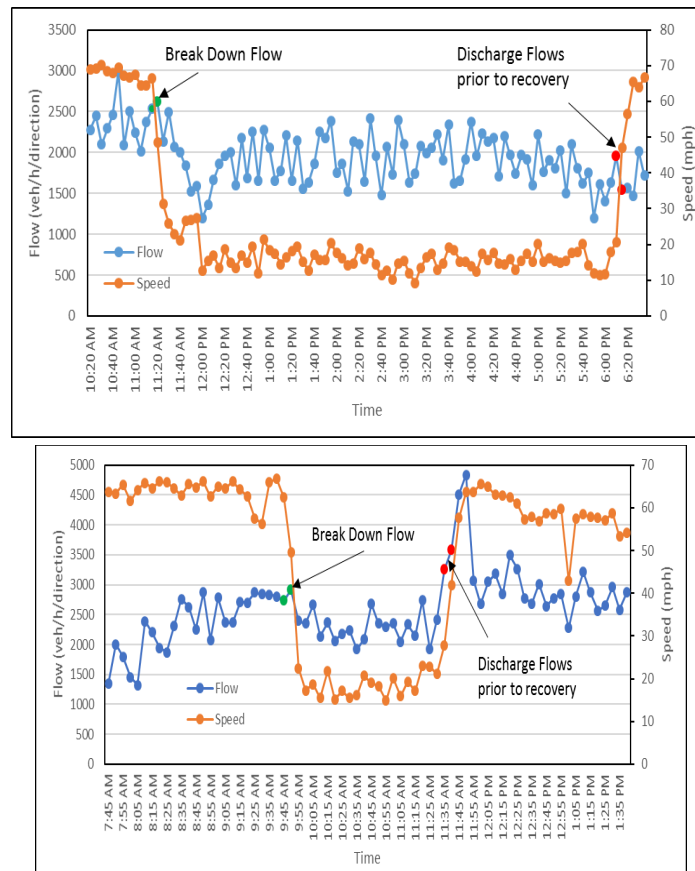


**Figure ES.2. Speed-flow plot in order of time for capacity identification**

For this study, two single-regime models proposed by Li (2008) and Van Aerde (1995) and the two-regime model by Gipps (1981) were calibrated using real-world data from the selected work zone locations. The speed-flow plots were developed by direction for both work zone and non-work zone days while plots by lane were developed for work zone days. A goodness of fit test was performed to determine the best fit among the three models, and the Van Aerde model was

the best fit model for most of the study locations (mean average percent error < 20% for all locations). The Gipps and Newell-Franklin models were good fits for a few locations but resulted in high errors at other locations. The Gipps model provided a good fit for locations where the traffic stream speed was not sensitive to flow in the uncongested regime (i.e., free-flow speed and speed at capacity were similar), whereas the Newell-Franklin model provided a good fit for locations where the traffic stream speed was sensitive to flow in uncongested regimes. These speed-flow models are the mathematical backbone of work zone traffic impact tools that reflect work zone activity.

The reduction factors for free-flow speed and capacity were computed using the work zone and non-work zone values obtained from the speed-flow curves for all sites and are shown in Table ES.1.

**Table ES.1. Capacity and free-flow speed reduction factors**

Locations and work activity (1)	Lane closure configuration (2)	Site number (3)	Work Zone			Non-work Zone			Capacity reduction factor (10 = 5/8) (10)	FFS reduction factor (11 = 6/9) (11)
			Capacity (vph)		FFS (mph) (6)	Capacity (vph)		FFS (mph) (9)		
			Directional (all lanes) (4)	Lane wise (all lanes / no. lanes) (5)		Directional (all lanes) (7)	Lane wise (all lanes / no. lanes) (8)			
Eastbound I-64 at Boone Bridge (work: restriping)	(3,2)	(a)	3,414	1,707	65.5	6,012	2,004	66	0.85	0.99
* Eastbound I-64 at Boone Bridge (work: bridge work)	(3,2)	(b)	3,172	1,586	59.4	6,012	2,004	66	0.79	0.90
Eastbound I-64 from Chesterfield Parkway to I-270 (work: paving operations)	(3,2)	(c)	3,540	1,770	66.3	5,748	1,916	67.5	0.92	0.98
Eastbound I-70 at Foristell (work: pavement repair)	(2,1)	(d)	1,380	1,380	65	3,360	1,680	67	0.82	0.97
Westbound I-70 at Foristell (work: paving operations)	(2,1)	(e)	1,560	1,560	67	3,360	1,680	67	0.93	1.00
Eastbound I-270 from McDonnell Boulevard to Route 367 (work: bridge work)	(4,2)	(f)	3,408	1,704	55	7,212	1,803	62.7	0.95	0.88
Westbound I-270 from I-170 to 367 (work: pavement work)	(3,2)	(g)	3,720	1,860	69.7	5,976	1,992	70.2	0.93	0.99
Eastbound I-44 at I-270 (Meramec Bridge) (work: bridge work)	(3,2)	(h)	3,372	1,686	61	5,304	1,768	70.7	0.95	0.86
Westbound I-44 (work: resurfacing)	(3,2)	(i)	2,520	1,260	55	5,584	1,861	70.5	0.68	0.78
Eastbound I-44 at Hampton (work: bridge rehabilitation)	(4,2)	(j)	3,624	1,812	57.8	7,872	1,968	62	0.92	0.93

The results show that all work zone activities in the study sample had an adverse effect on capacity and free-flow speed. The range of reduction factors for capacity and free-flow speed, shown in Table ES.1, can be extensive, depending on the nature of work and lane closure configurations. The capacity reduction factor for work zone conditions was found to be in the range of 0.68 to 0.95 while the free-flow speed reduction factor was found to be in the range of 0.78 to 1.0.

Further analysis was conducted for bridge-related and pavement-related work activities. A comparison of the speed-flow plots for bridge and pavement activities for three lane closure configurations is shown in Figure ES.3.

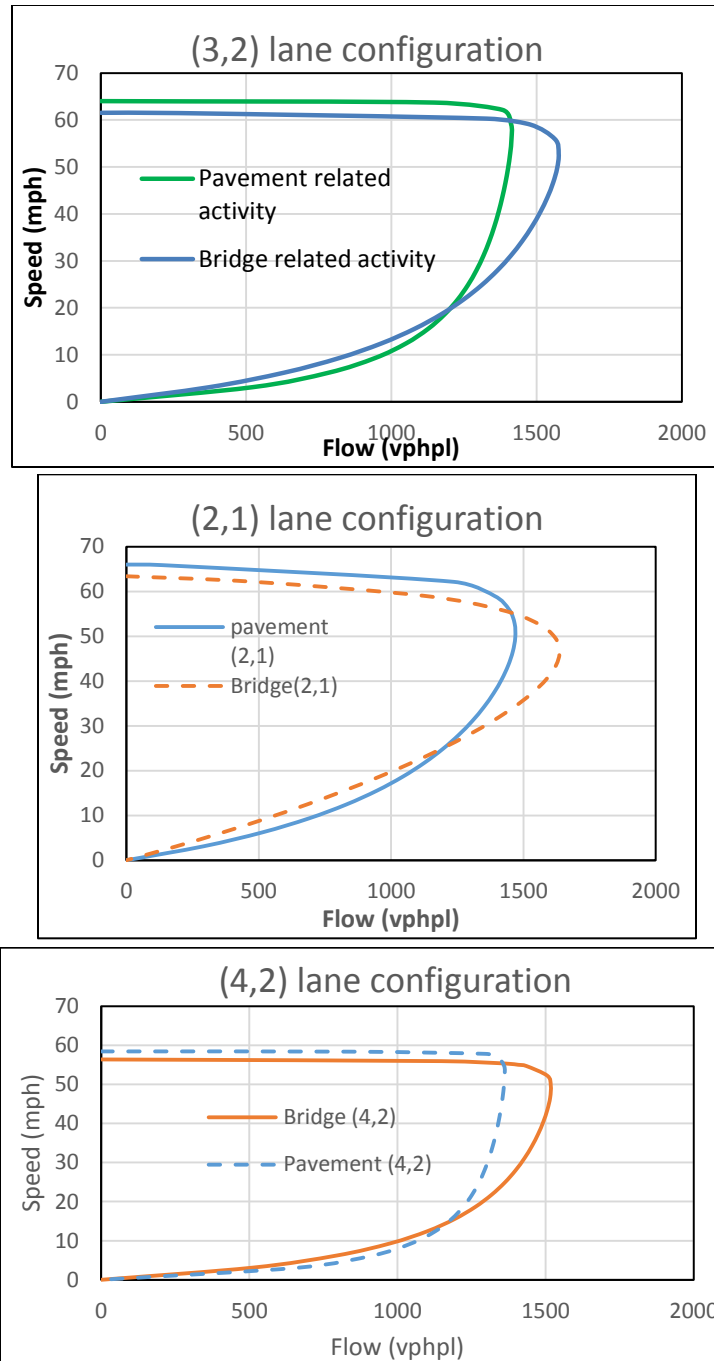


**Figure ES.3. Comparison of speed-flow plots for bridge- and pavement-related activities for (3,2), (2,1), and (4,2) lane drop configurations**

The variation in capacity values was found to be much lower for bridge-related work than pavement-related work. The higher variation in the capacity values for the pavement-related work may be due to the wider range of activities that are cataloged as pavement-related work in the MoDOT database. In terms of capacity, the (4,2) configuration experienced the lowest capacity while the (2,1) configuration experienced the highest capacity.

## 1. INTRODUCTION

All types of work zones have adverse impacts of some kind on traffic. The magnitude of the impact, however, varies from one work zone to another based on a variety of factors. These factors include geographical differences, demand differences (daily traffic volumes, hourly distribution of traffic), type of work activity, capacity reductions, and lane closure configurations. Existing traffic impact analysis tools are capable of incorporating the demand and geometric effects of work zones. However, there is limited understanding of how work activity type influences traffic operations in work zones.

This project takes a step toward understanding the relationship between work activity type and traffic flow characteristics. The effects of work activity are explored using three different traffic flow measures: (1) traffic speed versus flow curves, (2) capacity reduction factors, and (3) free-flow speed (FFS) reduction factors. Many traffic impact analysis tools, such as Quick Zone and custom spreadsheets, rely on hourly traffic volumes and capacity values (normal conditions and restricted conditions) as input to determine queue length and delay in work zones. These analytical tools incorporated the methodology for estimating delay and queue length from the 2010 edition of the Highway Capacity Manual (HCM) (TRB 2010). The 2010 edition of the HCM does not have speed-flow curves specifically developed for work zone conditions, let alone different work activities. The 2016 edition of the HCM does include an extension to the methodology for development of speed-flow curves. The new version includes adjustment factors for free-flow speed and capacity of work zones based on various geometric factors, but it lacks specific guidance on how work activity effects can be incorporated. By addressing this gap in existing knowledge, this research helps to develop future guidance for the HCM work zone methodology.

The remaining chapters of the report are structured as follows: Chapter 2 contains a brief literature review of the state of practice of traffic flow characteristics related to work zones. Chapter 3 contains descriptions of the study location and data used in this study. Chapter 4 describes the overall methodology adopted in this study, followed by descriptions of various methods applied to quantify traffic flow characteristics in work zone locations. Chapter 5 presents the estimation of traffic parameters and calibration of macroscopic speed-flow models. The chapter also offers a comparison between the work zone and non-work zone day speed-flow diagram. Finally, Chapter 6 presents the conclusions and summarizes the results.

## **2. LITERATURE REVIEW**

A literature review was conducted to gain insight into the state of the existing knowledge regarding work zone capacity. The sources reviewed included research studies, the 2010 and 2016 version of the HCM, and other resources.

### **2.1 Research Studies on Work Zone Capacity**

#### *2.1.1 Work Zone Capacity Adjustment Factors*

In some previous studies, work zone capacity adjustment factors were developed to account for the presence of work zone activity. A multiplicative capacity model based on data from six freeway reconstruction work zones in Ontario, Canada, was developed by Al-Kaisy and Hall (2003). Several factors were considered, including proportion of heavy vehicles, driver population, work activity, side of lane closure, rain, light condition, and non-additive interactive effects. Only one of the six sites had sufficient data to estimate work zone capacity based on construction activity. The capacity drop due to work zone activity ranged from 1.85 percent to 12.5 percent. The developed model included an adjustment factor of 0.93 for the presence of work activity at the construction site.

In a study by Elefteriadou et al. (2007), work zone capacity models were developed using simulations for three work zone merge configurations: two lanes to one lane, three lanes to two lanes, and three lanes to one lane. Both planning and operational models were developed for each of the three configurations. Work zone intensity was taken into account through a rubbernecking factor that was based on the study by Al-Kaisy and Hall (2003).

In research undertaken by Heaslip et al. (2009), a methodology was developed to estimate freeway work zone capacity using both simulation and field data collected from an Interstate freeway work zone in Jacksonville, Florida. Three work zone lane closure configurations were studied: two-to-one, three-to-two, and three-to-one. Work zone activity was incorporated through the use of a rubbernecking factor. However, this factor was not derived from the field data but was instead based on the values determined by Al-Kaisy and Hall (2003).

In a study by Krammes and Lopez (1994), new capacity values for short-term freeway work zone lane closures were developed using data from 33 freeway work zones. Five different lane closure configurations were investigated: three lanes to one lane, two lanes to one lane, four lanes to two lanes, five lanes to three lanes, and four lanes to three lanes. Most of these work zones involved maintenance activities. The study recommended a base work zone capacity value of 1,600 passenger cars/per hour/per lane (pcphpl). The authors suggested that this value should be adjusted for heavy vehicles, presence of ramps, and type and intensity of work activity. The recommended adjustment for type and intensity of work activity adjustment varies from -160 to 160 pcphpl. As indicated by Krammes and Lopez (1994), these adjustment values represent general guidance since a more definitive relationship could not be determined from the data.

### *2.1.2 Work Zone Activity Levels*

The effects of work zone activity on work zone capacity have been investigated by several researchers through the use of qualitative activity level variables. For example, work zone capacity values were developed by Dixon et al. (1996) based on data from 24 freeway work zones in North Carolina. Four different lane closure scenarios were studied. Variables that were evaluated included nighttime versus daytime construction, work zone intensity, work zone proximity to active lanes, and work zone proximity to interchanges. Work zone intensity was categorized as heavy, moderate, or light. The study found that rural work zone capacity was lower at the activity area than at the end of the transition area.

In a study by Jiang (1999), traffic flow characteristics for freeway work zones were investigated utilizing a sample of four Interstate work zones in Indiana. Two configurations were included in the research: a single-lane closure in one direction and a crossover. Work zone intensity was characterized by three levels: medium, nonadjacent, and high. The mean work zone capacities for the three levels of work intensity were found to be statistically equal.

Through research undertaken by Kim et al. (2001), a multiple regression model to estimate work zone capacity was developed using data collected from 12 work zone sites. The configuration studied involved lane closures on four lanes in one direction. Intensity of work activity was investigated through use of dummy variables for medium intensity and heavy intensity. The dummy variable for heavy intensity was included in the final model. Other variables in the model included number of closed lanes, location of closed lanes, proportion of heavy vehicles, lateral distance to open lanes, work zone length, and work zone grade.

Grey correlation analysis and multivariate linear regression were utilized by Li et al. (2013) to develop a model for work zone capacity. Intensity of work activity was investigated through use of dummy variables for medium intensity and heavy intensity. The dummy variable for medium intensity was found to be a significant variable in the model. The model also included variables for number of open lanes, speed, proportion of heavy vehicles, lateral distance to the open lanes, work zone length, time of day, location of closed lanes, and grade.

The effects of construction activity and intensity on the capacity of rural freeway work zones were investigated by Luna and Mohammadi (2014) using field and sensor data from a long-term Interstate work zone. Two categories of work zone intensity (light construction and heavy construction) were studied based on the number of personnel in the work zone. The study found that heavy construction activity led to a reduction in capacity.

In a study by Zheng et al. (2011), several different work zone capacity prediction models were compared, including the HCM model, two multi-linear regression models, and a fuzzy logic-based artificial neural network model. The models were evaluated using traffic and work zone data from Dutch freeways. The study found that the neuro-fuzzy model was the most accurate. Work intensity was considered through either an adjustment factor applied to the capacity or a dummy variable representing the work zone intensity level.

### *2.1.3 Regression Models*

In a study by Benekohal et al. (2004), a methodology for estimating operating speed and capacity in work zones was developed based on data collected from 11 work zones that included the closure of one lane. A relationship between speed reduction and work intensity was developed. Work intensity was quantified based on the number of workers in the active work area, amount of equipment in the work area, and distance between the active work area and open lane. The methodology used the HCM speed reductions for narrow lane width and lateral clearance.

### *2.1.4 Site-Specific Studies*

Several studies have investigated work zone capacity at specific sites but have not investigated the effects of work zone activity on capacity. Data from two lane closures at the same construction site in Toronto, Ontario, were used by Al-Kaisy et al. (2000) to investigate freeway capacity. Several factors were studied, including temporal variation, grade, day of the week, and weather conditions. Although there was considerable variation in freeway capacity over the four days of data collection, the values developed were relatively close to the values predicted by the 2010 edition of the HCM (TRB 2010).

Historical detector data from two urban freeway work zones in Milwaukee, Wisconsin, were used to analyze work zone capacity in a study by Notbohm et al. (2009). The first work zone involved the use of two separate tapers to go from four lanes to two lanes, while the second work zone was a two-lane-to-one-lane merge. The capacity values determined during the morning peak were 2,100 vehicles per hour per lane (vphpl) for the four-lane-to-two-lane case and 1,900 vphpl for the two-lane-to-one-lane case. The study recommended that capacity for urban long-term work zones should be determined based on throughputs observed over several hours.

In a study by Venugopal and Tarko (2001), capacity models for rural freeways were developed based on data from a 15-mile Interstate work zone in Indiana. The work zone utilized a lane drop from two lanes to one lane and included high intensity activity such as pavement rehabilitation and resurfacing. The study found that rainfall, heavy vehicles, police presence, and the presence of an innovative traffic control system called the Indiana Lane Merge System (ILMS) reduced the work zone capacity. The type of lane drop (left or right) was also investigated but was not found to affect capacity significantly.

The capacity of bidirectional eight-lane urban expressways was estimated by Shao and Chen (2010) using both field data from five work zone sites in China and simulation. The study found that the work zone capacity varied between 1,500 vphpl and 1,700 vphpl. The simulation portion of the study evaluated three different lane closure configurations: four lanes to one lane, four lanes to two lanes, and four lanes to three lanes. The study did not consider the effects of work zone intensity, work zone length, or work zone configuration.

### *2.1.5 Inconclusive Results for Work Zone Activity and Capacity*

In some studies, the effects of work zone activity on work zone capacity were investigated, but a relationship could not be found due to limitations of the data. In a study by Dudek and Richards (1981), freeway work zone capacity was investigated through use of data from 28 maintenance and construction work zones in Houston and Dallas, Texas. The following lane closure configurations were studied: three lanes to one lane, two lanes to one lane, five lanes to two lanes, four lanes to two lanes, three lanes to two lanes, and four lanes to three lanes. Capacity values were developed for different types of work, such as bridge repair, asphalt removal, patch and overlay, shoulder repair, pavement repair, freeway widening, concrete median barrier installation, and resurfacing. However, a relationship between work zone capacity and the type of work could not be developed due to data limitations. Other factors such as presence of on-ramps and off-ramps, grades, alignment, and percentage of trucks were not considered in the study.

In research by Sarasua et al. (2004), a model was developed for short-term work zone capacity for Interstate work zones in South Carolina. Data were collected from 22 work zone sites during a 12-month period. The sites included various types of work such as paving, median cable guardrail, rumble strips, bridge maintenance, and barrier wall erection. The final model included a base value of 1,460 pchpl adjusted by the proportion of heavy vehicles and number of lanes. The authors investigated the effects of work zone type through use of a dummy variable for high activity. However, the variable was not statistically significant. It was determined that the sample size was not sufficient to make any conclusions regarding the effects of work zone activity, intensity, and length on work zone capacity.

### *2.1.6 Arterial Work Zone Capacity*

While most of the existing research has focused on freeway work zone capacity, there have been some studies pertaining to arterial work zone capacity. As part of a study by Hawkins et al. (1992), the capacity of an arterial lane closure was estimated using video data collected from an urban study site in Arlington, Texas. The results indicated that the work zone capacity for the arterial lane closure was less than the work zone capacity for a freeway lane closure with similar geometric characteristics. A table of estimated work zone capacities for lane closures on urban arterials was developed based on these results. In another study by Elefteriadou (2008), arterial work zone capacity was investigated using simulation. Five regression equations were developed to predict arterial work zone capacity for lane groups based on different lane configurations: the capacity of two lanes with no left turns allowed, the capacity of two lanes with one left turn lane and one through/right lane, and the capacity of left turns, through/right turns, and the approach for arterials with three to six lanes. Several factors were found to affect the arterial work zone capacity, including the percentage of left-turning vehicles, the distance between the work zone and the nearest downstream intersection, the ratio of green time to cycle length, and the ratio of the number of open lanes to the total number of lanes.

### 2.1.7 Other Studies

In other research studies, various aspects of work zone capacity were investigated, but the effects of work zone activity on work zone capacity were not quantified. In research by Maze et al. (2000), the capacity of an Interstate work zone in Iowa was measured using field data collection. The work zone included a lane closure. The results indicated that the capacities ranged from 1,400 to 1,600 pcphpl. The type or intensity of work zone activity was not explicitly considered in this study. Using Missouri field data, three different methods for computing work zone capacity were compared by Edara et al. (2012): maximum sustained flow, rescaled cumulative flow curves, and 85th percentile flow. The most conservative capacity estimates were found using the queue discharge flow values. The study also included a survey of state departments of transportation (DOTs), which found that 30 percent of respondents considered work zone intensity in estimating work zone capacity while 74 percent considered the work zone configuration. In another study by Chatterjee et al. (2009), a method was developed to determine driver behavior parameters in Vissim that correspond with work zone capacities. Two merging cases in an early-merge system were studied: two lanes to one lane and three lanes to two lanes. Two car-following model parameters and one lane changing parameter were estimated.

### 2.1.8 Summary of Existing Literature

Table 2.1 summarizes the key findings from the existing literature.

**Table 2.1 Summary of key findings from literature**

Reference	Summary of Findings
Al-Kaisy and Hall 2003	<ul style="list-style-type: none"> <li>• Multiplicative work zone capacity model developed from field data</li> <li>• Mean queue discharge rate considered as capacity</li> <li>• Factors affecting work zone capacity               <ul style="list-style-type: none"> <li>• Percentage of heavy vehicles</li> <li>• Driver population</li> <li>• Light conditions</li> <li>• Work zone configuration</li> <li>• Weather conditions</li> <li>• Work activity</li> </ul> </li> <li>• Adjustment factor of 0.93 for presence of work zone activity</li> </ul>

Reference	Summary of Findings
Al-Kaisy et al. 2000	<ul style="list-style-type: none"> <li>• Investigated the capacity at work zones with long-term closures using field data</li> <li>• Mean queue discharge flow rate considered as capacity</li> <li>• Factors affecting work zone capacity <ul style="list-style-type: none"> <li>• Temporal variation</li> <li>• Grade</li> <li>• Day of week</li> <li>• Weather conditions</li> </ul> </li> <li>• Results reasonably close to the 2010 HCM values</li> <li>• Work zone activity not considered</li> </ul>
Benekohal et al. 2004	<ul style="list-style-type: none"> <li>• Developed methodology for work zone capacity using field data</li> <li>• Based on reductions in vehicle speed</li> <li>• Factors considered <ul style="list-style-type: none"> <li>• Work intensity</li> <li>• Lane width</li> <li>• Lateral clearance</li> </ul> </li> <li>• Quantification of work zone intensity <ul style="list-style-type: none"> <li>• Number of workers in active work area</li> <li>• Amount of equipment in work area</li> <li>• Distance between active work area and open lane</li> </ul> </li> </ul>
Chatterjee et al. 2009	<ul style="list-style-type: none"> <li>• Defined various sets of driving behavior parameters in microscopic simulation software Vissim for work zone capacity estimation</li> <li>• Estimated two car-following model parameters and one lane changing parameter for Vissim</li> <li>• Work zone activity not considered</li> </ul>
Dixon et al. 1996	<ul style="list-style-type: none"> <li>• Investigated freeway work zone capacity using field data</li> <li>• Based on flow rate at which traffic switches from uncongested to queued</li> <li>• Factors considered <ul style="list-style-type: none"> <li>• Time of day</li> <li>• Work zone intensity</li> <li>• Work zone proximity to active lanes</li> <li>• Work zone proximity to interchanges</li> </ul> </li> <li>• Categorization of work zone intensity <ul style="list-style-type: none"> <li>• Heavy</li> <li>• Moderate</li> <li>• Light</li> </ul> </li> <li>• Importance of both collapse volume and queue discharge values</li> </ul>

Reference	Summary of Findings
Dudek and Richards 1981	<ul style="list-style-type: none"> <li>• Investigated freeway work zone capacity using field data</li> <li>• Developed capacity values for different types of work               <ul style="list-style-type: none"> <li>• Bridge repair</li> <li>• Asphalt removal</li> <li>• Patch and overlay</li> <li>• Shoulder repair</li> <li>• Pavement repair</li> <li>• Freeway widening</li> <li>• Concrete median installation</li> <li>• Resurfacing</li> </ul> </li> <li>• Unable to determine relationship between work zone capacity and type of work</li> </ul>
Edara et al. 2012	<ul style="list-style-type: none"> <li>• Estimated capacity of short-term work zones using three methods               <ul style="list-style-type: none"> <li>• Maximum sustained flow</li> <li>• Rescaled cumulative flow curves (queue discharge flow)</li> <li>• 85th percentile of flow</li> </ul> </li> <li>• Most conservative estimation of capacity from queue discharge flow</li> <li>• Survey of state DOTs               <ul style="list-style-type: none"> <li>• 30 percent consider work zone intensity when estimating work zone capacity</li> <li>• 74 percent consider work zone configuration</li> </ul> </li> </ul>
Elefteriadou et al. 2007	<ul style="list-style-type: none"> <li>• Developed freeway work zone capacity models using simulation</li> <li>• Developed both planning and operational models</li> <li>• Work zone intensity incorporated through rubbernecking factor from Al-Kaisy and Hall (2003)</li> </ul>
Elefteriadou et al. 2008	<ul style="list-style-type: none"> <li>• Developed arterial work zone capacity models using simulation</li> <li>• Significant factors affecting work zone capacity               <ul style="list-style-type: none"> <li>• Percentage of left-turning vehicles</li> <li>• Distance between work zone and nearest downstream intersection</li> <li>• Ratio of green time to cycle length</li> <li>• Ratio of number of open lanes to total number of lanes</li> </ul> </li> <li>• Work zone activity not considered</li> </ul>
Hawkins et al. 1992	<ul style="list-style-type: none"> <li>• Estimated work zone capacity for lane closure on urban arterial using field data</li> <li>• Arterial work zone capacity less than freeway work zone capacity</li> <li>• Provided table of values for arterial work zone capacity</li> <li>• Work zone activity not considered</li> </ul>

Reference	Summary of Findings
Heaslip et al. 2009	<ul style="list-style-type: none"> <li>• Developed models and procedures for estimating freeway work zone capacity using both simulation and field data</li> <li>• Significant factors affecting work zone capacity <ul style="list-style-type: none"> <li>• Heavy vehicles</li> <li>• Presence of work zone activity</li> <li>• Location of upstream warning sign</li> <li>• Lane distribution</li> <li>• Speed</li> <li>• Lane width</li> <li>• Lateral clearance</li> <li>• Lighting</li> <li>• Driver population</li> <li>• Weather</li> <li>• Presence of ramps</li> </ul> </li> <li>• Work zone intensity incorporated through rubbernecking factor from Al-Kaisy and Hall (2003)</li> </ul>
Jiang 1999	<ul style="list-style-type: none"> <li>• Estimated freeway work zone capacity for both single-lane closure and crossover using field data</li> <li>• Defined capacity as flow just before the significant decrease in speed</li> <li>• Mean queue discharge flow rates were less than capacity</li> <li>• Categorization of work zone intensity <ul style="list-style-type: none"> <li>• Medium</li> <li>• Non-adjacent</li> <li>• High</li> </ul> </li> <li>• Mean work zone capacities for all work intensity categories statistically equal</li> </ul>
Kim et al. 2001	<ul style="list-style-type: none"> <li>• Developed multiple regression model for freeway work zone capacity using field data</li> <li>• Significant factors affecting work zone capacity <ul style="list-style-type: none"> <li>• Number of closed lanes</li> <li>• Location of closed lanes</li> <li>• Proportion of heavy vehicles</li> <li>• Lateral distance to open lanes</li> <li>• Work zone length</li> <li>• Work zone grade</li> <li>• Heavy work zone intensity</li> </ul> </li> <li>• Categorization of work zone intensity <ul style="list-style-type: none"> <li>• Medium</li> <li>• Heavy</li> </ul> </li> </ul>

Reference	Summary of Findings
Krammes and Lopez 1994	<ul style="list-style-type: none"> <li>• Developed capacity values for short-term freeway work zone lane closures using field data</li> <li>• Base work zone capacity measured as 1,600 pcphpl</li> <li>• Adjustments for work zone capacity <ul style="list-style-type: none"> <li>• Intensity of work activity</li> <li>• Heavy vehicles</li> <li>• Presence of ramps</li> </ul> </li> <li>• Adjustment for intensity of work varies -160 to +160 pcphpl</li> <li>• Factors affecting work zone intensity adjustment <ul style="list-style-type: none"> <li>• Number of workers</li> <li>• Size of equipment</li> <li>• Presence of flaggers</li> <li>• Noise and dust levels</li> <li>• Type of work</li> <li>• Location of work activity</li> </ul> </li> </ul>
Li et al. 2013	<ul style="list-style-type: none"> <li>• Used grey correlation and multivariate linear regression to develop model for freeway work zone capacity based on data from Kim et al. (2001)</li> <li>• Significant factors affecting capacity <ul style="list-style-type: none"> <li>• Number of open lanes</li> <li>• Speed</li> <li>• Proportion of heavy vehicles</li> <li>• Number of closed lanes</li> <li>• Lateral distance to the open lanes</li> <li>• Work zone length</li> <li>• Time of day</li> <li>• Location of closed lanes</li> <li>• Grade</li> <li>• Medium work intensity</li> </ul> </li> <li>• Categorization of work zone intensity <ul style="list-style-type: none"> <li>• Medium</li> <li>• Heavy</li> </ul> </li> </ul>
Luna and Mohammedi 2014	<ul style="list-style-type: none"> <li>• Investigated effects of construction activity and intensity on capacity of rural freeway work zones using field and sensor data</li> <li>• Categorization of work zone intensity <ul style="list-style-type: none"> <li>• Light</li> <li>• Heavy</li> </ul> </li> <li>• Heavy construction activity led to capacity reduction</li> </ul>

Reference	Summary of Findings
Maze et al. 2000	<ul style="list-style-type: none"> <li>• Estimated capacity of a rural Iowa freeway work zone using field data</li> <li>• Capacity defined as the average of ten highest values of flow immediately before and after queuing conditions</li> <li>• Estimated capacity of rural Iowa work zone varied from 1,400 to 1,600 pchpl</li> <li>• Work zone activity not considered</li> </ul>
Notbohm et al. 2009	<ul style="list-style-type: none"> <li>• Analyzed urban freeway work zone capacity using historical detector data from two work zones</li> <li>• Work zone capacity calculated as maximum hourly volume counted</li> <li>• Morning peak capacity values 2,100 vphpl (four-lane to two-lane) and 1,900 vphpl (two-lane to one-lane)</li> <li>• Work zone activity not considered</li> </ul>
Sarasua et al. 2004	<ul style="list-style-type: none"> <li>• Developed model for short-term freeway work zone capacity from field data</li> <li>• Capacity of work zone determined from speed-flow relationship</li> <li>• Base capacity 1,460 pchpl <ul style="list-style-type: none"> <li>• Adjustment factors</li> <li>• Proportion of heavy vehicles</li> <li>• Number of lanes</li> </ul> </li> <li>• High work zone activity investigated but found to be not statistically significant</li> </ul>
Shao and Chen 2010	<ul style="list-style-type: none"> <li>• Estimated capacity for eight-lane urban expressway work zones using both field data and simulation</li> <li>• Work zone capacity defined as saturation flow rate</li> <li>• Range of capacity values (four-lane to two-lane) 1,500 to 1,700 vphpl</li> <li>• Regression models for speed and flow developed</li> <li>• Work zone activity not considered</li> </ul>
Venugopal and Tarko 2001	<ul style="list-style-type: none"> <li>• Developed additive and multiplicative capacity prediction models for rural freeway work zones capacity</li> <li>• Base values 1,433 vphpl (additive) and 1,320 vphpl (multiplicative)</li> <li>• Significant factors affecting capacity <ul style="list-style-type: none"> <li>• Rainfall</li> <li>• Percentage of heavy vehicles</li> <li>• Police presence</li> <li>• Presence of Indiana Lane Merge System (ILMS)</li> </ul> </li> <li>• Work zone activity not considered</li> </ul>

Reference	Summary of Findings
Zheng et al. 2011	<ul style="list-style-type: none"> <li>• Compared several different work zone capacity prediction models using field data <ul style="list-style-type: none"> <li>• HCM model</li> <li>• Two multi-linear regression models</li> <li>• Fuzzy logic based artificial neural network model</li> </ul> </li> <li>• Neuro-fuzzy model most accurate</li> <li>• Work intensity considerations <ul style="list-style-type: none"> <li>• Adjustment factor</li> <li>• Use of dummy variable</li> </ul> </li> </ul>

## 2.2 Current Practice of Work Zone Capacity Estimation (2010 HCM)

The 2010 HCM (TRB 2010) provides some guidance regarding the estimation of work zone capacity. In this manual, work zones are divided into two types based on work activity and nature of barriers used:

1. Short-term work zone lane closures, usually for maintenance (standard channeling devices such as traffic cones, drums, etc.)
2. Long-term work zone lane closures, usually for construction (portable concrete barriers)

### 2.2.1 Capacity of Short-Term Work Zones

Based on the study performed by Krammes and Lopez (1994), the capacity of short-term freeway work zones is measured as 1,600 pchpl for all lane closure configurations. However, the base value of capacity is adjusted based on factors such as the intensity of work activity, effect of heavy vehicles, and presence of ramps.

#### 2.2.1.1 Intensity of Work Activity

The intensity of work activity is calculated by using an index derived from factors for the number of workers, size of equipment, presence of flaggers, and noise and dust level at the site (Krammes and Lopez 1994).

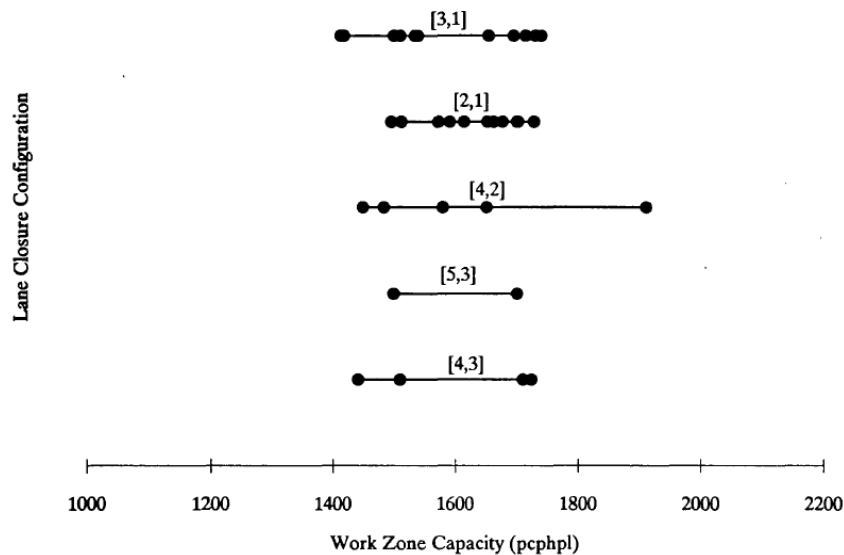
Studies cited in the 1985 HCM (TRB 1985) and Dudek et al. (1981) reported that work zone capacity decreased with increased intensity of work activity. The studies also reported that mean speeds of traffic streams decreased as work activities were moved closer to the travel lane. Table 2.2, which is derived from the 1985 HCM, shows capacity values for various lane closure configurations and types of activity.

**Table 2.2. Work zone capacity (vphpl) variation by lane closure configuration and type of work**

Type of Work	Lane Closure Configuration (Normal, Open)				
	[3,1]	[2,1]	[5,2]	[4 or 3,2]	[4,3]
Median Barrier/Guardrail Installation/Repair	--	1,500	--	1,600 (1,470)	1,600 (1,523)
Pavement Repair	1,050	1,400	--	1,500 (1,450)	1,500
Resurfacing, Asphalt Removal	1,050	1,200 (1,300)	-- (1,375)	1,300 (1,450)	1,333
Striping, Slide Removal	--	1,200	--	1,300	1,333
Pavement Markers	--	1,100	--	1,200	1,200
Bridge Repair	-- (1,350)	-- (1,350)	--	1,100	1,133

Source: TRB 1985

According to the 2010 HCM (TRB 2010), the recommended adjustment for work activity is within the range of approximately +/- 10 percent of 1,600 pcphpl. This recommendation stems from the study conducted by Krammes and Lopez (1994) and is illustrated in Figure 2.1.



Krammes and Lopez 1994, Transportation Research Record: Journal of the Transportation Research Board

**Figure 2.1. Short-term freeway work zone lane closure capacity**

### 2.2.1.2 Effect of Heavy Vehicles

The HCM recommends that a heavy vehicle factor be incorporated to adjust capacity since the base value of capacity is given in terms of pcphpl (TRB 2010). The heavy vehicle factor is calculated based on the formula in the HCM manual for basic freeway segments.

### 2.2.1.3 Presence of Ramps

The presence of entrance ramps within the taper area or just immediately downstream of the beginning of the full lane closure has an adverse effect on work zone capacity. The vehicles from the ramp will try to force their way into the mainline traffic stream, resulting in a reduction of upstream main lane queue discharge. Additional capacity reduction can arise because of the added turbulence in the merge area.

The HCM also recommends that the on-ramp be located at least 1,500 ft upstream of the beginning of the lane closure. However, if this distance allowance is not possible, either the ramp volume should be added to the mainline volume or the capacity of the work zone should be decreased by the ramp volume up to one-half of the capacity of one open lane through the work zone.

### 2.2.1.4 Calculation of Estimated Work Zone Capacity

Work zone capacity is calculated using the following equation (TRB 2010):

$$c = (1,600 \text{ pcphpl} + I - R) \times H \times N \quad (2.1)$$

where

$c$  = estimated work zone capacity (vph)

$I$  = adjustment for type and intensity of work activity (pcphpl)

$R$  = adjustment for presence of ramps (pcphpl)

$H$  = heavy vehicle adjustment factor (vehicles/passenger car)

$N$  = number of lanes open through work zone

To review, the recommended values for the base capacity and the various adjustments are as follows:

$I$  = range (-160 to + 160 pcphpl), depending on type, intensity, and location of work activity

$R$  = minimum of average entrance ramp volume in pcphpl during lane closure period for ramps located within channelizing taper or within 152 m (500 ft) downstream of the beginning of full lane closure, or one-half of capacity of one lane open through work zone (i.e.,  $1,600 \text{ pcphpl}/2N$ )

$H$  = various percentages of heavy vehicles and passenger car equivalents, given in the 2010 HCM

### 2.2.2 Capacity of Long-Term Work Zones

The capacities of long-term work zones vary greatly and depend on various site-specific characteristics. Table 2.3 summarizes how capacities vary for different locations and lane configurations. The HCM recommends that capacity be estimated based on local data and experience. In the absence of data, the values shown in Table 2.3 can be used.

**Table 2.3. Capacity of long-term work zones (vphpl)**

State	Normal Lanes to Reduced Lanes					
	2 to 1	3 to 2	3 to 1	4 to 3	4 to 2	4 to 1
TX	1,340		1,170			
NC	1,690		1,640			
CT	1,500–1,800		1,500–1,800			
MO	1,240	1,430	960	1,480	1,420	
NV	1,375–1,400		1,375–1,400			
OR	1,400–1,600		1,400–1,600			
SC	950		950			
WA	1,350		1,450			
WI	1,560–1,900		1,600–2,000		1,800-2,100	
FL	1,800		1,800			
VA	1,300	1,300	1,300	1,300	1,300	1,300
IA	1,400–1,600	1,400–1,600	1,400–1,600	1,400–1,600	1,400–1,600	1,400–1,600
MA	1,340	1,490	1,170	1,520	1,480	1,170
Default	1,400	1,450	1,450	1,500	1,450	1,350

Source: Adapted from Chatterjee et al. 2010

### 2.2.3 2010 HCM Enhancements

A study by Zegeer et al. (2014) included some enhancements to the 2010 HCM work zone capacity methodology. In the first enhancement, a method was developed to modify the discharge rate from a signalized intersection on an urban street due to the presence of an incident or work zone lane closure downstream. For freeway work zones, a table extrapolating the 2010 HCM values to freeway work zones with five moving lanes was developed as shown in Table 2.4.

**Table 2.4. Work zone capacity and minimum free-flow speed adjustment factors for freeway work zones**

Work Zone		Minimum Allowable Free-Flow Speed Adjustment Factors				
Lanes Open	CAF	55 mph	60 mph	65 mph	70 mph	75 mph
		(2,250 pcphpl)	(2,300 pcphpl)	(2,350 pcphpl)	(2,400 pcphpl)	(2,400 pcphpl)
1	0.68	0.60	0.56	0.53	0.50	0.47
2	0.70	0.62	0.58	0.55	0.52	0.49
3	0.72	0.64	0.60	0.57	0.54	0.50
4	0.74	0.66	0.62	0.58	0.55	0.52
5	0.77	0.68	0.64	0.60	0.57	0.53

Note: The minimum allowable free-flow speed adjustment factors are according to base free-flow and base capacity. CAF = capacity adjustment factor  
Source: Zegeer et al. 2014

### 2.3 2016 HCM Method for Work Zone Capacity Calculations

In the 2016 HCM (TRB 2016), the capacity of the work zone is estimated in terms of queue discharge rate (congested conditions). This rate is convenient and is easier to measure than direct estimation from pre-breakdown capacity (maximum sustainable flow rate before breakdown).

The work zone capacity is estimated from the following relationship:

$$\text{Work zone capacity} = C_{wz} = \frac{\text{Mean queue discharge rate (QDR)}}{100 - \alpha} \quad (2.2)$$

where

$\alpha$  = Percentage drop in pre-breakdown capacity at the work zone due to queue conditions. In the absence of field data, 13.4 percent can be used for  $\alpha$  for freeway work zones.

#### 2.3.1 Estimation of Queue Discharge Rate

There are many factors such as lane closure configuration, type of barrier, land use type, lateral distance between barrier and edge of travel lane, time of the day, etc., which can affect the queue discharge rate. To estimate the queue discharge rate, all of the aforementioned factors need to be considered. The relationship among the factors and queue discharge rate is stated below:

$$QDR_{wz} = 2093 - (154 \times f_{LCSI}) - (194 \times f_{Br}) - (179 \times f_A) + (9 \times f_{LAT}) - (59 \times f_{DN}) \quad (2.3)$$

where

$QDR_{wz}$  = work zone queue discharge rate (pcphpl)

$f_{LCSI}$  = lane closure severity index

$f_{Br}$  = barrier type (0 = concrete and hard barrier separation, 1 = cone, plastic drum, or other soft barrier separation)

$f_A$  = area type (0 = urban areas with high development densities or concentrations of population, 1 = rural areas with widely scattered development and low housing and employment densities)

$f_{LAT}$  = lateral distance from the edge of travel lane adjacent to the work zone to the barrier, barricades, or cones (0 to 12 ft)

$f_{DN}$  = daylight/night (0 = daylight, 1 = night)

The lane closure severity index, which is a function of lane closure configuration, can be estimated from Table 2.5:

**Table 2.5. Lane closure severity index**

Total Number of Lane(s)	Total Number of Lane(s)	Open Ratio	$f_{LCSI}$
3	3	1.00	0.33
2	2	1.00	0.50
4	3	0.75	0.44
3	2	0.67	0.75
4	2	0.50	1.00
2	1	0.50	2.00
3	1	0.33	3.00
4	1	0.25	4.00

Source: TRB 2016

### 2.3.2 Estimation of Free-Flow Speed

The free-flow speeds in work zones are observed to be less than the free-flow speeds in non-work zone segments. Factors such as lane closure, intensity of work, and the number of ramps present upstream or downstream of the work zone can reduce the free-flow speed. Free-flow speeds for work zones can be estimated by using the following formula, which incorporates the effects of several factors associated with work zone speeds (TRB 2016):

$$FFS_{wz} = 9.95 + (33.49 \times f_{Sr}) + (0.53 \times f_S) - (5.60 \times f_{LCSI}) - (3.84 \times f_{Br}) - (1.71 \times f_{DN}) - (1.45 \times f_{Nr}) \quad (2.4)$$

where

$FFS_{wz}$  = work zone free-flow speed (mph)

$f_{Sr}$  = speed ratio (decimal), i.e., the ratio of non-work zone speed limit to work zone speed limit

$f_S$  = work zone speed limit (mph)

$f_{LC SI}$  = lane closure severity index

$f_{Br}$  = barrier type (0 = concrete and hard barrier separation, 1 = cone, plastic drum, or other soft barrier separation)

$f_{DN}$  = daylight/night (0 = daylight, 1 = night)

$f_{Nr}$  = number of on-ramps and off-ramps within three miles upstream and downstream of the work zone area

### 2.3.3 Speed-Flow Model Development for Work Zones

The generalized speed-flow curve used in both the 2010 HCM and 2016 HCM suggests that for low and medium flow rates, the decrease in speed is negligible. As flow continues to increase, speed decreases significantly before capacity is reached. The speed-flow model of work zones can be built by performing the following steps:

1. The vehicular traffic flow should be converted to equivalent passenger car traffic by using the formula suggested by the HCM for basic freeway segments.
2. The break point between the straight and curved segments should be estimated by using the following equation (TRB 2016):

$$BP = [1000 + 40 \times (75 - FFS_{wz}) \times CAF^2 \quad (2.5)$$

where

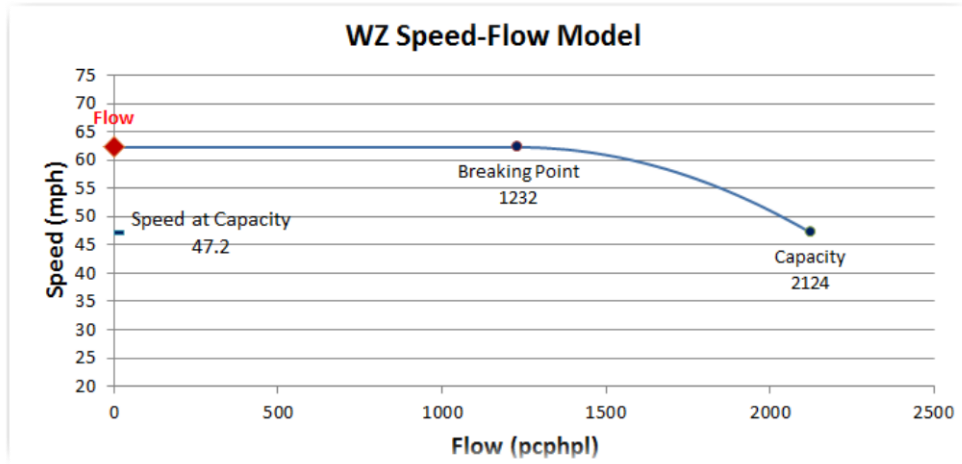
$FFS_{wz}$  = free-flow speed of the work zone (mph)

$CAF$  = capacity adjustment factor (ratio of work zone capacity to freeway base section capacity)

3. The curved segment can be estimated for any flow level ( $v_p$ ) greater than break point by using the following formula (TRB 2016):

$$S = FFS_{wz} - \frac{(FFS_{wz} - \frac{C_{wz}}{45})(v_p - BP)^2}{(C_{wz} - BP)^2} \quad (2.6)$$

The representative figure of the work zone speed-flow model is depicted in Figure 2.2.



HCM, TRB 2016

**Figure 2.2. Representative work zone speed-flow model**

## 2.4 Other Existing Guidance

Some DOTs provide guidance regarding work zone capacity. For example, the Massachusetts Department of Transportation (MassDOT) design guide (MassDOT 2006) provides a table with expected vehicle capacities based on the number of lanes and number of closed lanes, as shown in Table 2.6.

**Table 2.6. Work zone capacities from MassDOT design guide**

Number of Lanes		Estimated Capacity	
Normally open	During construction	Vehicles per hour per lane	Total vehicles per hour
2	1	1,340	1,340
3	2	1,490	2,980
3	1	1,170	1,170
4	3	1,520	4,560
4	2	1,480	2,980
4	1	1,170	1,170

Source: Adapted from MassDOT 2006

The work zone guidelines from the Missouri Department of Transportation (MoDOT) also present some information regarding work zone capacities (MoDOT 2004). According to the MoDOT guide, the maximum traffic capacity for a freeway with two lanes in each direction and one closed lane is 1,240 vphpl. The MoDOT guide also indicates that the estimated work zone capacity for a multi-lane roadway is approximately 1,000 vphpl. MoDOT recommends that mitigation strategies to reduce congestion in work zones for two-lane roadways should be

considered when volumes reach 600 vphpl. The MoDOT guide includes a table of estimated work zone capacities for various scenarios, as shown in Table 2.7.

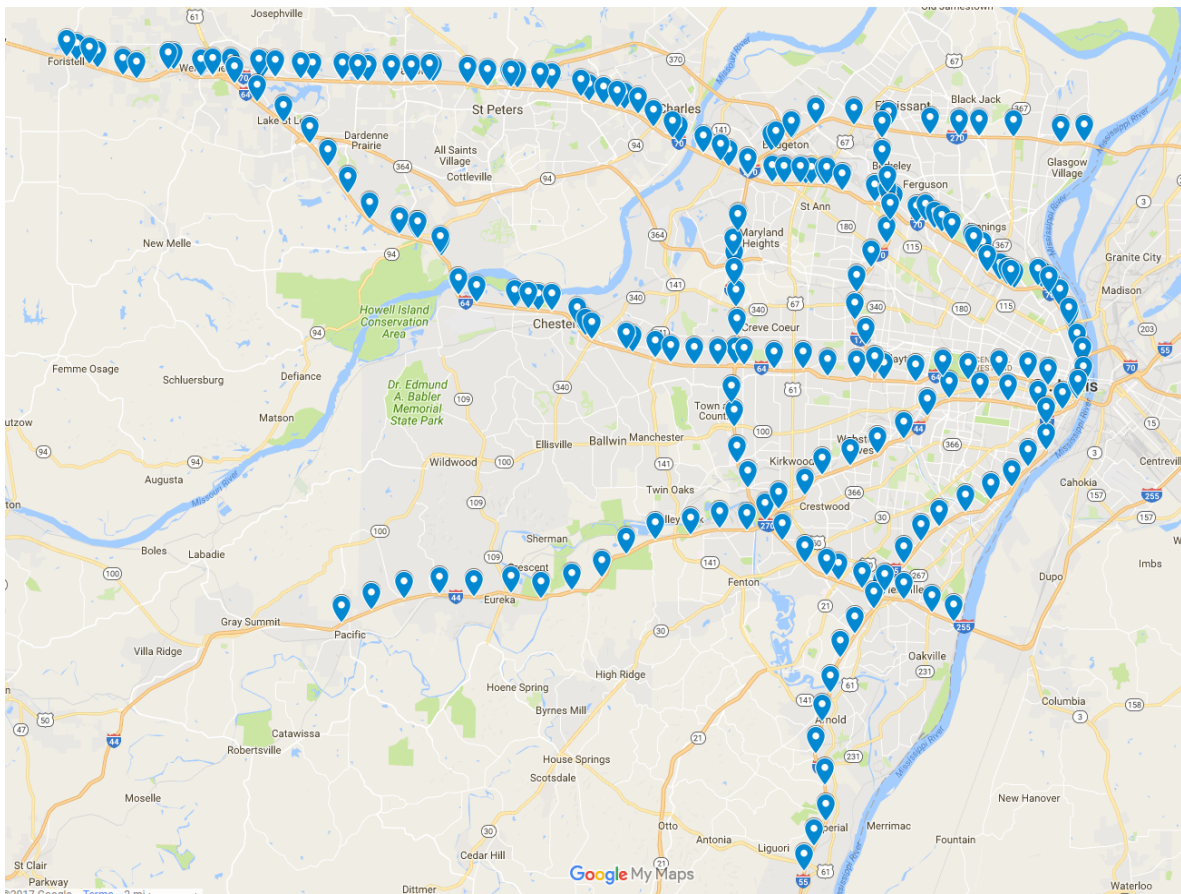
**Table 2.7. Work zone capacities from MoDOT design guide**

<b>Interstate and Freeway Lane Conditions</b>		<b>Capacity Restrictions</b>		<b>Cautionary Zone</b>	
<b>Total number of lanes</b>	<b>Number of open lanes</b>	<b>Vehicles per hour per lane</b>	<b>Total capacity in open lanes</b>	<b>Vehicles per hour per lane</b>	<b>Total capacity in open lanes</b>
3	1	960	960	750	750
2	1	1,240	1,240	1,000	1,000
5	2	1,320	2,640	1,000	2,000
4	2	1,420	2,840	1,100	2,200
3	2	1,430	2,860	1,100	2,200
4	3	1,480	4,440	1,100	3,300

Source: MoDOT 2004

### 3. STUDY AREA AND DATA COLLECTION

The goal of this study was to evaluate the impacts on traffic due to various work activities in work zones. The type of work and lane closure configuration can significantly influence traffic mobility in a work zone. To capture the impacts of different work activities and lane closure configurations on traffic, Interstate freeways in the St. Louis District of MoDOT were selected for study. The St. Louis District contains six Interstate freeways: I-44, I-55, I-64, I-70, I-170, and I-270, connecting most of the regional highways. The traffic flow characteristics data for Interstate highways were collected using a combination of sensor and probe data. The University of Missouri, with MoDOT's permission, has access to real-time traffic data throughout the state of Missouri. Probe-based speed and travel time data are available via the Regional Integrated Transportation Information System (RITIS) and Nokia HERE (a map application). Point-based sensor data of traffic flow variables are also available for different regions in the state based on sensor coverage. For example, coverage in the St. Louis region is extensive, with nearly 700 sensors deployed on freeways and arterials. The geographical distribution of fixed traffic sensors for all Interstate highways in the St. Louis District is illustrated in Figure 3.1.



© 2016 Google

**Figure 3.1. Geographical distribution of fixed traffic sensors for all Interstate highways in the St. Louis District**

### 3.1. Identification of Work Zone Locations

The work zone locations selected for this study were identified from the bimonthly Regional Mobility Report published by MoDOT. The report for the St. Louis District records the events that significantly affect traffic mobility for the specified months. The events, such as work zones and accidents, that cause significant impacts on mobility are recorded with relevant information. Based on travel time, the impacts of work zones in the report are classified as major, moderate, and minor. The major- and moderate-impact work zones have more than 10 minutes additional travel time. For this study, major- and moderate-impact work zones were selected because traffic conditions ranging from free-flow to below capacity can be experienced in these work zones. The classification of work zones observed in a bimonthly report is shown in Table 3.1.

**Table 3.1. Classification of work zones observed in two months**

<b>May 2015</b>		<b>June 2015</b>	
<b>Level of Travel Time Impact</b>	<b>Number of Work Zones</b>	<b>Level of Travel Time Impact</b>	<b>Number of Work Zones</b>
Major Impact	0	Major Impact	1
Moderate Impact	1	Moderate Impact	1
Minor Impact	240	Minor Impact	300
Total	241	Total	302

Source: MoDOT 2015–2016

The report also includes information about the route, location, date, and type of work for the work zones with major and moderate impacts. A sample of the reported information is illustrated in Figure 3.2.

**Major Impact (15 Minutes or Above Additional Travel Time)**

**6/27 (Saturday) AM Eastbound I-64 at Technology (Boone Bridge) — 2 Right Lanes Closed**

- Bridge work scheduled throughout the day
- Removing barrier and placing striping for bridge opening
- All mitigation efforts were in use
- RITIS data showed motorists experienced an additional 17 minutes of travel time

**Moderate Impact (10-14 Minutes Additional Travel Time)**

**6/27 (Saturday) AM Eastbound I-64 at Technology (Boone Bridge) — 2 Right Lanes Closed**

- Bridge work scheduled throughout the day
- Removing barrier and placing striping for bridge opening
- All mitigation efforts were in use
- RITIS data showed motorists experienced an additional 14 minutes of travel time

**5/18 (Monday) PM Southbound US 67 I-55 to Route 110 — Right Lane Closed**

- Project being administered through the Southeast District
- Resurfacing Project
- All mitigation efforts were in use
- RITIS data showed motorists experienced an additional 14 minutes of travel time

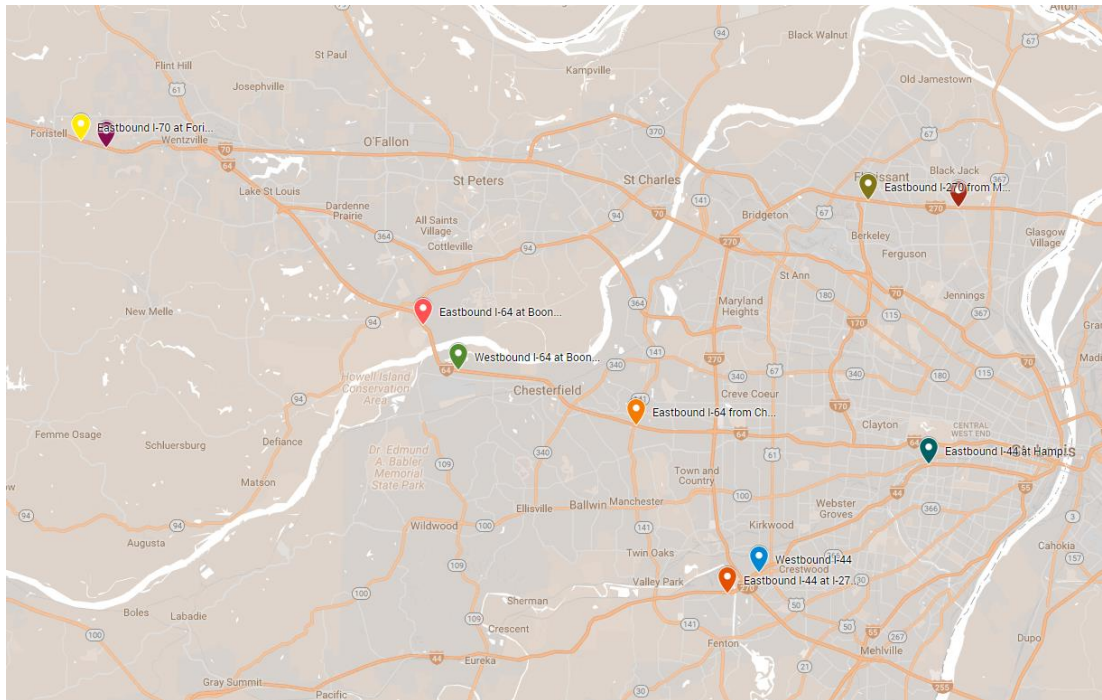
MoDOT 2015–2016

**Figure 3.2. Information related to route, location, date, and type of work for the work zones**

The mobility reports were available from January 2015 through August 2016 during the time of work zone activity data collection. So, the mobility reports from January 2015 through August 2016 were reviewed, and 11 work zone locations were identified with major and moderate impacts on travel time. Details of the work zone locations, along with the work activities, are listed in Table 3.2 and illustrated in Figure 3.3.

**Table 3.2. Details of the work zone locations**

No.	Location	Work description	Lane closure configuration (total no. of lanes, no. of open lanes)
1.	Eastbound I-64 at Boone Bridge	restriping	(3,2)
2.	Eastbound I-64 at Boone Bridge	bridge work	(3,2)
3.	Westbound I-64 at Boone Bridge	bridge demolition preparation	(3,2)
4.	Eastbound I-64 from Chesterfield Parkway to I-270	paving operations	(3,2)
5.	Eastbound I-70 at Foristell	pavement repair	(2,1)
6.	Westbound I-70 at Foristell	paving operations	(2,1)
7.	Eastbound I-270 from McDonnell Boulevard to Route 367	bridge work	(4,2)
8.	Westbound I-270 from I-170 to 367	pavement work	(3,2)
9.	Eastbound I-44 at I-270 (Meramec Bridge)	bridge work	(3,2)
10.	Westbound I-44	resurfacing	(3,2)
11.	Eastbound I-44 at Hampton	bridge rehabilitation	(4,2)

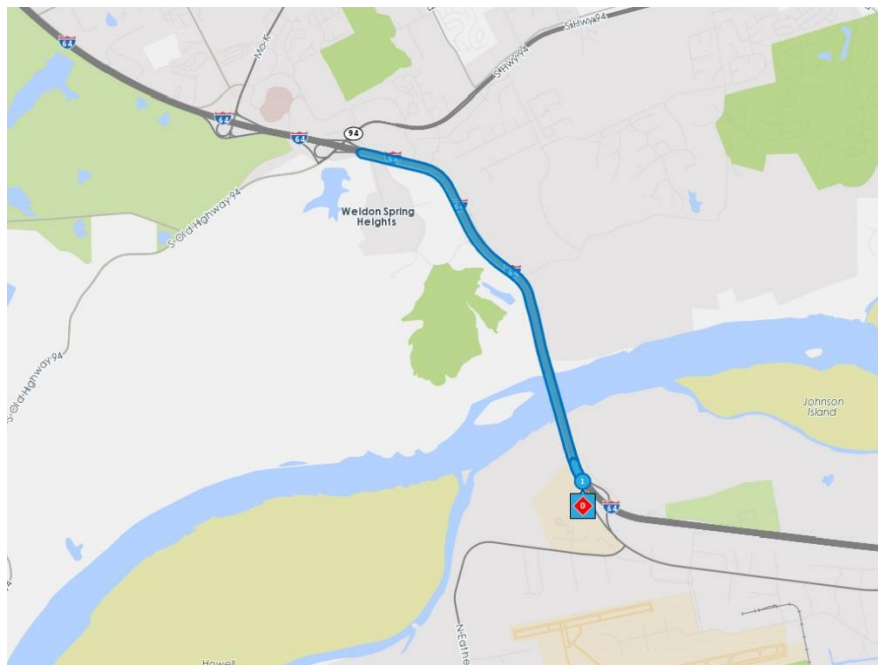


© 2016 Google

**Figure 3.3. Geographical distribution of work zone locations for all Interstate highways in the St. Louis District**

### 3.2. Identification of Work Zone Segments

In some cases, the bimonthly Regional Mobility Report is not sufficient to identify the exact work zone segments because it only mentions the locations with nearby routes or landmarks. To identify the exact segments, the Missouri Analytics application in RITIS was used. The Missouri Analytics application has historical information about work zones and other bottlenecks. The application shares information such as location of segment, maximum queue length, congestion, and total duration in the form of tables and maps. Location information from Missouri Analytics can be checked on a sensor deployment map (Figure 3.1), and sensors affected by work zone activities can be identified. Identification of one of the work zone locations on I-64 (the major impact work zone in Figure 3.2) with the help of Missouri Analytics is shown in Figure 3.4.



RITIS (Missouri Analytics), University of Maryland CATT Lab

**Figure 3.4. Identification of work zone segment at I-64 Boone Bridge**

To identify the work zone, basic information such as route, location, date, and type of work were collected from the bimonthly Regional Mobility Report (Figure 3.2). Then, information such as date, road, and region were used as inputs for the Missouri Analytics application to query information related to the location, length, and duration of the bottleneck. After the location was identified in the sensor deployment map (Figure 3.1), the sensors affected by the bottleneck were identified.

### 3.3. Traffic Data Collection

Three major types of traffic information are collected regularly for individual lanes from each traffic sensor in a 30-second window: traffic volume, speed, and occupancy. The collected traffic information is transmitted in real time to a MoDOT database in extensible markup language

(XML) format. Figure 3.5 provides screenshots showing traffic sensor information and a segment of an XML file.

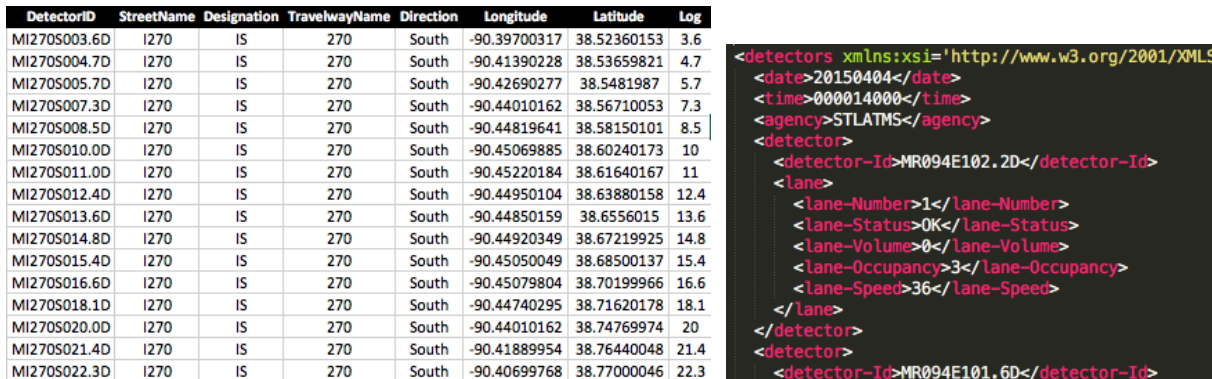


**Figure 3.5. Traffic sensor information (left) and XML feed detector information (right)**

The traffic sensor information (left side of Figure 3.5) consists of eight fields: detector ID (traffic sensor ID), street name, designation, travel way name, direction, longitude, latitude, and log-mile. The right side of Figure 3.5 shows specific detector information in XML format: date, time (in 30-second intervals), agency, detector ID, lane number, lane status, traffic volume, occupancy, and speed.

## 4. METHODOLOGY

The methodology used to develop speed-flow plots is depicted in the Figure 4.1.

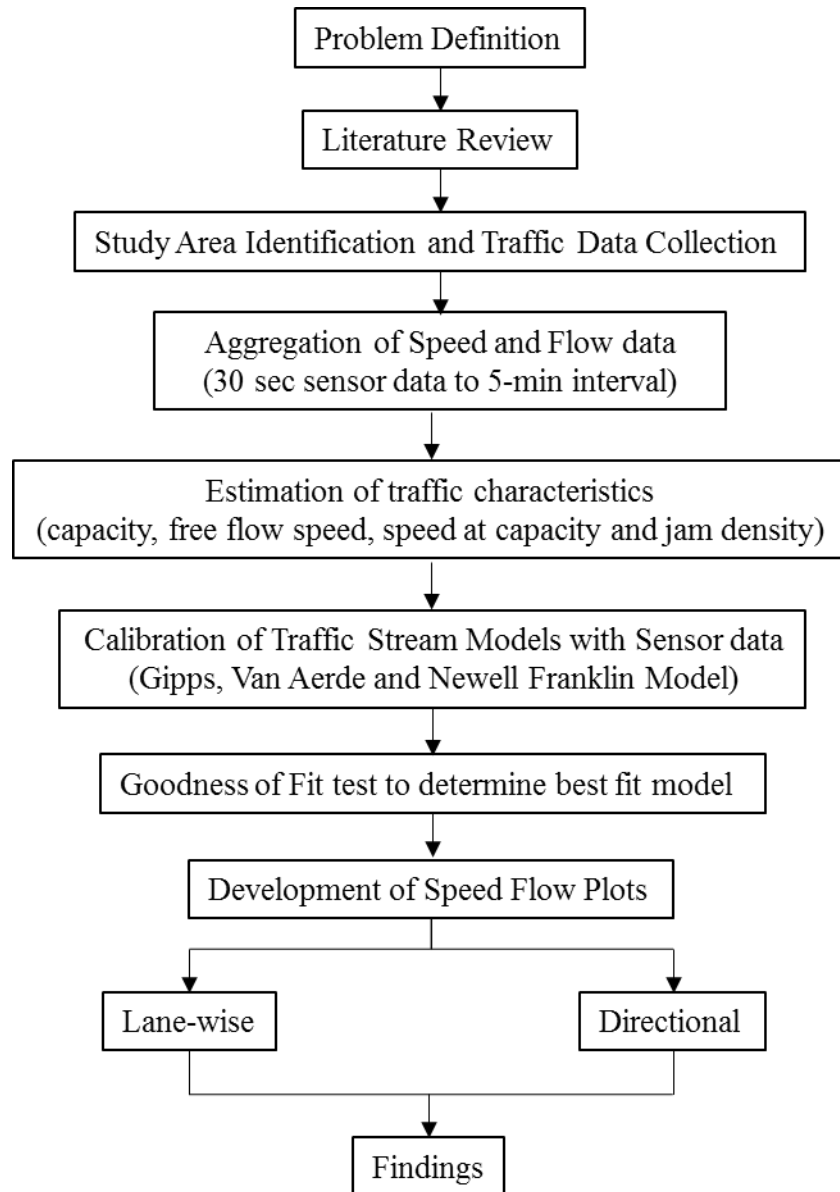


**Figure 4.1. Study methodology**

### 4.1. Identification of Work Zone Time

In many cases, the work zones were in place for less than a day. In those cases, it was important to identify work zone hours so that data from non-work zone times could be eliminated from the work zone analysis. After identifying the specific day of the work zone from the mobility report, work zone hours were identified by plotting traffic count data by lane. Work zone hours were

determined based on time periods in which there was no traffic in at least one lane while other lanes were operating normally. The identification process is illustrated in Figure 4.2 using sample data from a work zone on I-70 near the city of Foristell. The segment is a two-lane Interstate, and one of the lanes was closed overnight. The lane was opened at 5:18 a.m., which separates work zone time from non-work zone time in the same day, indicating the end of work zone time. The lane closed again at 8:15 p.m. (which is not shown in the figure), indicating the beginning of work zone activity.

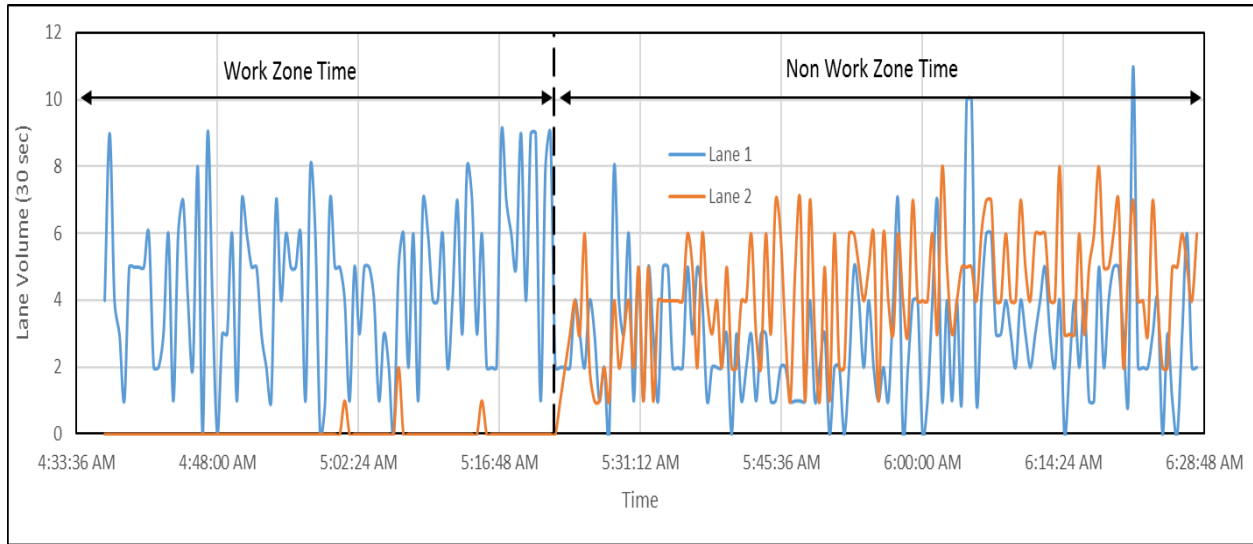


**Figure 4.2. Identification of work zone time at I-70 near Foristell**

#### 4.2. Aggregation of Speed-Flow Data

After identification of the work zone time, the 30-second speed and flow data from the detectors were aggregated into 5-minute intervals. A study conducted by Lorenz and Eleftheriadou (2001) showed that for longer periods (5 or 15 min), the breakdown probability at a higher flow rate is substantially higher, while for short periods (1 min), the probability is low for all range of flows (low and high). So, a 5-minute interval was considered to be reasonable for aggregation to capture measures of traffic flow characteristics. The flow is estimated by aggregating the 30-second counts to 5-minute counts and then converting the results to an hourly flow. The corresponding speed is estimated by taking the weighted average of the 30-second speed data. A general equation for the volume and speed processing is presented below.

$$Volume_t = \sum_{i=1}^n volume_i \times 12 \quad (4.1)$$

$$Speed_t = \frac{\sum_{i=1}^n (volume_i \times speed_i)}{\sum_{i=1}^n volume_i} \quad (4.2)$$

where

n =10 (since 30-second data is aggregated into 5 minutes)

### **4.3. Estimation of Traffic Flow Characteristics**

#### *4.3.1. Free-Flow Speed*

Free-flow speed is the mean speed of passenger cars under low-density conditions. The most accurate method for estimating segment free-flow speed is to measure it in the field during uncongested flow conditions (under 800 vphpl, according to the 2010 HCM). Hou et al. (2013) used the 85th percentile speed as a measure to evaluate the effectiveness of posted speed limits for short-term Interstate work zones. For this study, the 85th percentile speed of the traffic stream under low-flow conditions was considered to be the free-flow speed.

#### *4.3.2. Capacity and Speed at Capacity*

In much of the existing literature, capacity is defined based on breakdown flow or queue discharge flow. Some researchers define capacity as the traffic flow breakdown point. The breakdown point is the traffic flow just before a significant drop in speed followed by low speeds sustained for some time and fluctuating traffic flow rate (Jiang 1999, Dong and Mahmassani 2009, Heaslip et al. 2009), while others define capacity based on queue discharge flow (Al-Kaisy et al. 2000, Al-Kaisy and Hall 2003, Benekohal et al. 2004). Elefteriadou and Lertworawanich (2003) found that the magnitude of breakdown flows is almost always lower than that of discharge flows prior to recovery to non-congested conditions.

To identify capacity in this study, speed and flow data were plotted in order of time. The process was carried out for all work zone locations on both work zone and non-work zone days. The plots show that higher flow could occur either at breakdown or prior to recovery to non-congested conditions. In most cases, the breakdown flow is found to be higher. So, to prevent underestimation, the higher value of either the breakdown flow or the discharge flow before recovery was designated as capacity. The mean queue discharge rates in the study locations were lower than the work zone capacities. The identification of capacity values is illustrated in Figures 4.3.1 and 4.3.2 with time series plots for two selected work zone locations. Figure 4.3.1 shows the scenario when breakdown flow is higher than recovery flow, while the opposite scenario is shown in Figure 4.3.2.

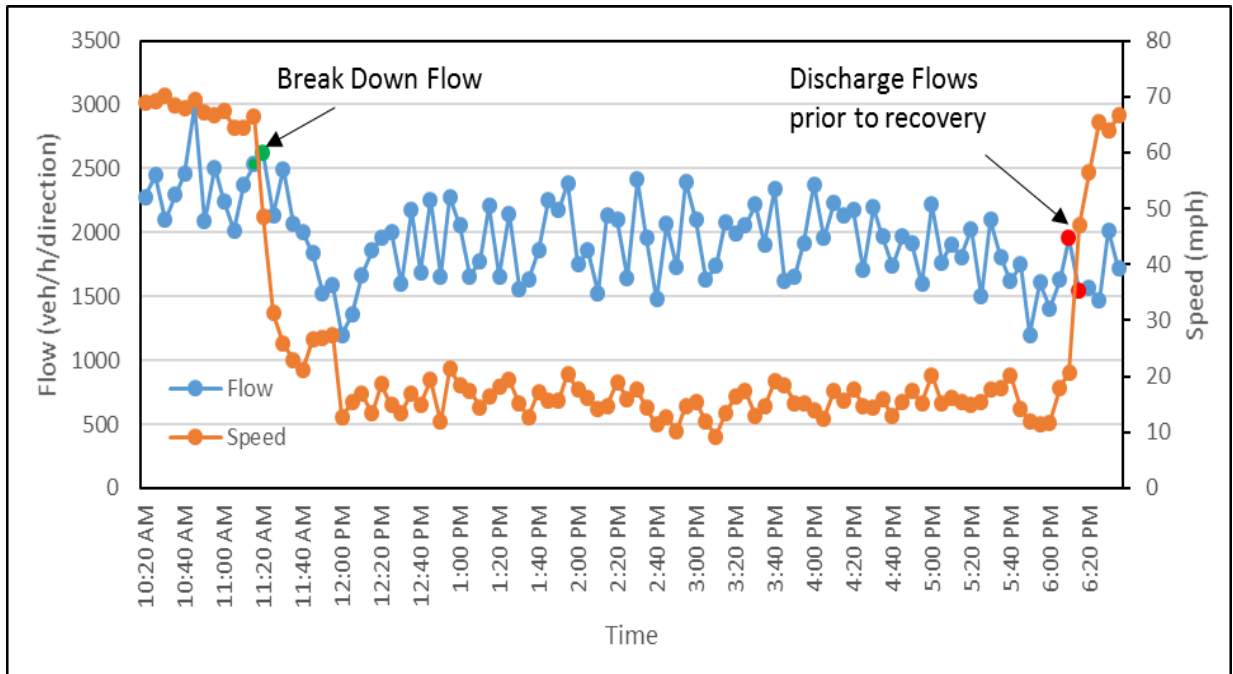


**Figure 4.3.1. Speed-flow plot in order of time for capacity identification when breakdown flow is higher than recovery flow**

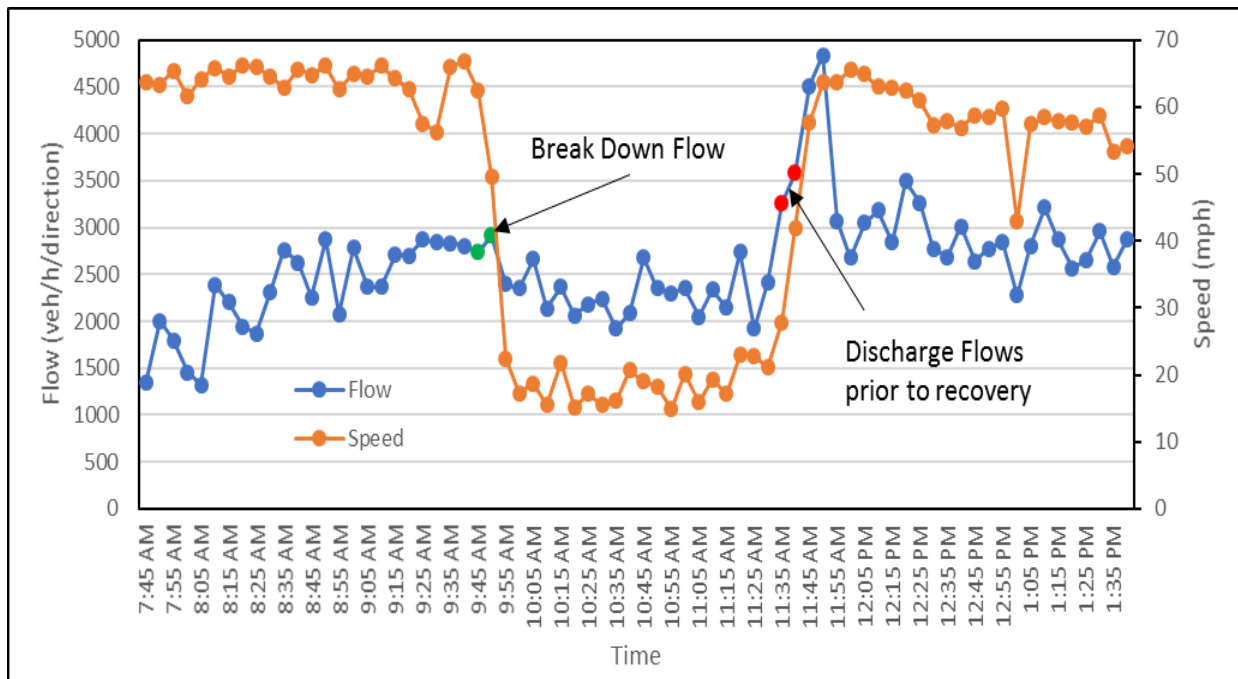


**Figure 4.3.2. Speed-flow plot in order of time for capacity identification when breakdown flow is lower than recovery flow**

Speed at capacity can also be identified from the time series plot of speed and flow. The speed at capacity, at breakdown, and at recovery delineates the uncongested and congested conditions.

### 4.3.3 Jam Density

After the identification of capacity and speed at capacity, field data points can be split into uncongested and congested conditions. A flow versus density plot was developed using field data points of the locations in this study. Linear regression was used to create best fit lines for both uncongested and congested conditions (Kianfar and Edara 2013, Dervisoglu et al. 2009). From field data points, it is difficult to estimate jam density due to the sparseness of data near jam condition. So, jam density can be estimated from the regression line for the congested state. The intersection of the x-axis with the regression line represents jam density for the location. Figure 4.4 shows the flow-density plot and jam density estimation for a work zone location at I-64 Boone Bridge.

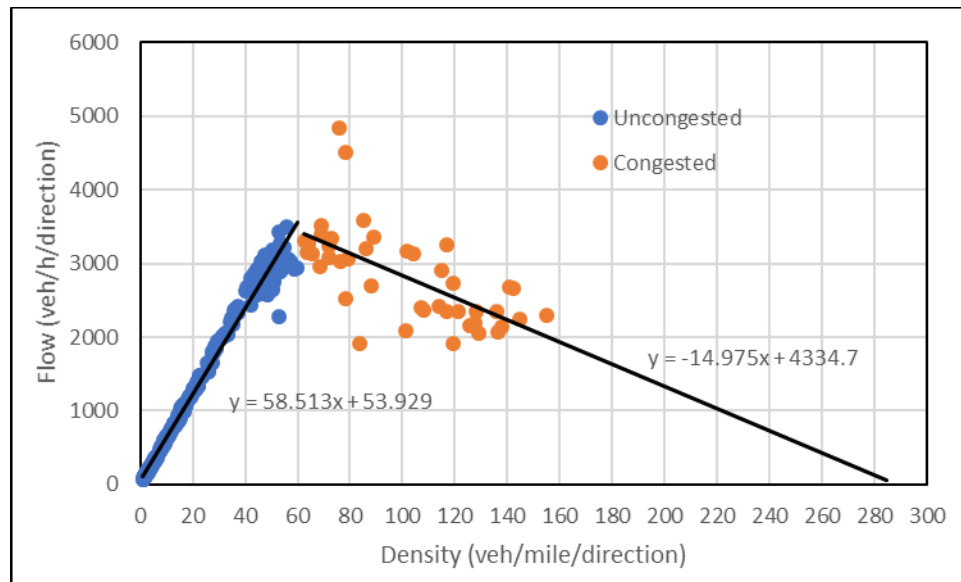


Figure 4.4. Creating flow-density diagram for work zone at I-64 Boone Bridge

## 4.4 Calibration of Traffic Stream Models with Macroscopic Sensor Data

### 4.4.1 Speed-Flow Models

Over the years, different approaches, such as empirical studies, hydrodynamic analogies, and car-following theories, have been used to develop speed-flow models. Traffic flow models can be broadly classified based on their functional forms. Single-regime functions can represent different traffic states with a continuous function while multi-regime functions address different traffic states with different equations. One tradeoff between the single- and multi-regime functions is simplicity versus the ability to capture multiple traffic states more accurately.

For this study, two single-regime models proposed by Li (2008) and Van Aerde (1995) and the two-regime model by Gipps (1981) were considered, and the models were calibrated with real-world data from 11 selected work zone locations. These three models were used because

previous literature (Burris and Patil 2008, Brilon and Lohoff 2011, Rakha 2009, Rakha and Gao 2010, Rakha et al. 2007) found that these three models were applicable to various traffic scenarios.

#### 4.4.2 Van Aerde Model

The Van Aerde model is a four-parameter car-following model, which combines the well-known Pipes and Greenshields models (Rakha and Crowther 2002). The generalized form proposed by Van Aerde was

$$h_n = c_1 + c_3 u_n + \frac{c_2}{u_f - u_n} \quad (4.3)$$

where

$h_n$  = the spacing (km) of vehicle  $n$

$u_n$  = the speed of vehicle  $n$  (km/h)

$u_f$  = the facility free-flow speed (km/h)

$c_1$  = fixed spacing constant (km)

$c_2$  = variable spacing constant (km<sup>2</sup>/h)

$c_3$  = variable spacing constant (h)

Rakha (2009) developed a procedure for the calibration of the four input parameters using real-world loop detector data. The macroscopic flow and speed relation derived from the model is shown below:

$$q = \frac{u}{c_1 + \frac{c_2}{u_f - u} + c_3 u} \quad (4.4)$$

where

$q$  = flow rate of traffic stream

$u$  = speed of traffic stream

The insertion of four parameters into the model as input provides a high degree of flexibility in capturing various human and geometric characteristics. However, the inclusion of many parameters in the function also results in a complicated speed-flow relationship.

#### 4.4.3 Gipps Model

The Gipps model is a two-stage model with an assumption that stream speed is insensitive to density in the uncongested state. The functional form of the model (Gipps 1981), including safety margin to driver's reaction time, is

$$u_n(t+T) = 3.6 \left[ -bT + \sqrt{b^2T^2 + b \left\{ 2[s_n(t) - L_{n-1}] - \frac{u_n(t)}{3.6}T + \frac{u_{n-1}t^2}{3.6^2 * b'} \right\}} \right] \quad (4.5)$$

where

$b$  and  $b'$  = deceleration parameters of vehicle  $n$  ( $m/s^2$ )

$L_{n-1}$  = the effective length of vehicle ( $m$ )

$s_n(t)$  = spacing between vehicle  $n$  and  $n-1$  at time  $t$  ( $m$ )

$u_{n-1}(t)$  = speed of the preceding vehicle ( $km/h$ )

$T$  = driver's reaction time

Wilson (2001) presented a simplified form of the steady state Gipps car-following model as

$$s = s_j + \frac{1}{2.4} Tu + \frac{1}{25.92 b} \left( 1 - \frac{b}{b'} \right) u^2 \quad (4.6)$$

Rakha et al. (2007) demonstrated a macroscopic speed-flow relationship based on the Gipps car-following model as

$$q = \frac{1000 u}{s_j + \frac{1}{2.4} Tu + \frac{1}{25.92 b} \left( 1 - \frac{b}{b'} \right) u^2} \quad (4.7)$$

where

$$T = 2.4 \left( \frac{1000}{q_c} - \frac{1000}{k_j u_c} - \frac{u_c}{25.92 b} \left( 1 - \frac{b}{b'} \right) \right) \quad (4.8)$$

#### 4.4.4 Re-specified Newell-Franklin Model

Li (2008) re-specified the traditional Newell-Franklin model (Newell 1961) by replacing jam density and kinematic wave speed with capacity and speed at capacity. The proposed generalized form is illustrated below:

$$q = q_o \left( \frac{u}{u_c} \right) \left( 1 - \frac{1}{\beta} \ln \frac{u_f - u}{u_f - u_c} \right)^{-1} \quad (4.9)$$

where

$$\beta = \frac{u_c}{(u_f - u_c)} \quad (4.10)$$

$q_o$  = capacity

$u_c$  = speed at capacity

$u_f$  = free-flow speed

The model follows the standard practice specified by the HCM of using  $q_o$ ,  $u_c$ , and  $u_f$  to develop speed-flow plots and provides a good fit for uncongested conditions.

### 4.5 Goodness of Fit

The three traffic models, Li, Van Aerde, and Gipps, were evaluated using goodness of fit measures. In other words, how close were the model estimations to the observed field data? Mean absolute percentage error (MAPE) and root mean square error (RMSE) served as the goodness of fit measures. MAPE uses percentages, which are easy to understand without requiring any insights into the units of variables. The RMSE uses the same units as the variable of interest. Both measures are commonly used for evaluating model performance.

#### 4.5.1. Mean Absolute Percentage Error (MAPE)

MAPE (Hyndman and Koehler 2006) describes the fit of a model in terms of a percentage and is defined as

$$MAPE = \frac{1}{N} \sum_{i=1}^N \left| \frac{Actual - Estimated}{Actual} \right| \quad (4.10)$$

where

N is the total number of observations

The Lewis scale (Lewis 1982), a popular scale used to define MAPE levels for error evaluation and interpretation in different fields, categorizes estimation accuracy using the following MAPE levels:

- Less than 10% – highly accurate
- 11% to 20% – good
- 21% to 50% – reasonable
- 51% or more – inaccurate

#### 4.5.2. Root Mean Square Error (RMSE)

RMSE (Hyndman and Koehler 2006) describes the fit of a model in terms of standard deviation of residuals and is defined as

$$RMSE = \sqrt{\frac{\sum_{i=1}^N (Actual - Estimated)^2}{N}} \quad (4.11)$$

where

N is the total number of observations

## 5. DEVELOPMENT OF SPEED-FLOW CURVES

Speed-flow models for work zone locations were developed both by lane and direction.

### 5.1. Speed-Flow Relationship by Direction

To estimate the impacts of work activity in work zones on the overall traffic flow characteristics of roadway segments, speed-flow plots based on directional traffic were developed. The plots were developed for both work zone days and non-work zone days to determine the reduction in capacity and free-flow speed of a roadway segment due to work activity. Since all work zones were selected for moderate or major impact on travel time, traffic conditions ranging from free-flow condition to below capacity condition were captured in all selected locations. To capture a full range of traffic flow characteristics for non-work zone days, speed-flow data were queried for up to 30 days before work activity and plotted as shown in Figure 5.1.

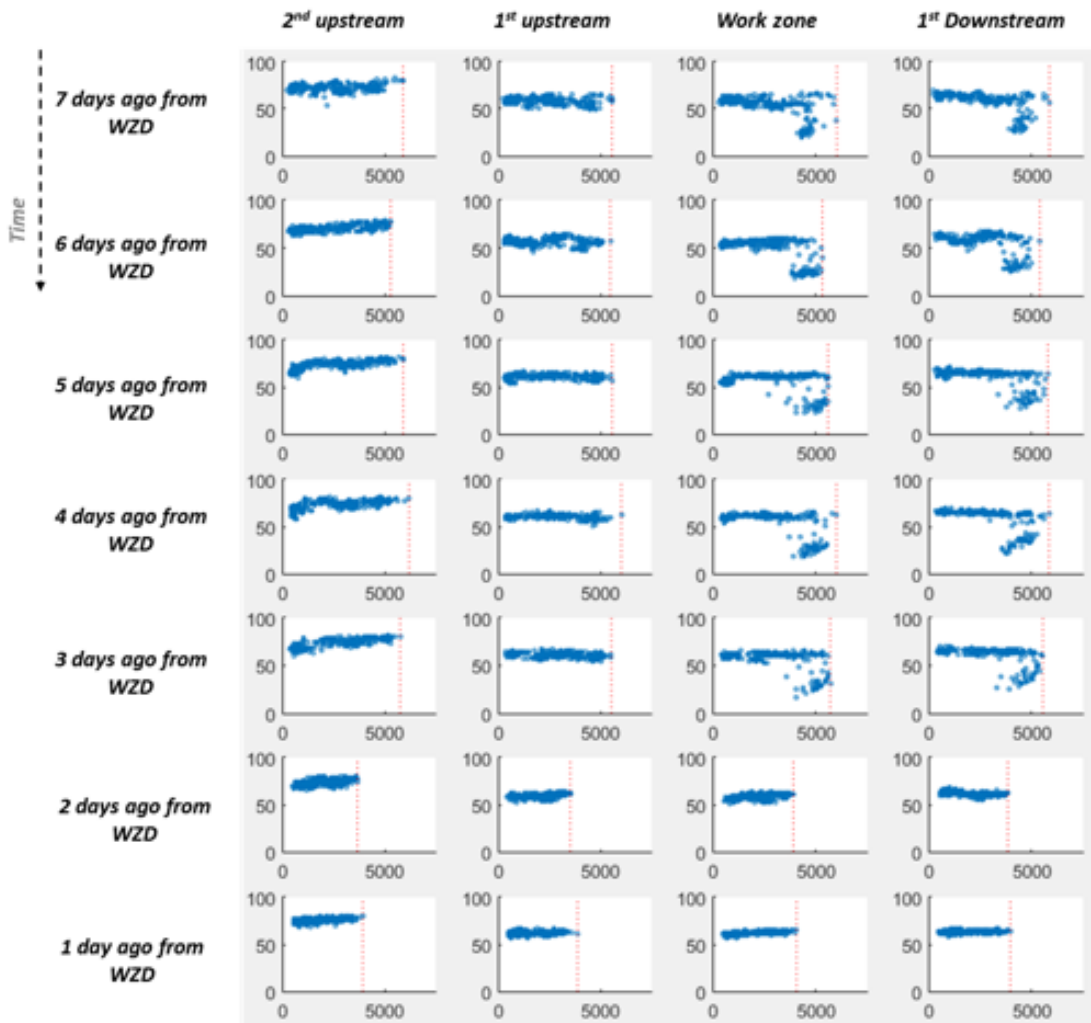
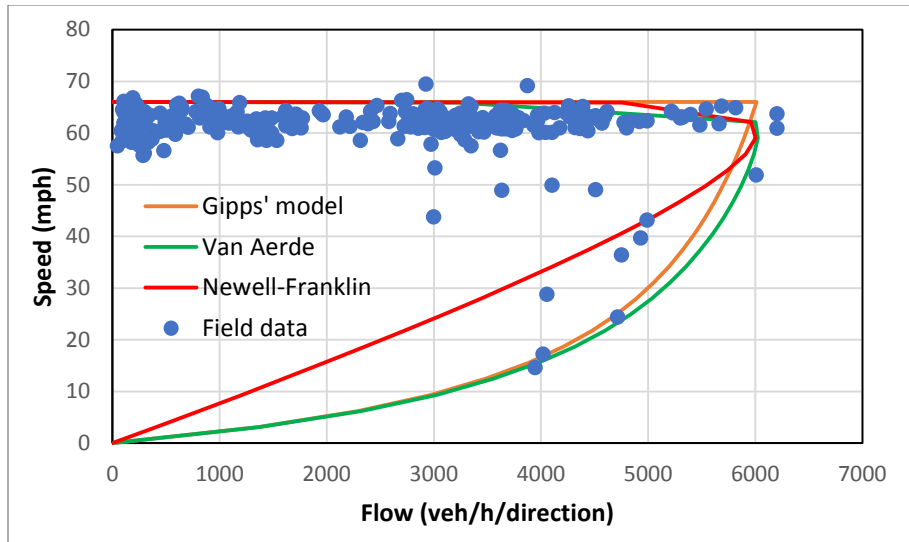


Figure 5.1. Sample of speed-flow plots for non-work zone days in a work zone location

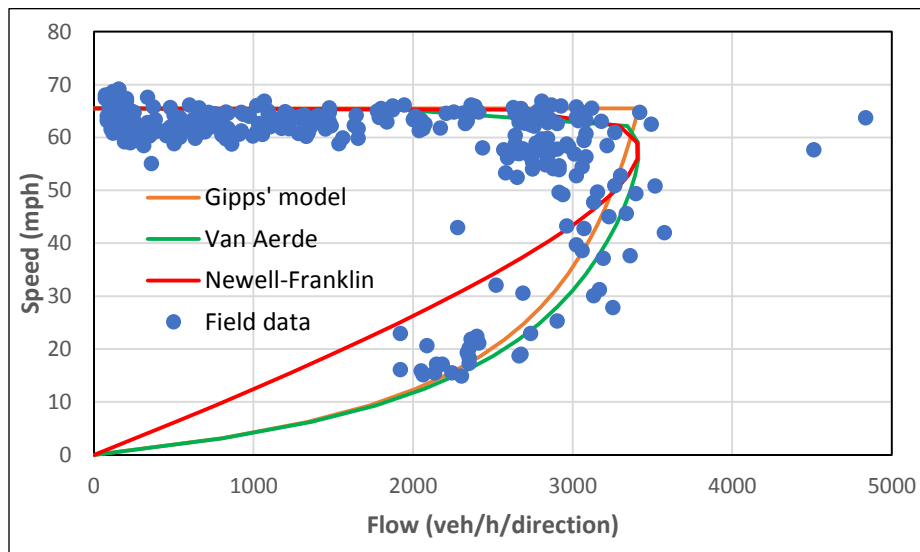
As shown in Figure 5.1, capacity was observed for the location on the third, fourth, fifth, sixth, and seventh days before the work zone was deployed. The shape of the speed-flow plots and capacity values was consistent for all days. A similar approach was applied to all selected work zone locations to develop speed-flow plots.

#### *5.1.1. Calibration of Traffic Stream Models with Field Data*

All three of the selected traffic stream models were calibrated with field data to test their performance for varying geometric and traffic scenarios. The plots for traffic stream models for selected work zone locations are illustrated in Figures 5.2.1 to 5.2.11. For each location, the type of work and the lane closure configuration are indicated in the figure label. For example, a (3,2) means a lane reduction from three lanes to two lanes.

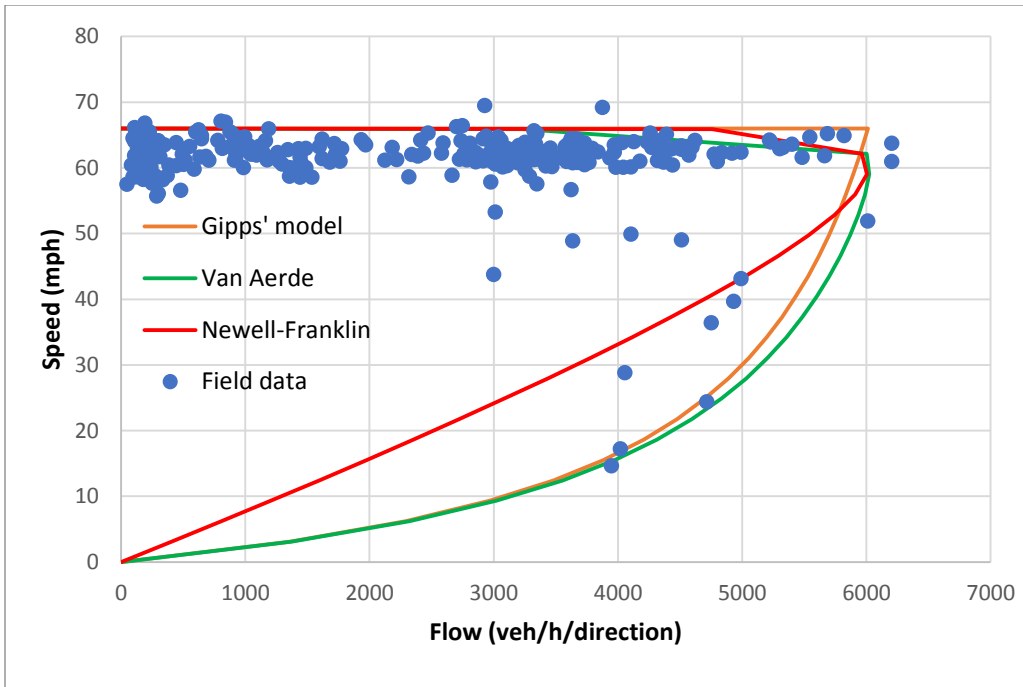


Non-work zone day

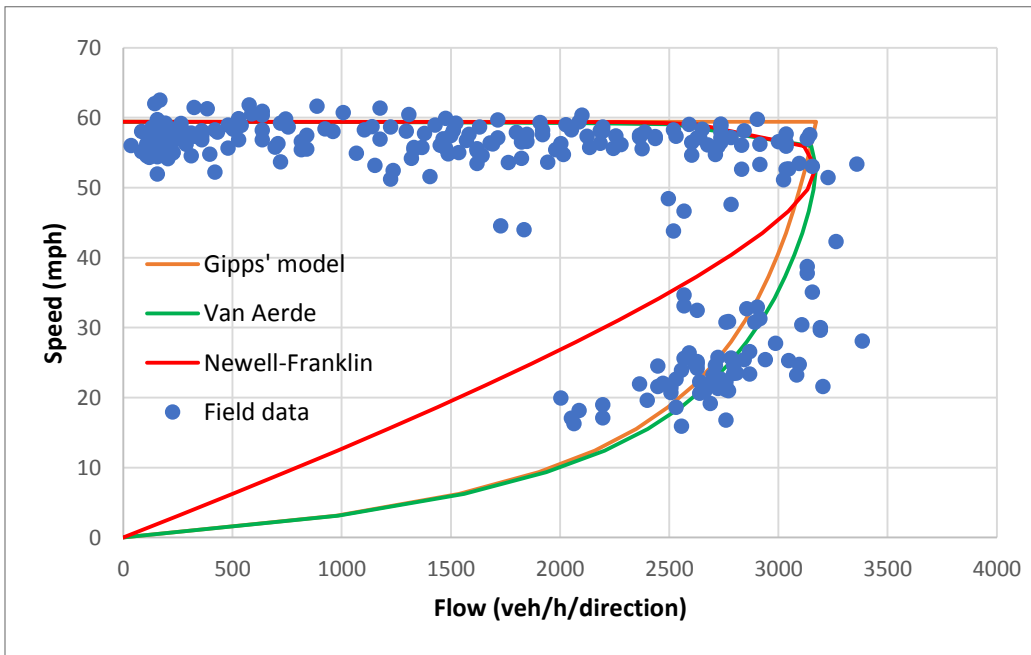


Work zone day

**Figure 5.2.1. Fitting traffic stream models for Eastbound I-64 at Boone Bridge (restriping, 3,2)**

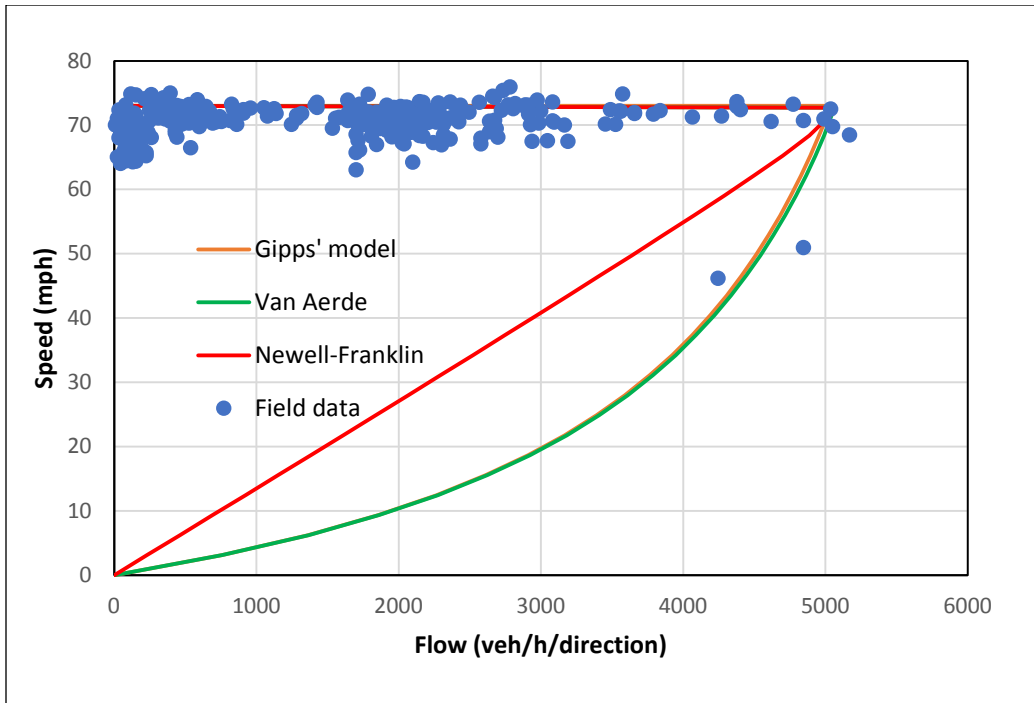


Non-work zone day

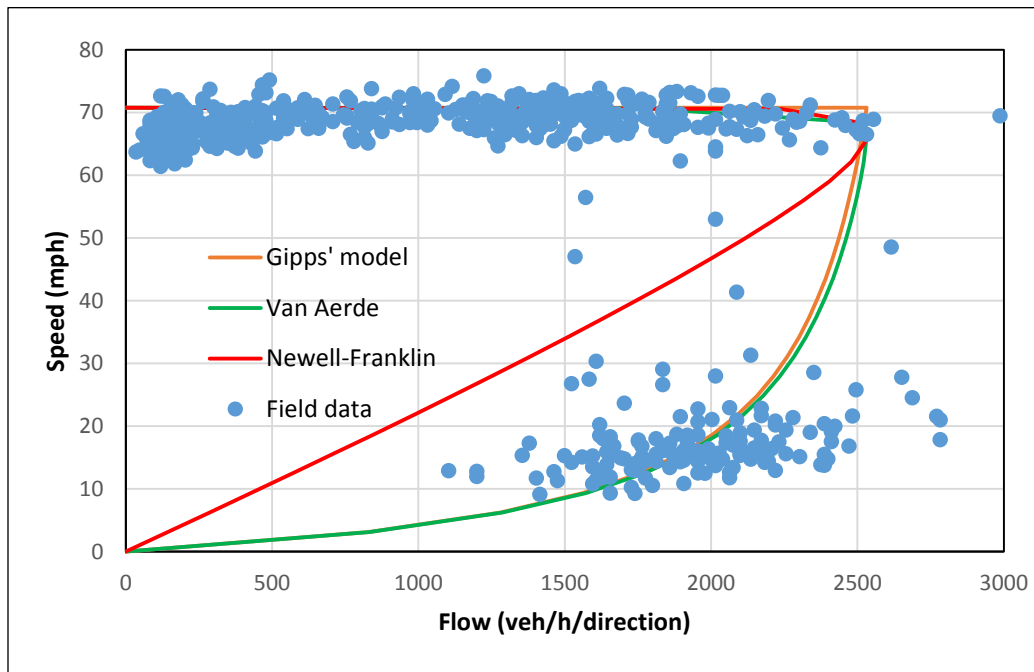


Work zone day

**Figure 5.2.2. Fitting traffic stream models for Eastbound I-64 at Boone Bridge (bridge work, 3,2)**

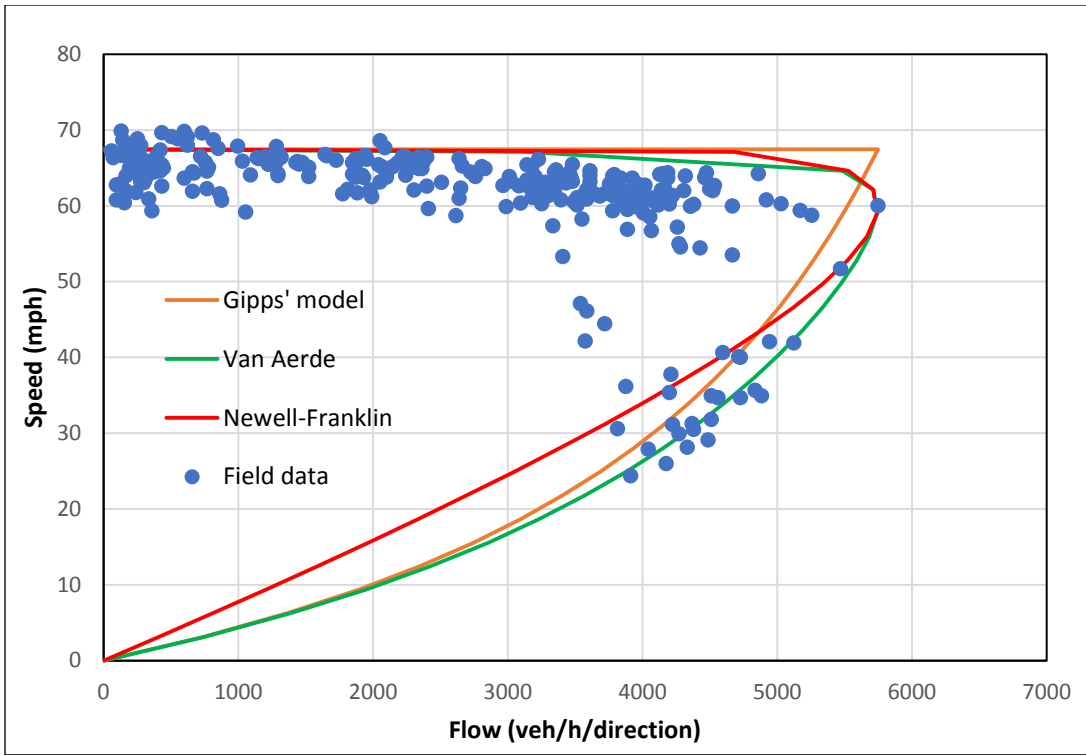


Non-work zone day

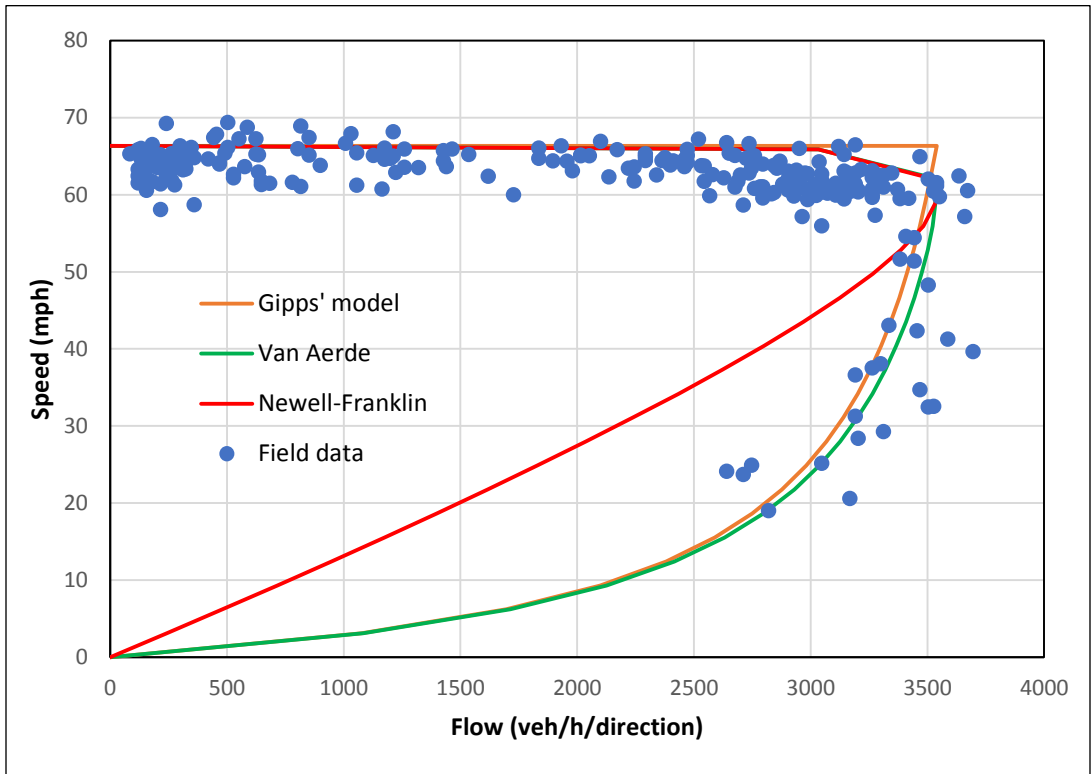


Work zone day

**Figure 5.2.3. Fitting traffic stream models for Westbound I-64 at Boone Bridge (bridge demolition preparation, 3,2)**

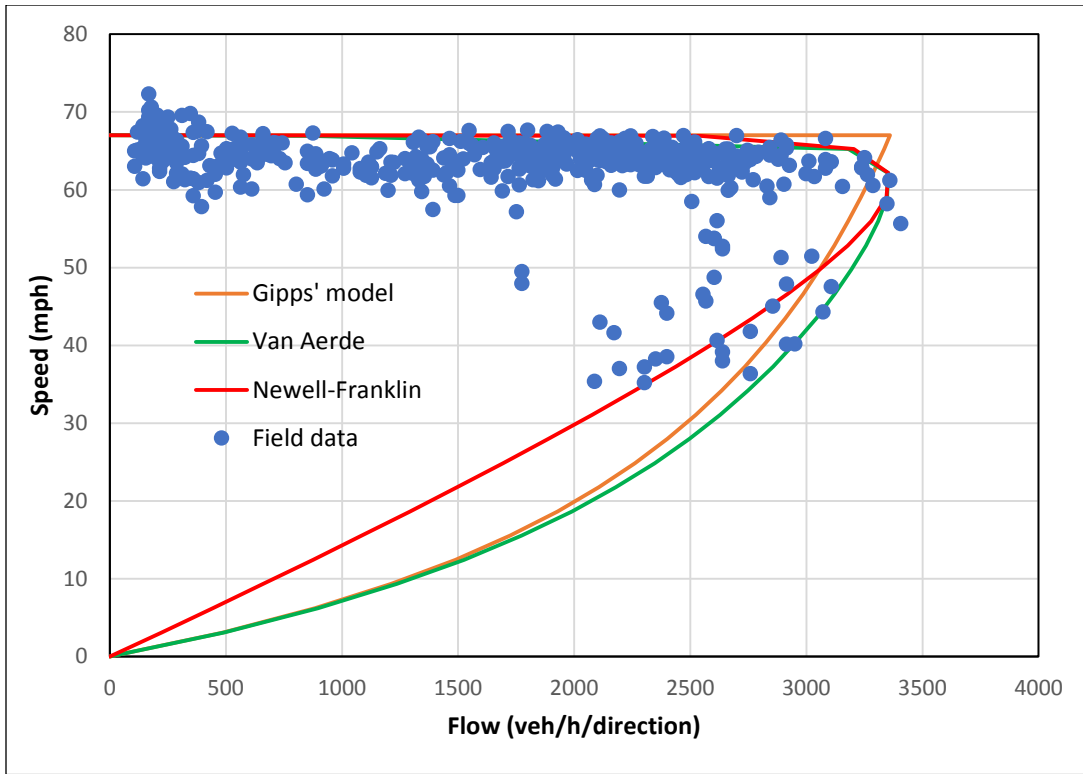


Non-work zone day

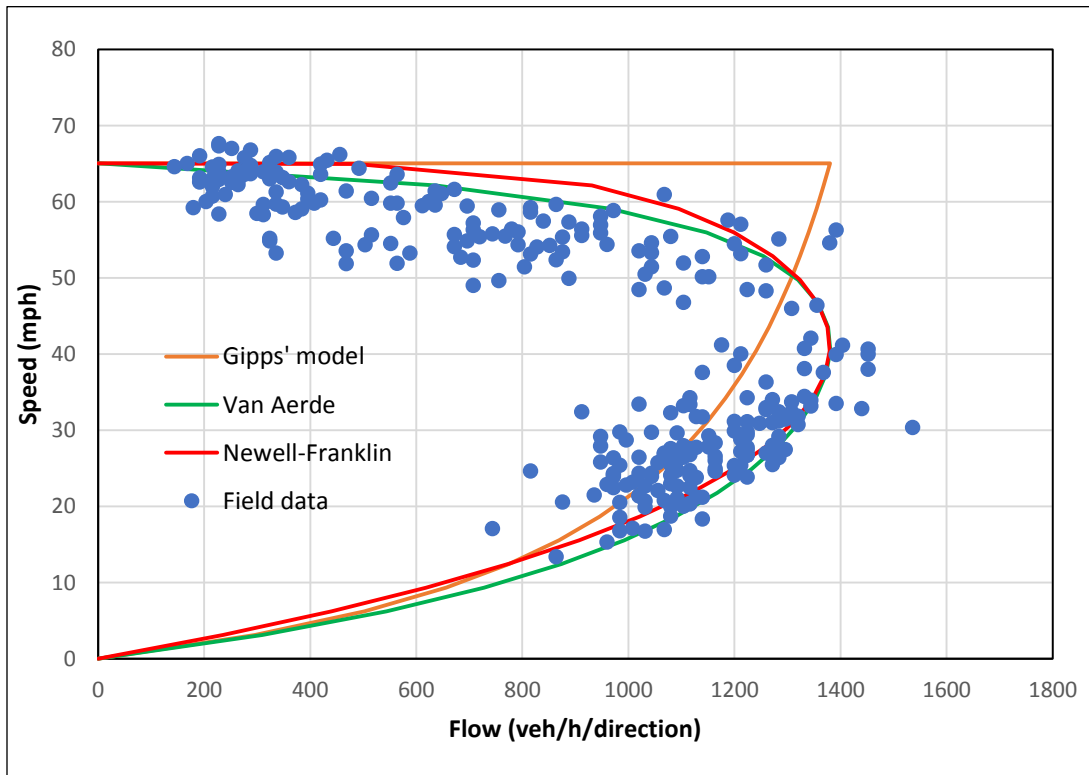


Work zone day

**Figure 5.2.4. Fitting traffic stream models for Eastbound I-64 from Chesterfield Parkway to I-270 (paving operations, 3,2)**

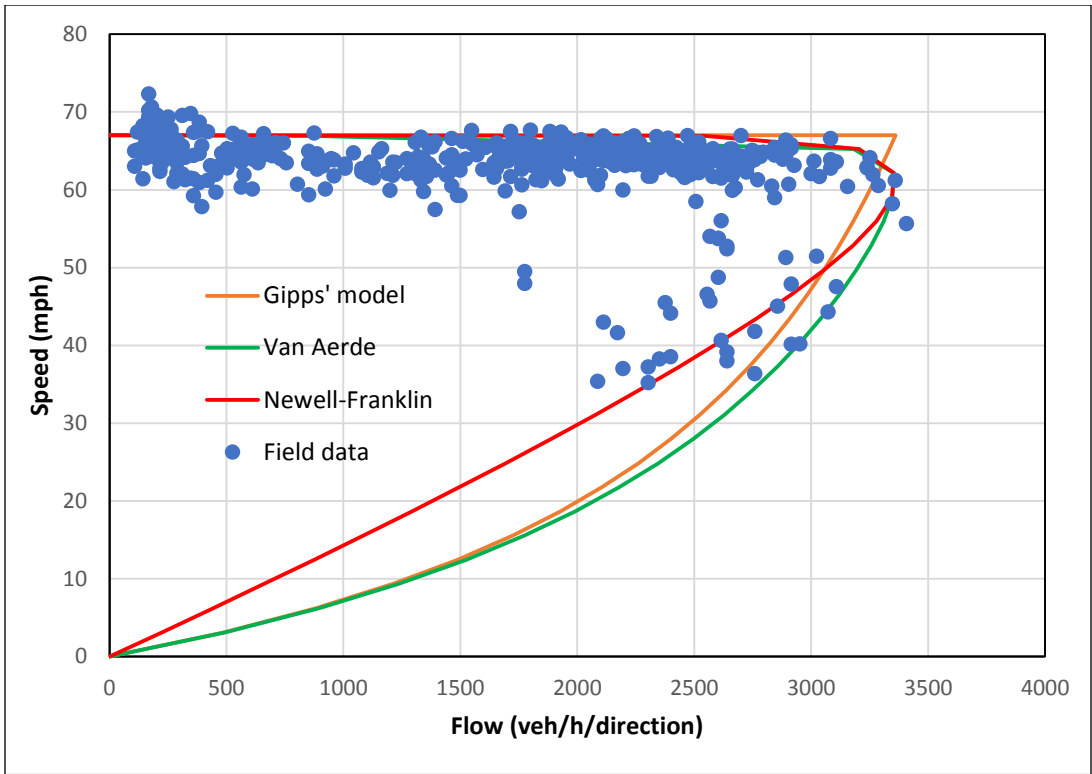


Non-work zone day

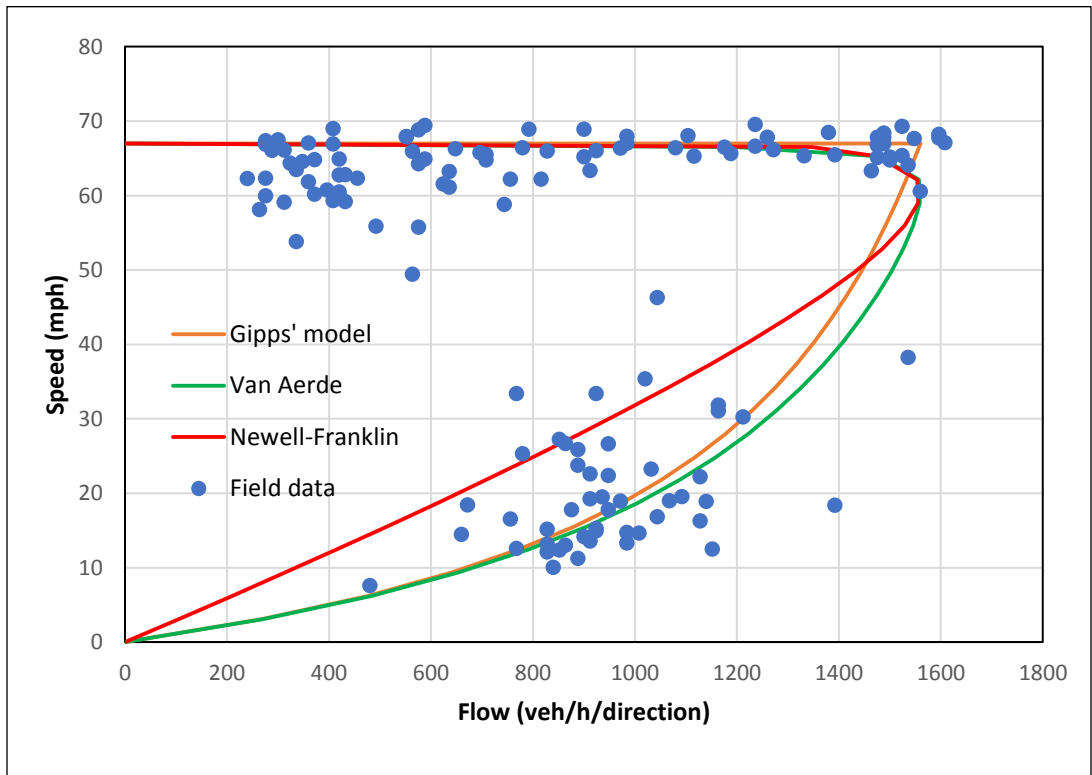


Work zone day

**Figure 5.2.5. Fitting traffic stream models for Eastbound I-70 at Foristell (pavement repair, 2,1)**

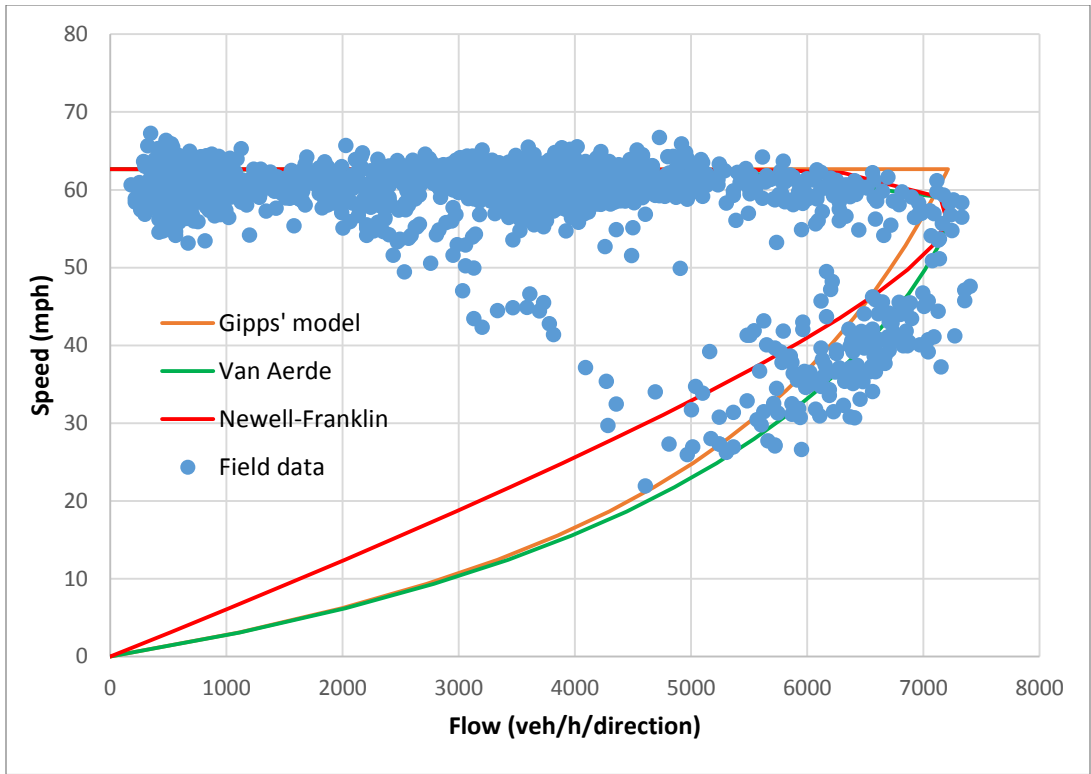


Non-work zone day

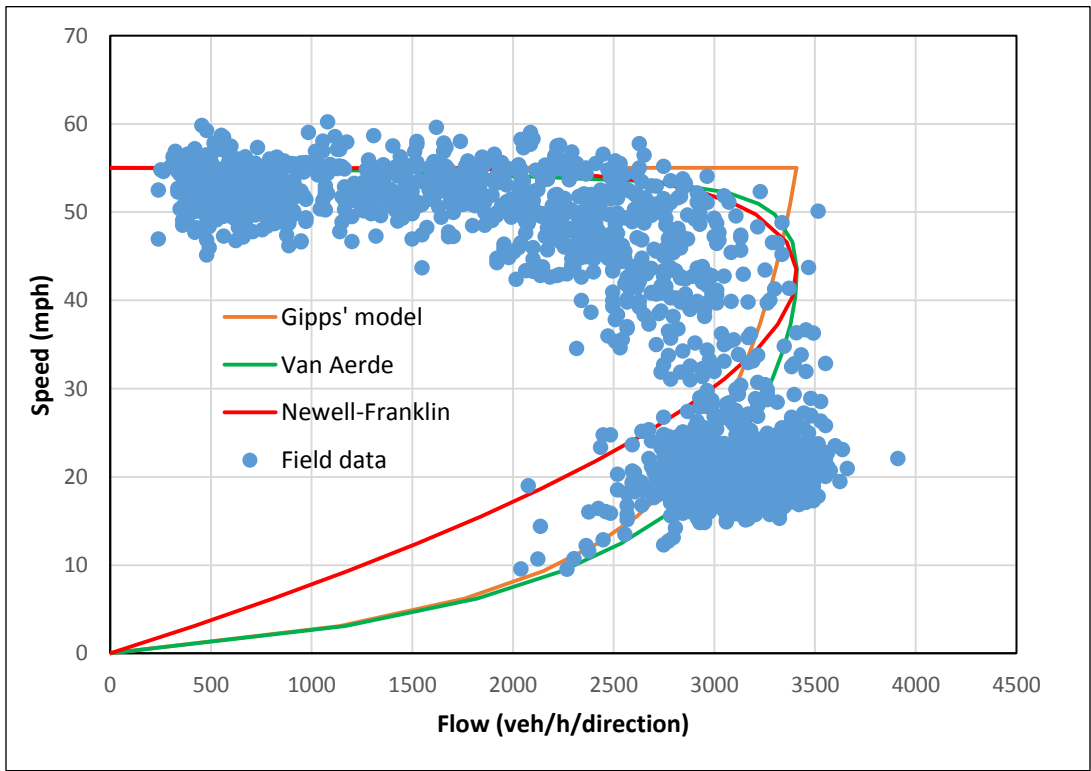


Work zone day

**Figure 5.2.6. Fitting traffic stream models for Westbound I-70 at Foristell (paving operations, 2,1)**

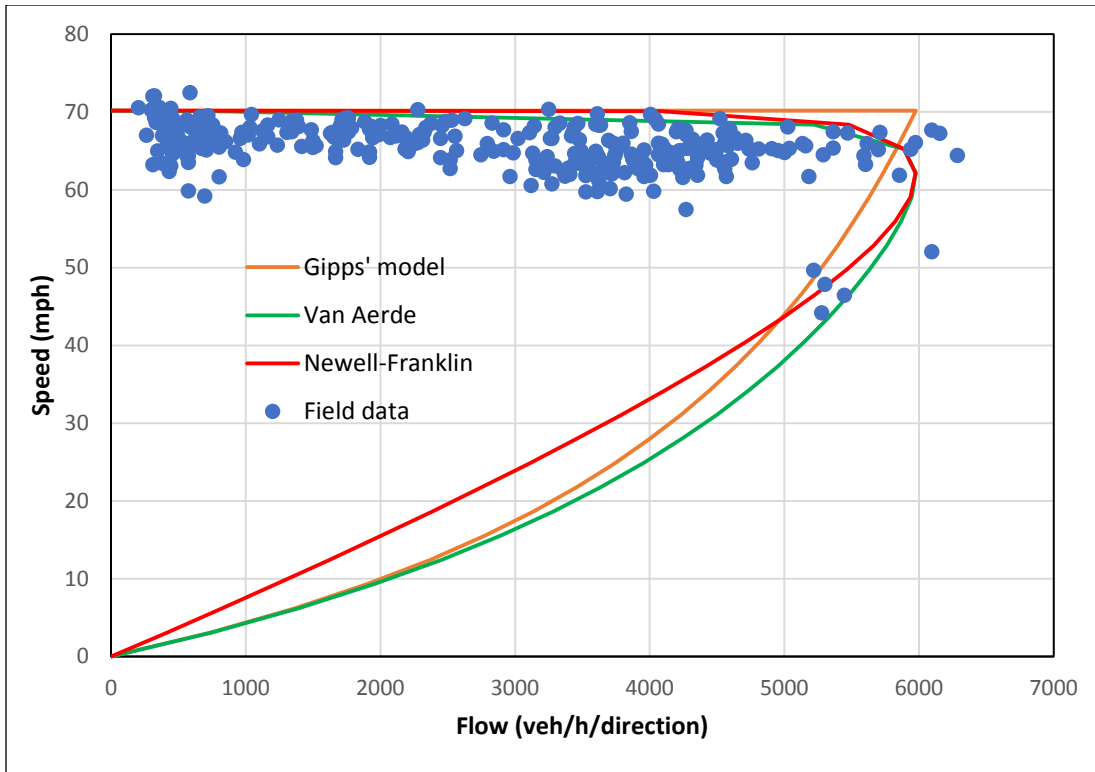


Non-work zone day

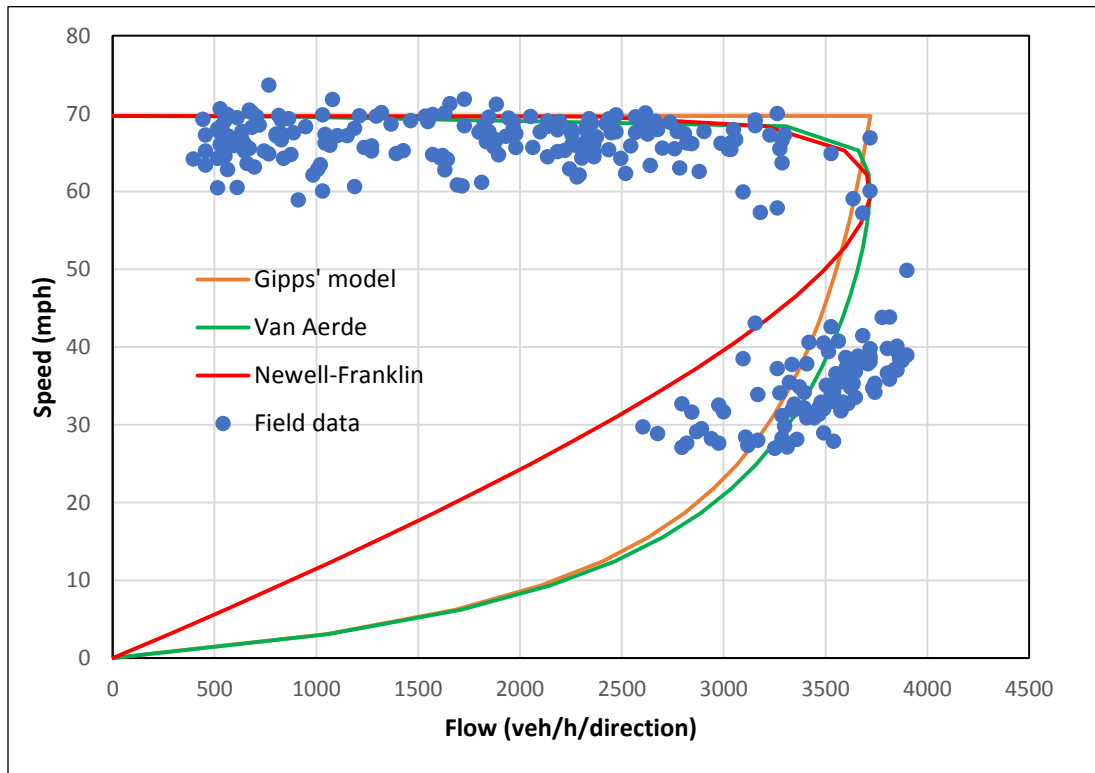


Work zone day

**Figure 5.2.7. Fitting traffic stream models for Eastbound I-270 from McDonnell Boulevard to Route 367 (bridge work, 4,2)**

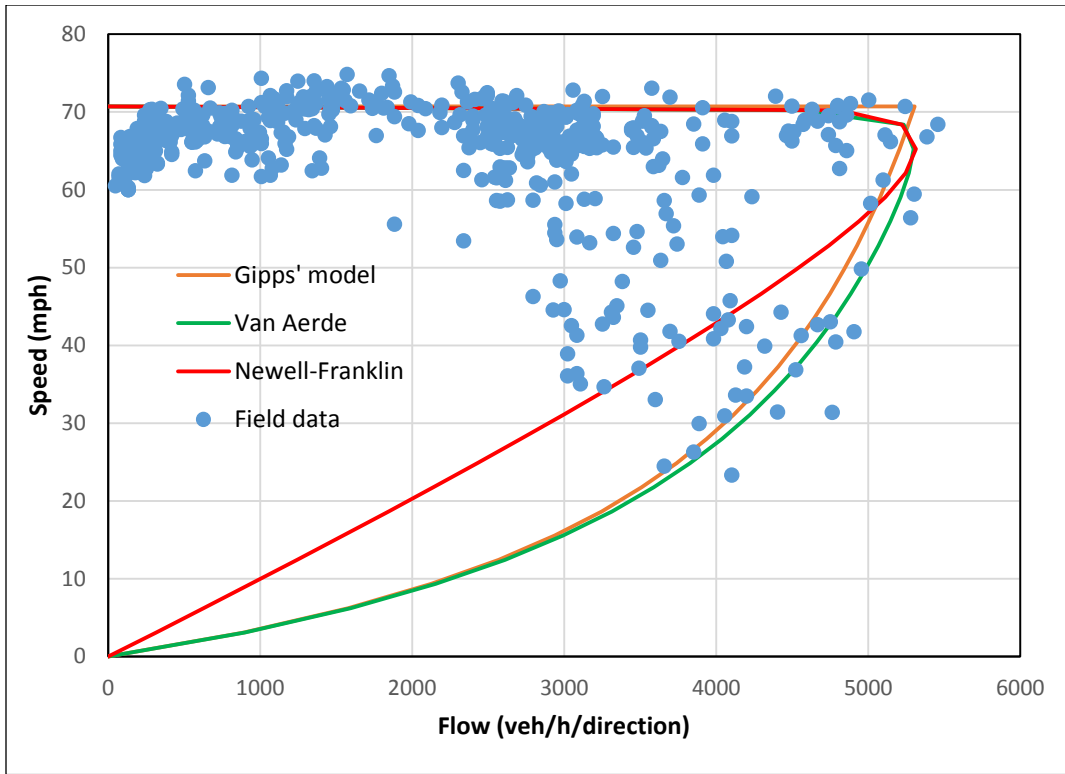


Non-work zone day

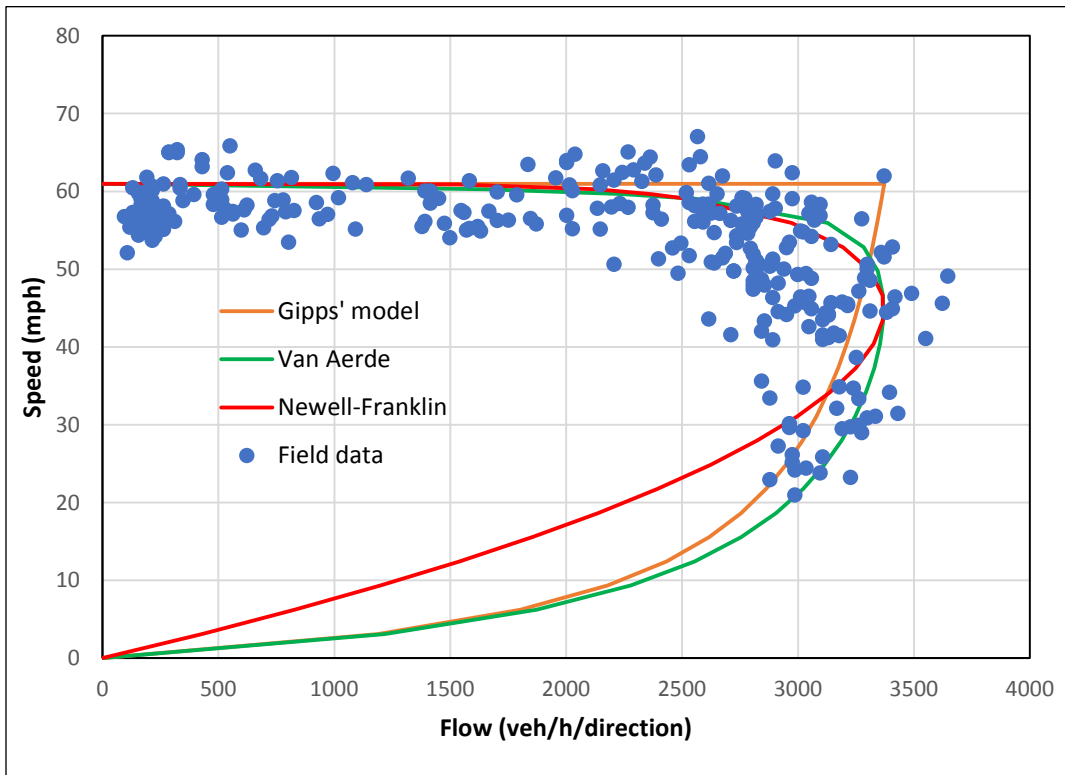


Work zone day

**Figure 5.2.8. Fitting traffic stream models for Westbound I-270 from I-170 to Route 367 (pavement work, 3,2)**

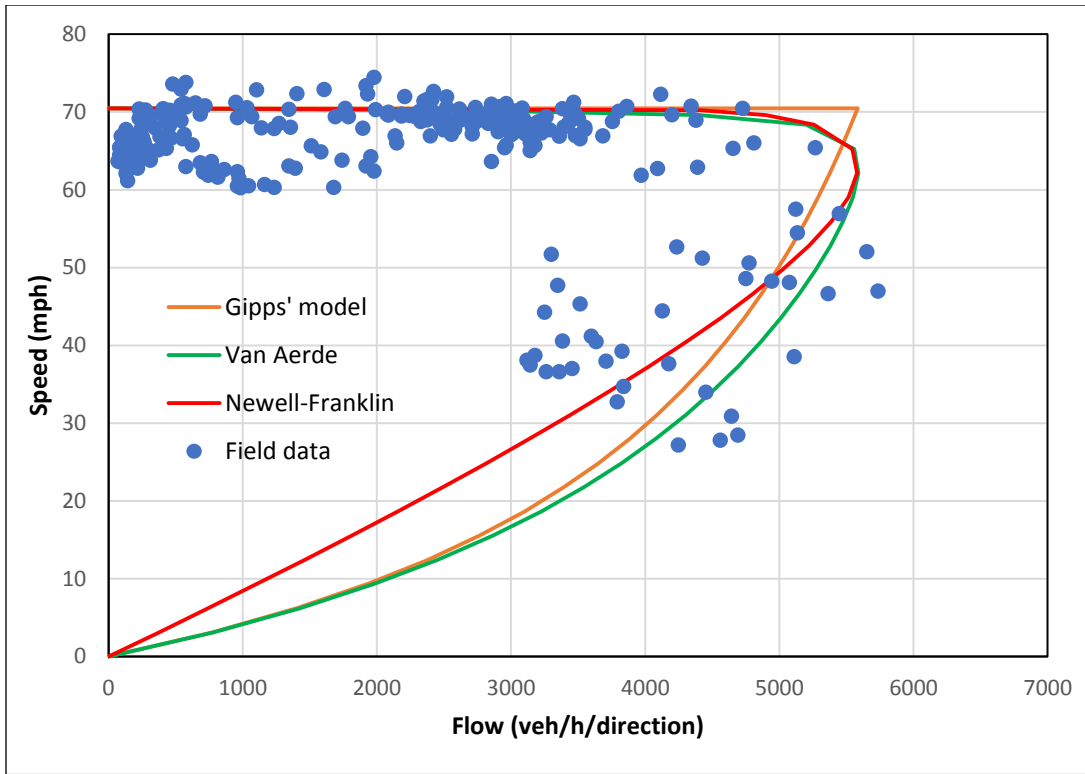


Non-work zone day

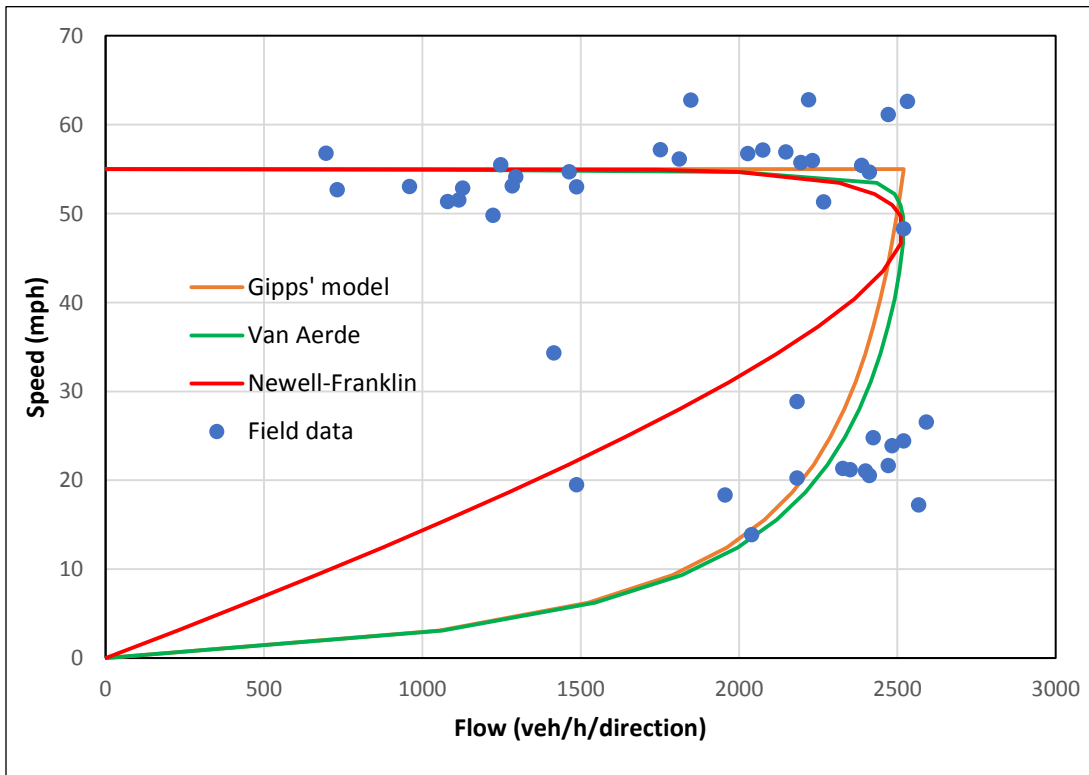


Work zone day

**Figure 5.2.9. Fitting traffic stream models for Eastbound I-44 at I-270 (Meramec Bridge) (bridge work, 3,2)**

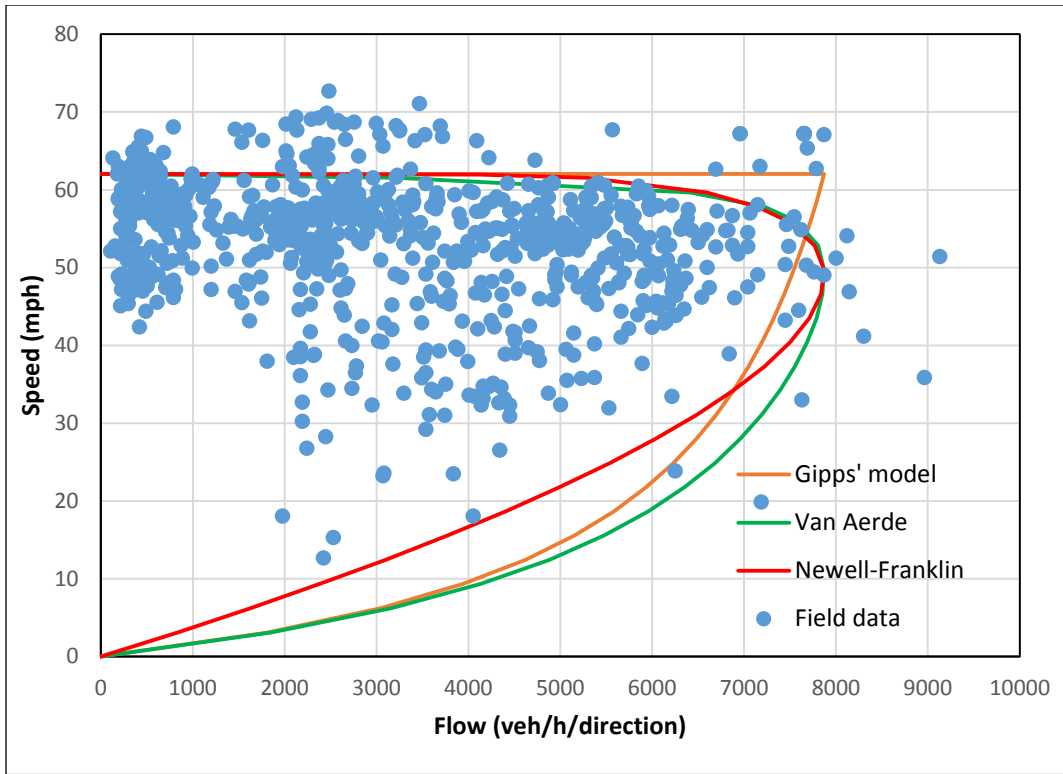


Non-work zone day

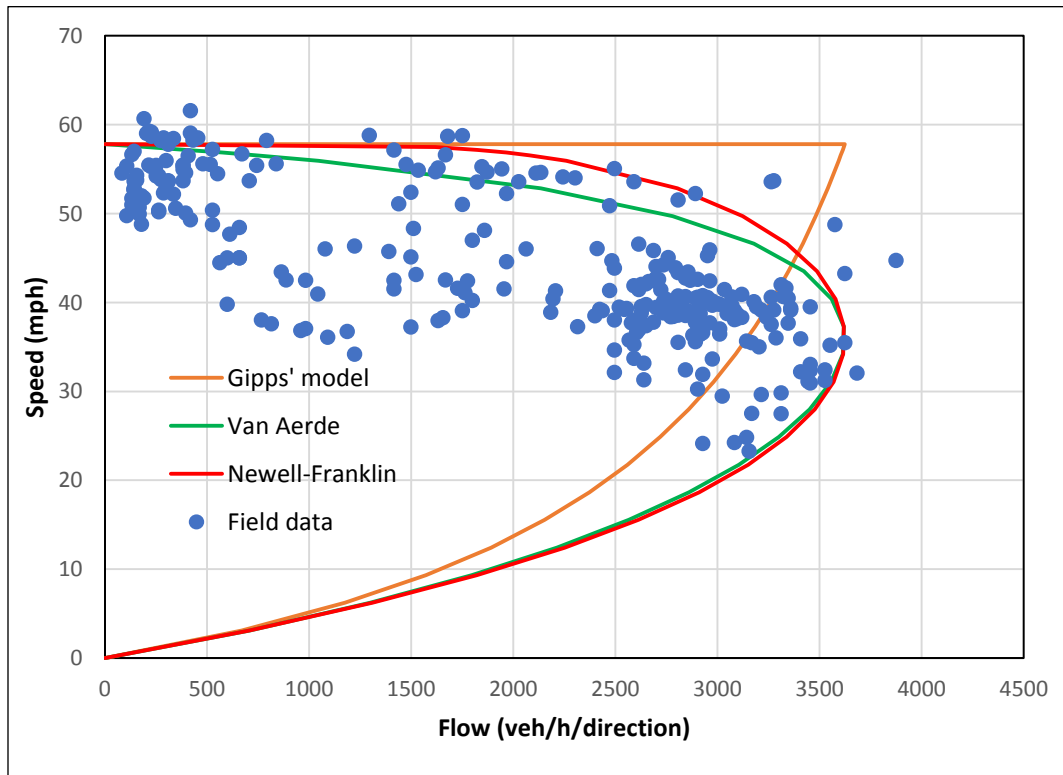


Work zone day

**Figure 5.2.10 Fitting traffic stream models for Westbound I-44 (resurfacing, 3,2)**



Non-work zone day



Work zone day

**Figure 5.2.11. Fitting traffic stream models for Eastbound I-44 at Hampton (bridge rehabilitation, 4,2)**

### *5.1.2. Goodness of Fit Test*

To determine the model with the best fit from among the three selected traffic stream models, a goodness of fit test was performed. Goodness of fit statistics, as summarized in Table 5.1, showed that the Van Aerde model is the best fit model for most of the study locations (MAPE < 20% for all locations). The Gipps and Newell-Franklin models fit well for a few locations but fit poorly in other locations. The Gipps model provides a reasonable fit for locations where the traffic stream speed is not sensitive to flow in the uncongested regime, whereas the Newell-Franklin model provides a good fit for locations where the traffic stream speed is sensitive to flow in uncongested regimes. Since the Van Aerde model fits well with the field data for all traffic scenarios, all speed-flow plots developed with the Van Aerde model were analyzed further.

**Table 5.1. Goodness of fit statistics**

Location	Traffic Characteristics			RMSE and MAPE			
	Capacity, veh/h/direction (lane wise in parenthesis, vphpl)	FFS (mph)	Speed at Capacity (mph)	K <sub>j</sub> , veh/mile/ direction	Van Aerde	Gipps	Newell- Franklin
Eastbound I-64 at Boone Bridge (work: restriping)	3,414 (1,707)	65.5	57.53	280 (140)	5.02213 (7.85%)	6.725286 (9.03%)	7.401302 (12.26%)
Eastbound I-64 at Boone Bridge (work: bridge work)	3,172 (1,586)	59.42	53	430 (215)	4.721195 (9.25%)	5.713379 (10.83%)	10.03836 (21.19%)
Westbound I-64 at Boone Bridge (work: bridge demolition preparation)	2,532 (1,266)	70.75	66.50	380 (190)	6.686216 (15.65%)	6.812487 (16.46%)	21.13868 (60.84%)
Eastbound I-64 from Chesterfield Parkway to I-270 (work: paving operations)	3,540 (1,770)	66.32	60	475 (238)	4.436011 (6.41%)	5.456148 (7.32%)	8.770458 (10.65%)
Eastbound I-70 at Foristell (work: pavement repair)	1,380 (1,380)	65	41	115 (115)	7.143565 (14.69%)	9.095556 (19.64%)	6.469169 (12.25%)
Westbound I-70 at Foristell (work: paving operations)	1,560 (1,560)	67	60.5	100 (100)	7.736523 (15.12%)	6.614910 (14.21%)	9.649916 (29.42%)
Eastbound I-270 from McDonnell Boulevard to Route 367 (work: bridge work)	3,408 (1,704)	55	43	520 (260)	6.745994 (19.23%)	10.76114 (33.21%)	9.795803 (34.56%)
Westbound I-270 from I-170 to 367 (work: pavement work)	3,720 (1,860)	69.68	60.04	450 (225)	6.168564 (10.36%)	8.794558 (14.42%)	8.913963 (16.09%)
Eastbound I-44 at I-270 (Meramec Bridge) (work: bridge work)	3,372 (1,686)	61	45	560 (280)	7.40334 (10.85%)	7.841082 (13.03%)	7.0456 (10.56%)
Westbound I-44 (work: resurfacing)	2,520 (1,260)	55	48.276	550 (275)	8.534911 (19.01%)	9.644866 (22.87%)	11.36845 (30.95%)
Eastbound I-44 at Hampton (work: bridge rehabilitation)	3,624 (1,812)	57.80	36	250 (125)	9.874358 (19.66%)	13.72484 (29.70%)	10.1343 (20.19%)

### 5.1.3 Comparison of Work Zone and Non-Work Zone Day Speed-Flow Plot

Reductions in capacity and free-flow speed from normal conditions due to different activities in work zones were estimated by comparing corresponding speed-flow curves. Work zone day and non-work zone day plots were developed by direction while considering all lanes together. The work zone and non-work zone day plots cannot be compared directly because the work zone plot accounts for reductions in capacity due to lane closure. For comparison purposes, the speed-flow plots by direction were scaled down to plots by lane by dividing all flow values by the corresponding number of lanes. The comparisons of normal day to work zone day speed-flow curves are illustrated in Figures 5.3.1 to 5.3.11.

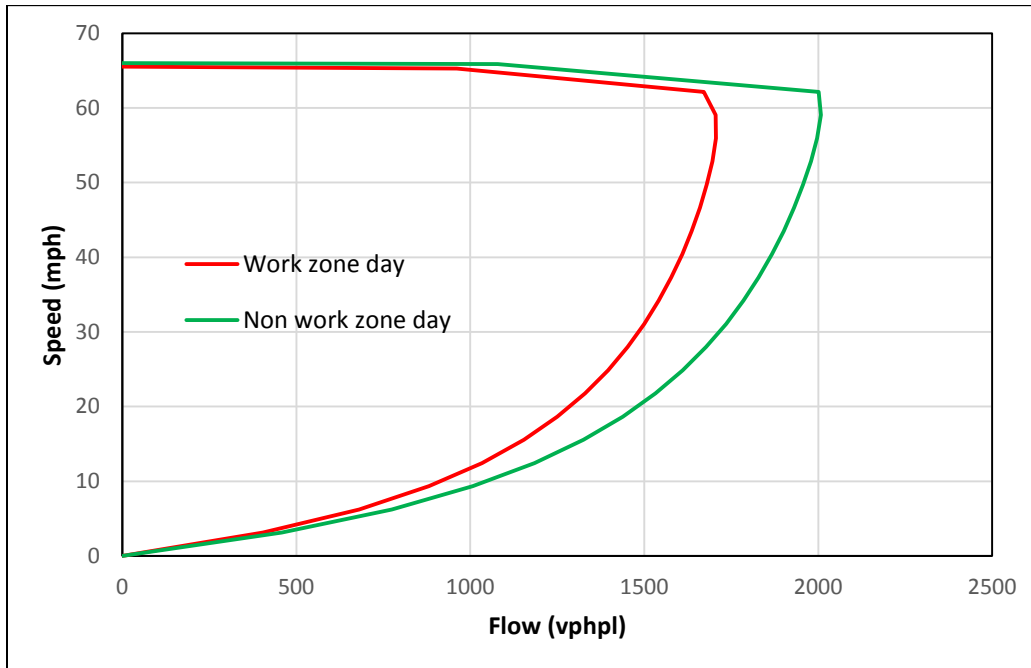


**Figure 5.3.1. Comparison of work zone versus non-work zone day speed-flow plots for Eastbound I-64 at Boone Bridge (restriping, 3,2)**

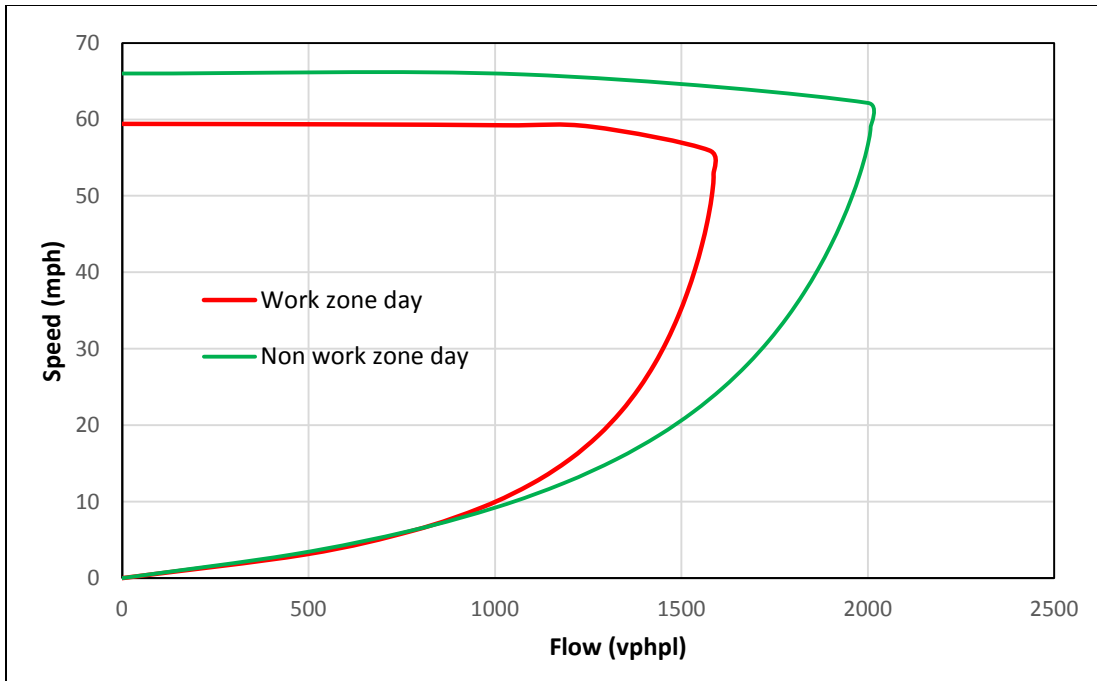


**Figure 5.3.2. Comparison of work zone versus non-work zone day speed-flow plots for Eastbound I-64 at Boone Bridge (bridge work, 3,2)**

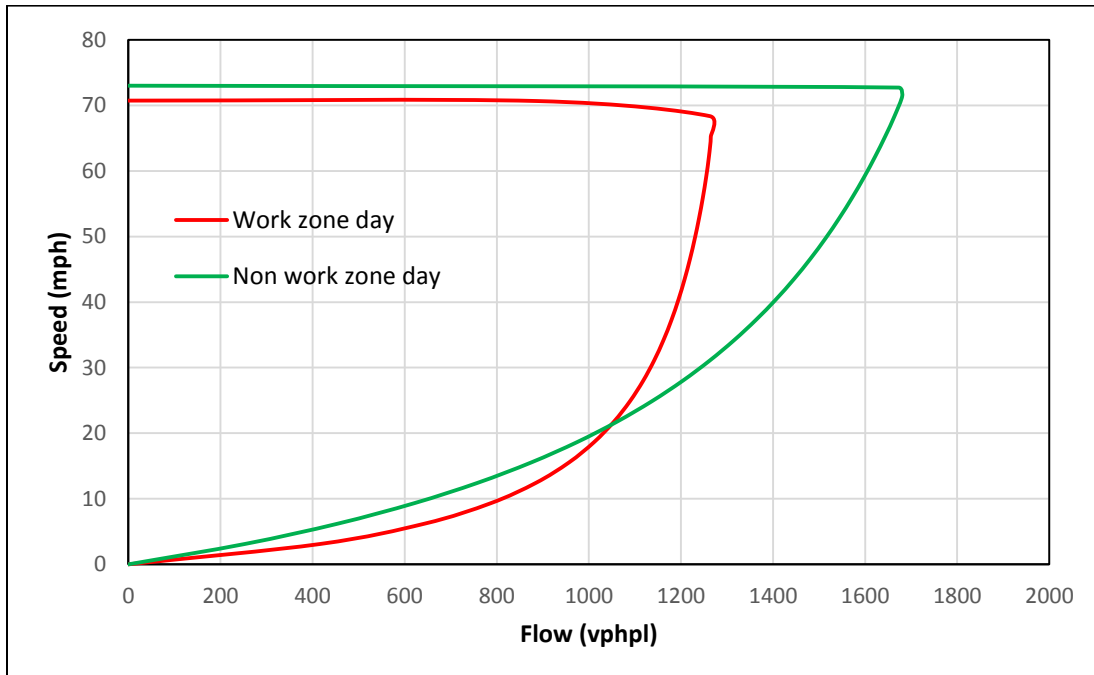


**Figure 5.3.3. Comparison of work zone versus non-work zone day speed-flow plots for Westbound I-64 at Boone Bridge (bridge demolition preparation, 3,2)**

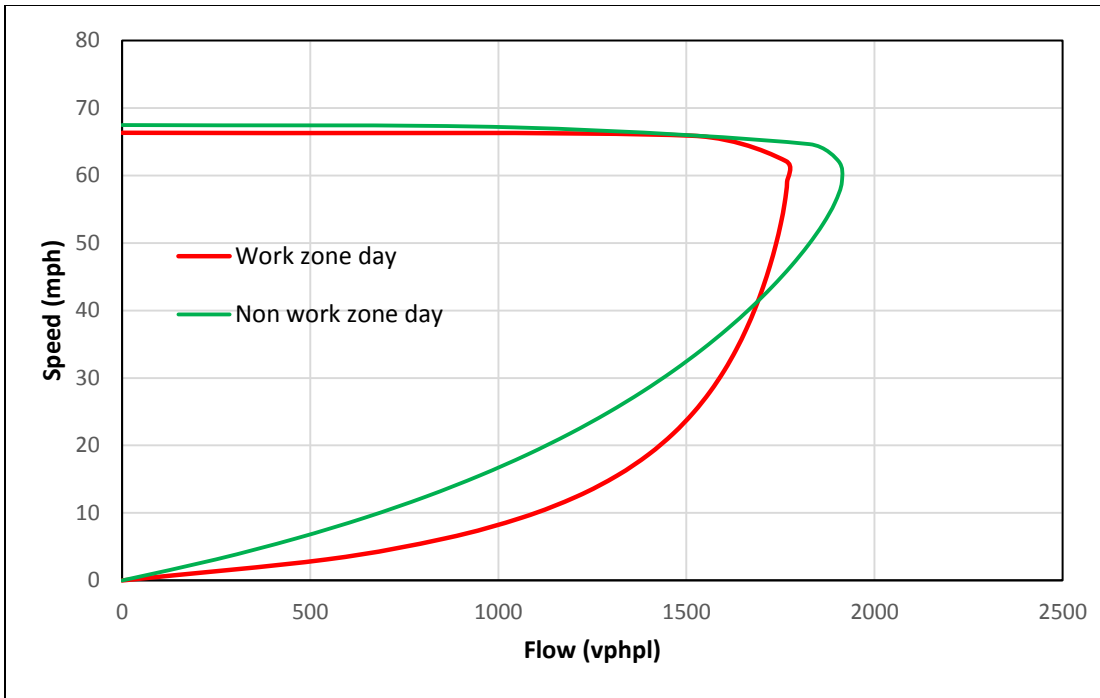


**Figure 5.3.4. Comparison of work zone versus non-work zone day speed-flow plots for Eastbound I-64 from Chesterfield Parkway to I-270 (paving operations, 3,2)**

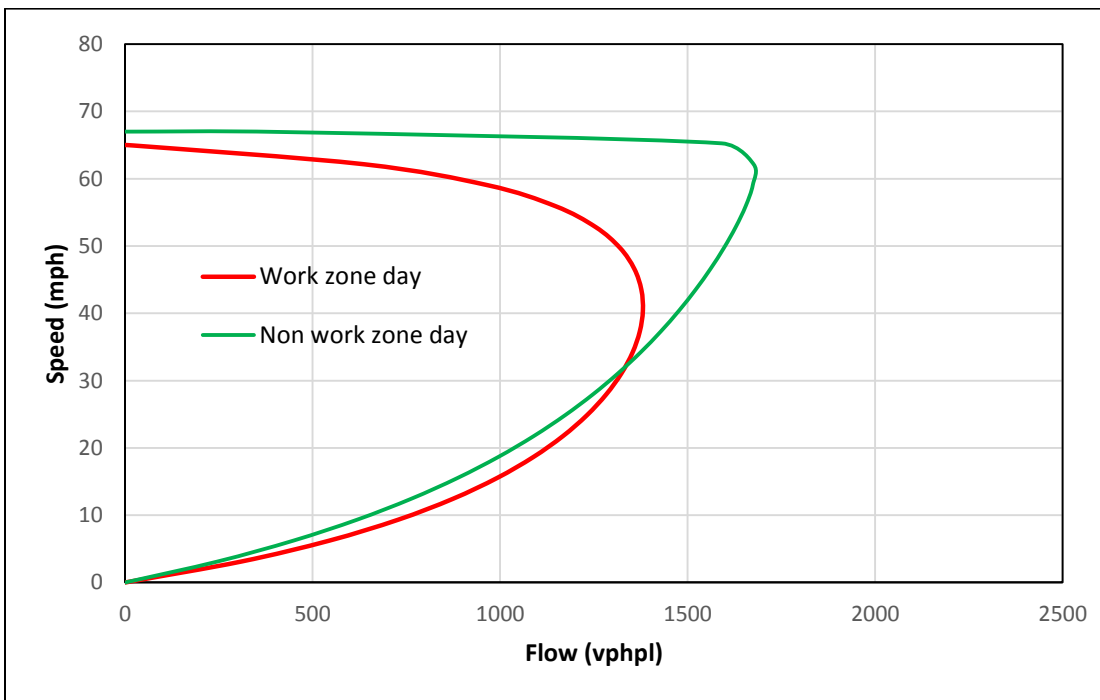


**Figure 5.3.5. Comparison of work zone versus non-work zone day speed-flow plots for Eastbound I-70 at Foristell (pavement repair, 2,1)**

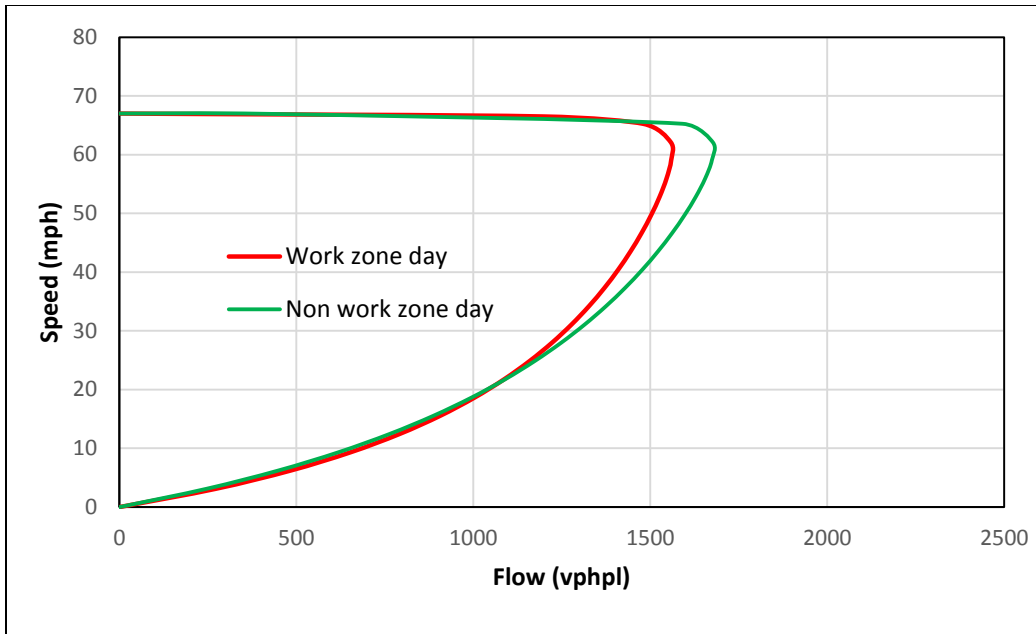


**Figure 5.3.6. Comparison of work zone versus non-work zone day speed-flow plots for Westbound I-70 at Foristell (paving operations, 2,1)**

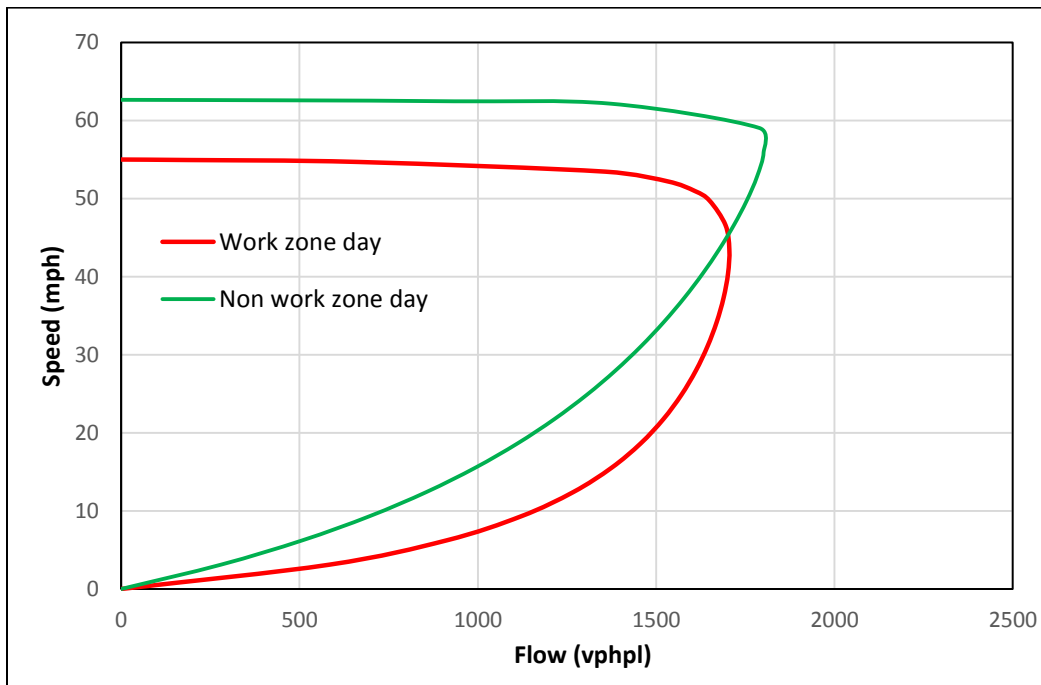


**Figure 5.3.7. Comparison of work zone versus non-work zone day speed-flow plots for Eastbound I-270 from McDonnell Boulevard to Route 36 (bridge work, 4,2)**

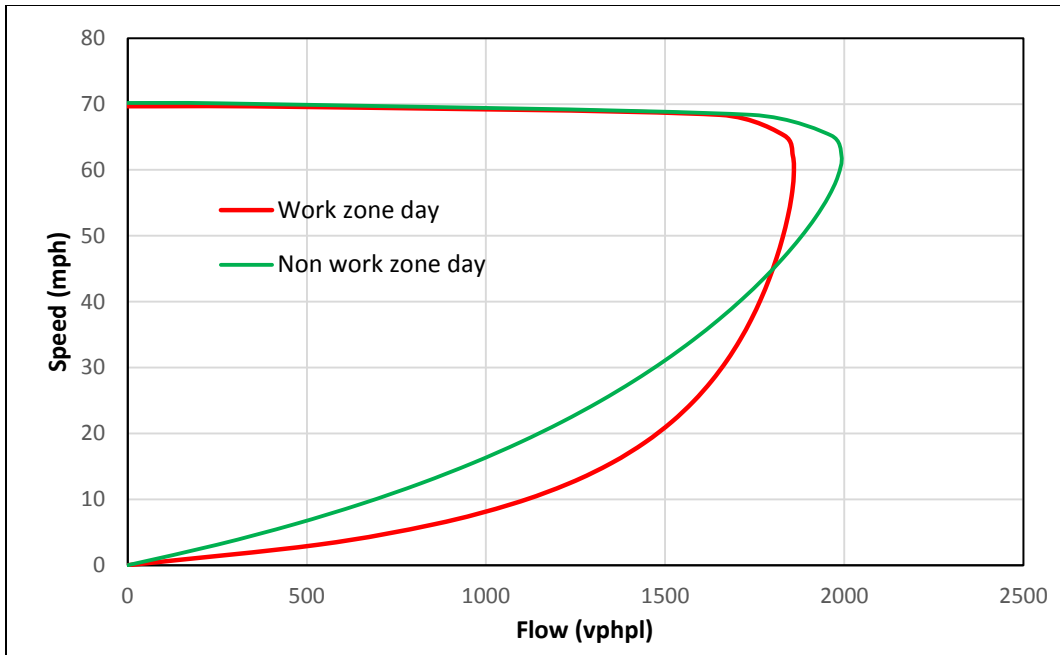


**Figure 5.3.8. Comparison of work zone versus non-work zone day speed-flow plots for Westbound I-270 from I-170 to 367 (pavement work, 3,2)**

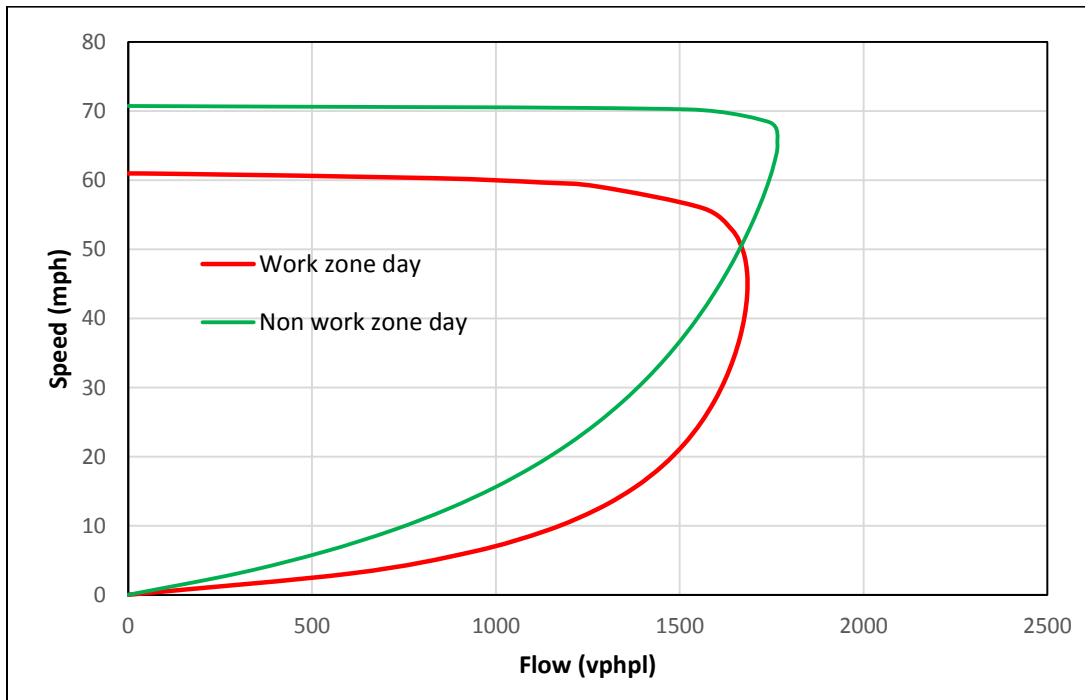


**Figure 5.3.9. Comparison of work zone versus non-work zone day speed-flow plots for Eastbound I-44 at I-270 (Meramec Bridge) (bridge work, 3,2)**

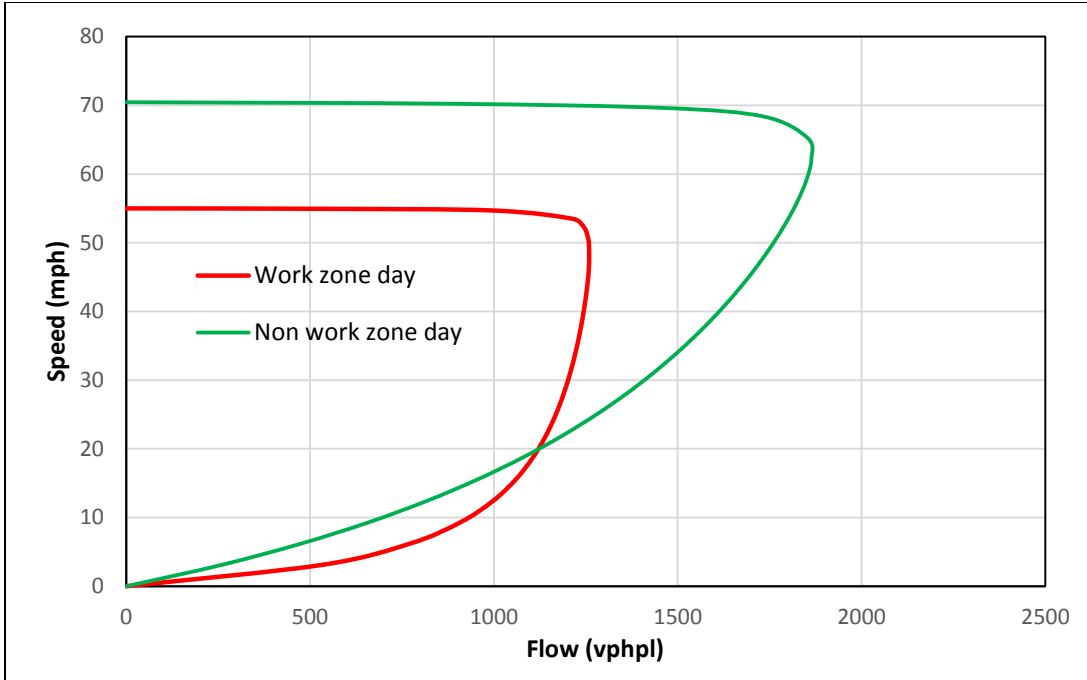


**Figure 5.3.10. Comparison of work zone versus non-work zone day speed-flow plots for Westbound I-44 (resurfacing, 3,2)**

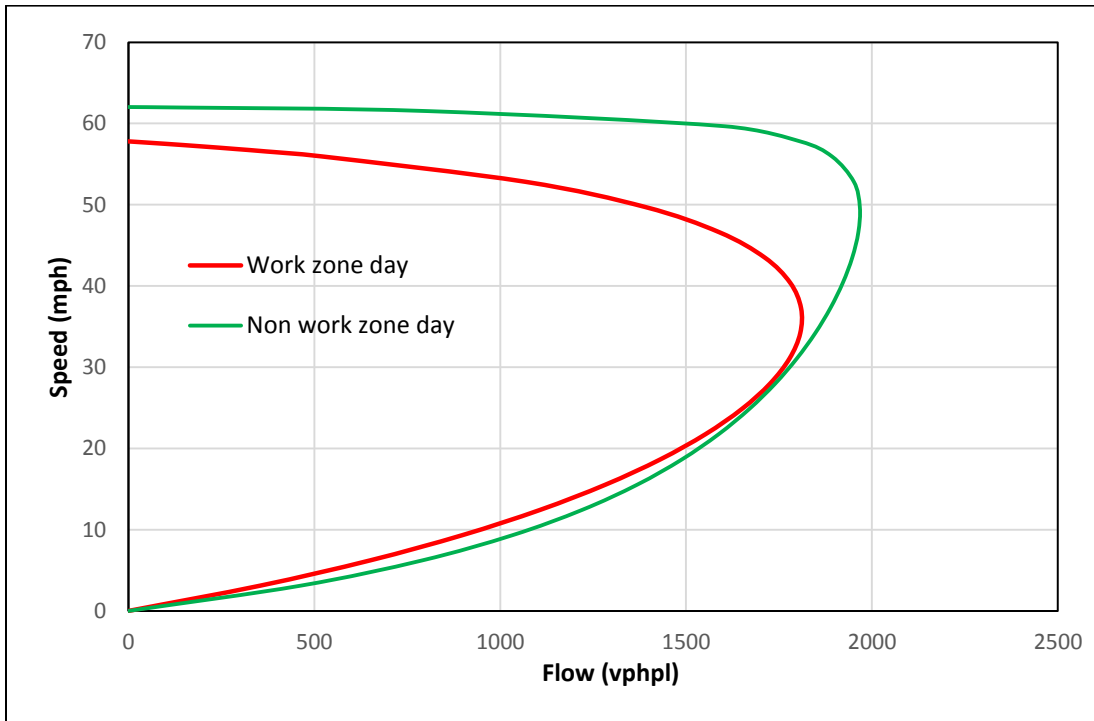


**Figure 5.3.11. Comparison of work zone versus non-work zone day speed-flow plots for Eastbound I-44 at Hampton (bridge rehabilitation, 4,2)**

Figures 5.3.1 to 5.3.11 show that work zone activities have an adverse effect on capacity and free-flow speed. The reduction in free-flow speed and capacity can be estimated from the figures to quantify the impact of work zone activities. The results are summarized in Table 5.2.

**Table 5.2. Capacity and free-flow speed reduction factors**

Locations (1)	Closure configuration (2)	Work zone day			Non-work zone day			Capacity reduction factor (9 = 4/7) (9)	FFS reduction factor (10 = 5/8) (10)
		Capacity (vph)			Capacity (vph)				
		Directional (all lanes) (3)	Lane wise (all lanes/no. of lanes) (4)	FFS (mph) (5)	Directional (all lanes) (6)	Lane wise (all lanes/no. of lanes) (7)	FFS (mph) (8)		
Eastbound I-64 at Boone Bridge (work: restriping)	(3,2)	3414	1707	65.5	6012	2004	66	0.85	0.99
Eastbound I-64 at Boone Bridge (work: bridge work)	(3,2)	3172	1586	59.42	6012	2004	66	0.79	0.90
Westbound I-64 at Boone Bridge (work: bridge demolition preparation)	(3,2)	2532	1266	70.75	5040	1680	73	0.75	0.97
Eastbound I-64 from Chesterfield Parkway to I- 270 (work: paving operations)	(3,2)	3540	1770	66.32	5748	1916	67.46	0.92	0.98
Eastbound I-70 at Foristell (work: pavement repair)	(2,1)	1380	1380	65	3360	1680	67	0.82	0.97
Westbound I-70 at Foristell (work: paving operations)	(2,1)	1560	1560	67	3360	1680	67	0.93	1.00
Eastbound I-270 from McDonnell Boulevard to Route 367(work: bridge work)	(4,2)	3408	1704	55	7212	1803	62.67	0.95	0.88
Westbound I-270 from I-170 to 367 (work: pavement work)	(3,2)	3720	1860	69.68	5976	1992	70.16	0.93	0.99
Eastbound I-44 at I-270 (Meramec Bridge) (work: bridge work)	(3,2)	3372	1686	61	5304	1768	70.7	0.95	0.86
Westbound I-44 (work: resurfacing)	(3,2)	2520	1260	55	5584	1861	70.45	0.68	0.78
Eastbound I-44 at Hampton (work: bridge rehabilitation)	(4,2)	3624	1812	57.80	7872	1968	62.03	0.92	0.93

## 5.2. Speed-Flow Relationship by Lane

The lane adjacent to the work activity was considered for the development of speed-flow curves. The developed plots for selected work zone locations are illustrated in Figures 5.4.1. to 5.4.11.

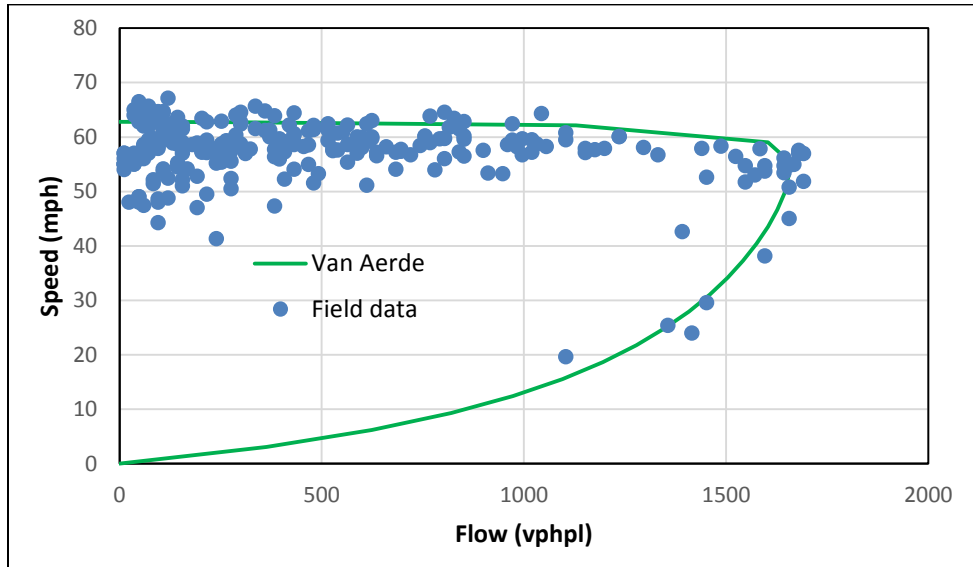


Figure 5.4.1. Speed-flow plot for Eastbound I-64 at Boone Bridge (restriping, 3,2)

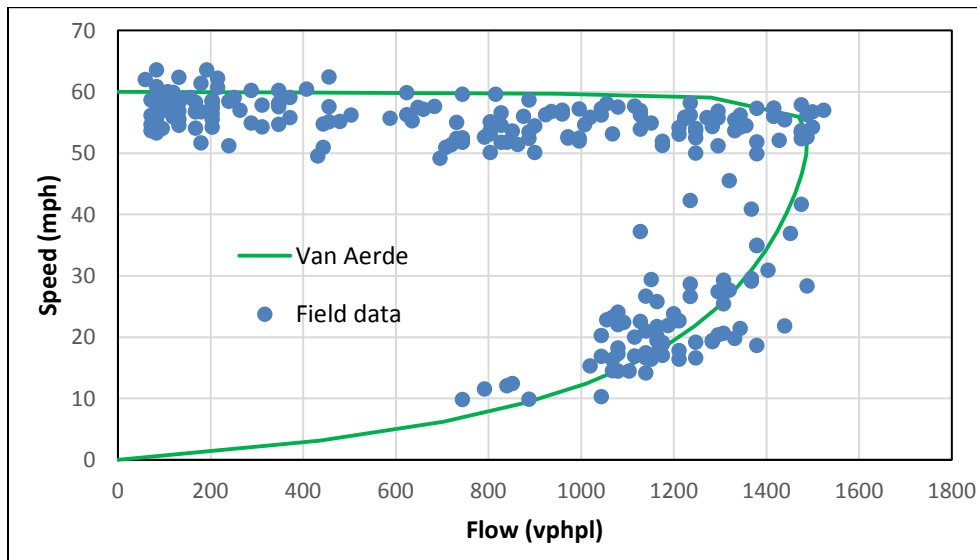
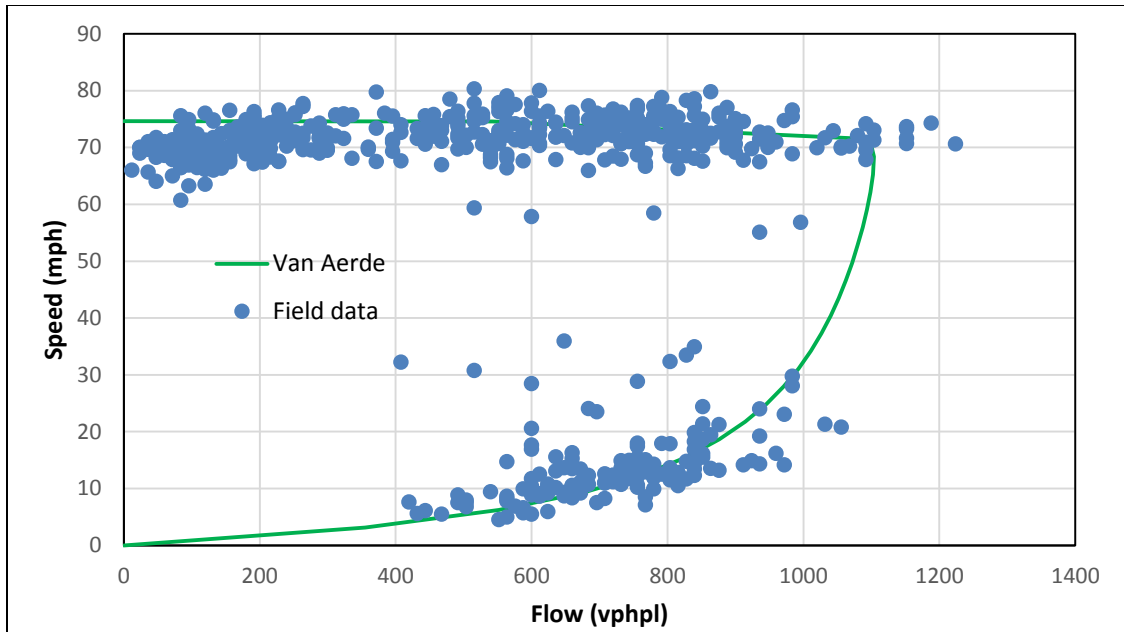
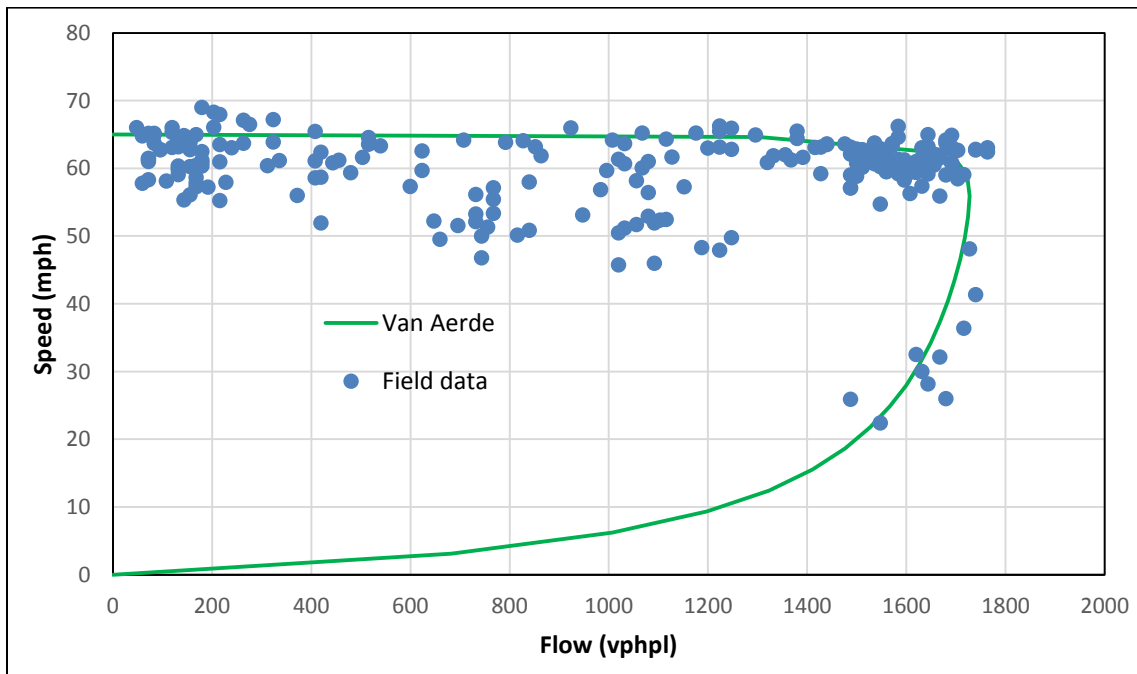


Figure 5.4.2. Speed-flow plot for Eastbound I-64 at Boone Bridge (bridge work, 3,2)



**Figure 5.4.3. Speed-flow plot for Westbound I-64 at Boone Bridge (bridge demolition preparation, 3,2)**



**Figure 5.4.4. Speed-flow plot for Eastbound I-64 from Chesterfield Parkway to I-270 (paving operations, 3,2)**

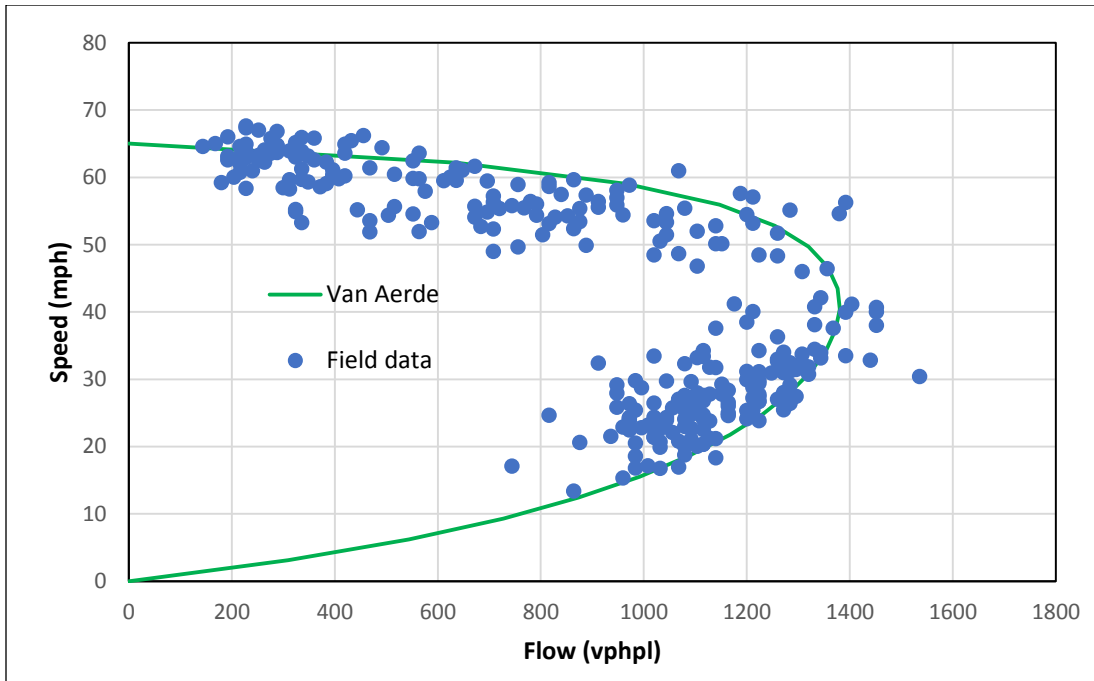


Figure 5.4.5. Speed-flow plot for Eastbound I-70 at Foristell (pavement repair, 2,1)

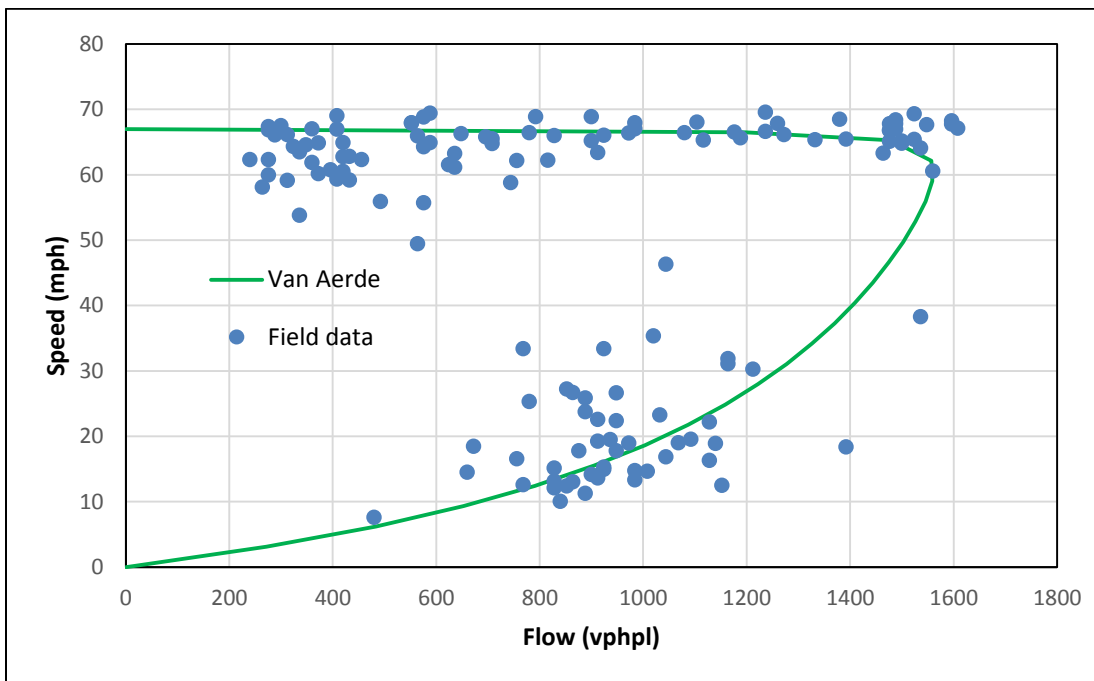
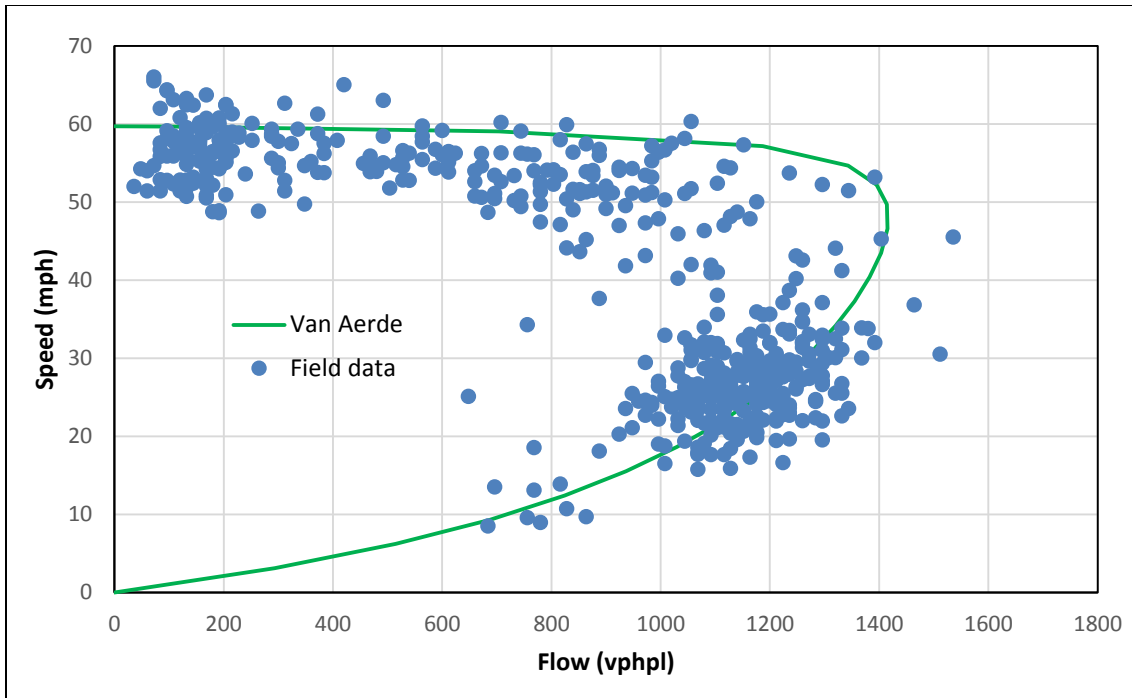
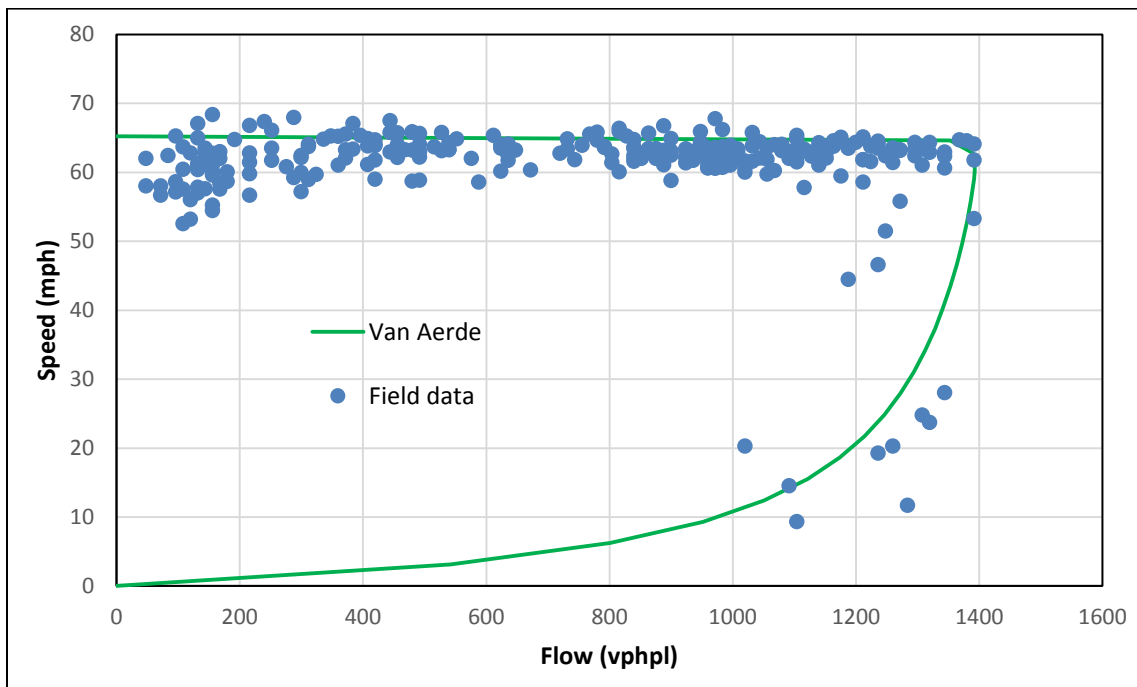


Figure 5.4.6. Speed-flow plot for Westbound I-70 at Foristell (paving operations, 2,1)



**Figure 5.4.7. Speed-flow plot for Eastbound I-270 from McDonnell Boulevard to Route 367 (bridge work, 4,2)**



**Figure 5.4.8. Speed-flow plot for Westbound I-270 from I-170 to Route 367 (pavement work, 3,2)**

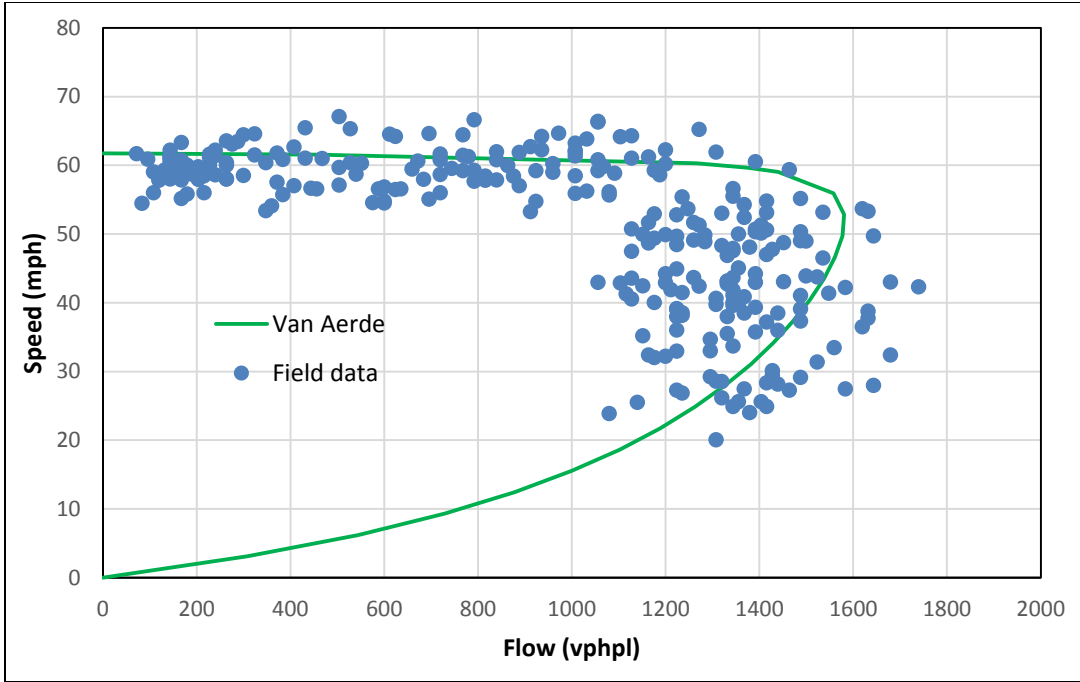


**Figure 5.4.9. Speed-flow plot for Eastbound I-44 at I-270 (Meramec Bridge) (bridge work, 3,2)**

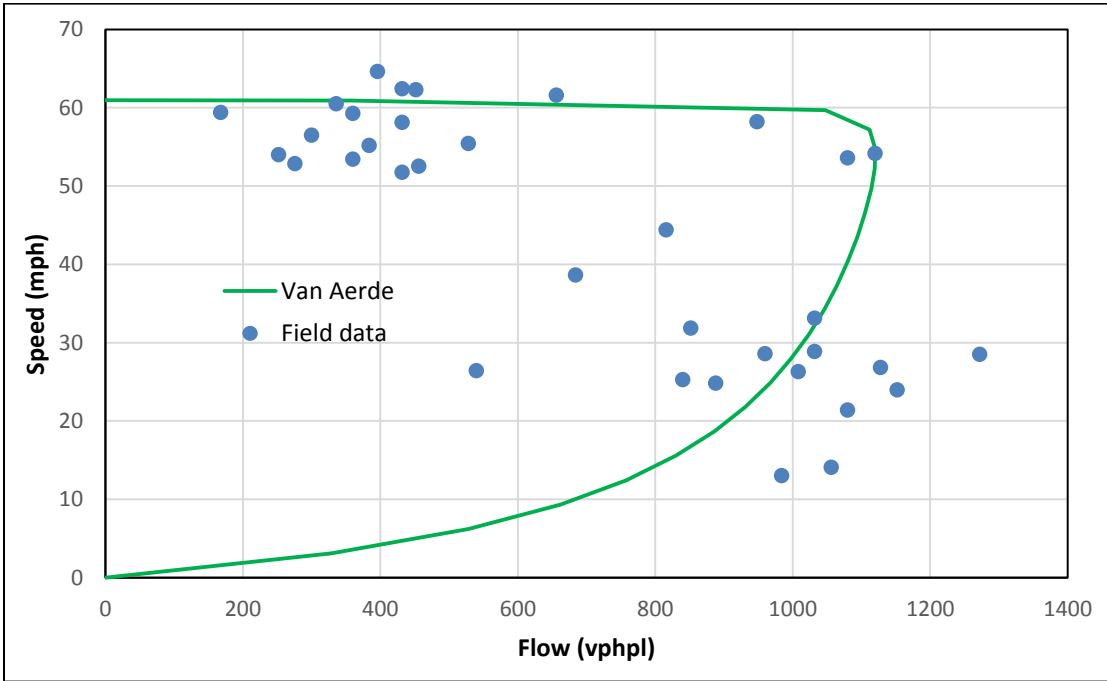


**Figure 5.4.10. Speed-flow plot for Westbound I-44 (resurfacing, 3,2)**

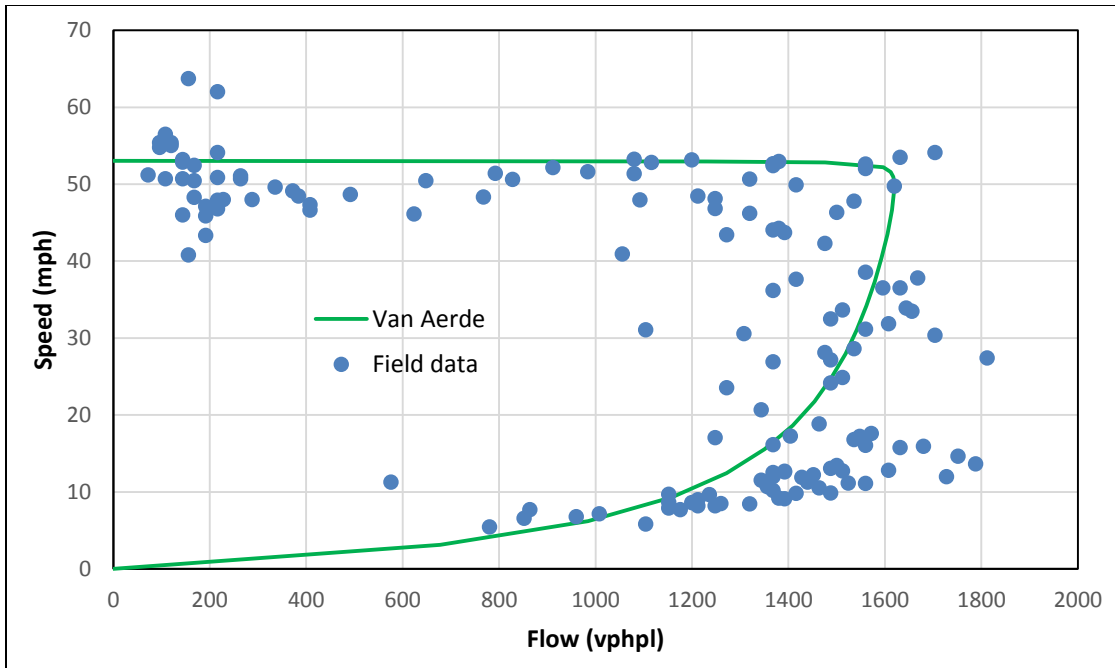


**Figure 5.4.11. Speed-flow plot for Eastbound I-44 at Hampton (bridge rehabilitation, 4,2)**

### 5.2.1 Comparison of Different Work Activities

MoDOT work activities in work zones can be broadly classified into two groups: activities related to bridges and activities related to pavements. Pavement work refers to construction and maintenance operations while bridge work includes reconstruction, joint replacement, etc. Table 5.3 lists all the activities related to pavement and bridge work in the MoDOT Transportation Management Systems (TMS) database.

**Table 5.3. Work activities related to bridges and pavements**

<b>Bridge-Related Work</b>	<b>Pavement-Related Work</b>
Bridge maintenance, Bridge reconstruction, Bridge flushing, Joint/Crack sealing,	Chip seal overlay, Cinder seal overlay, Concrete barrier wall, Concrete overlay, Core drilling, Culvert replacement, Diamond grinding, Fog seal, Grooving drive surface, Guard rail/Cable work, intersection improvement, Lighting/Signal/Sign work, Median or Shoulder, Microsurfacing, Milling drive surface, Mowing, New pavement construction, Patching drive surface, Pavement marking, Pavement repair, Pavement striping, Permit or utility work, Railroad maintenance, Resurfacing pavement, Road mix overlay, Roadside work, Scrub sealing pavement, Seal coat overlay, Shoulder work, Sweeping pavement, Undersealing

For comparison purposes, speed-flow curves developed for all selected locations were merged into these two groups. It was found that of the 11 selected locations, six were associated with bridge-related work while the remaining 5 were associated with pavement-related work. The comparison of speed-flow plots among study locations for bridge- and pavement-related activities is illustrated in Figures 5.5.1. and 5.5.2.

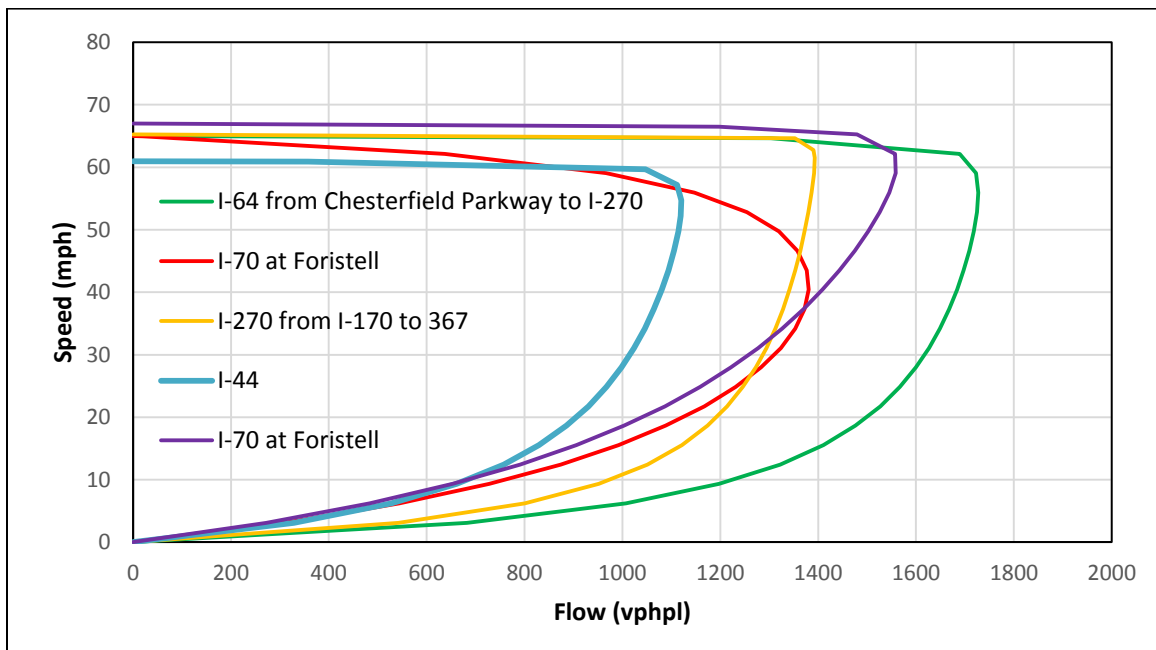


**Figure 5.5.1. Speed-flow plot for pavement-related activities**

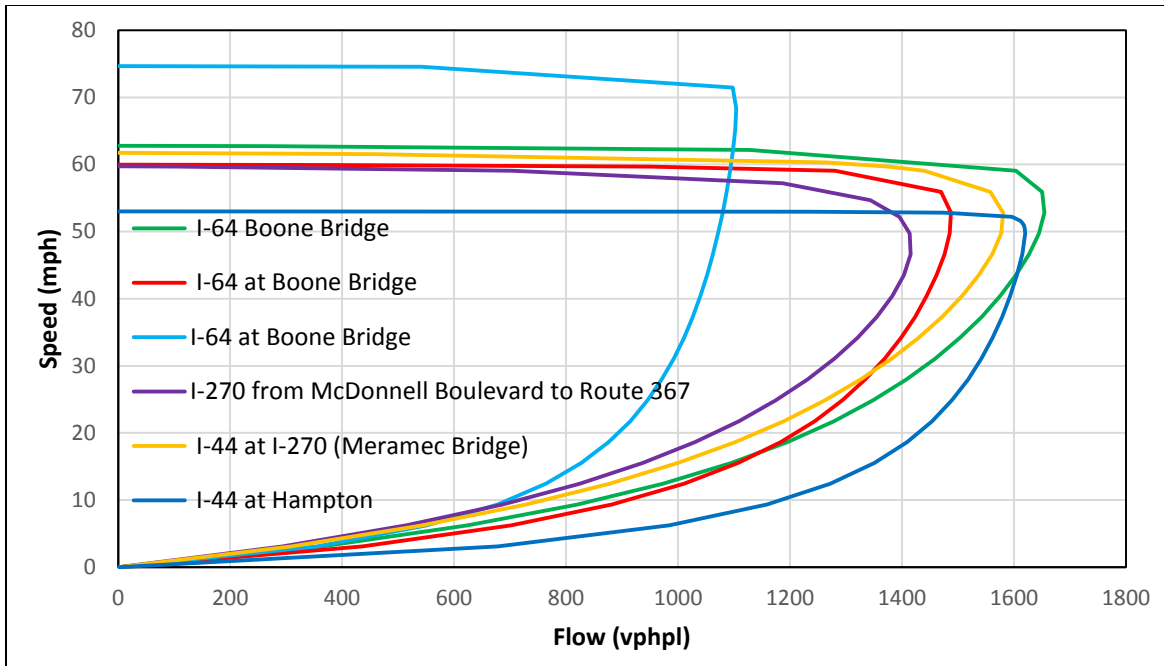


**Figure 5.5.2. Speed-flow plot for bridge-related activities**

### 5.2.2. Comparison of Different Work Activities by Lane Closure Configurations

From the literature review, it was found that work zone capacities were estimated separately for different lane closure configurations. In the 2010 HCM, capacity values of work zones with different lane closure configurations are illustrated for 13 different states. So, to maintain agreement with current practices, speed-flow plots developed in this study were organized according to lane closure configuration. For this study, 7 of the 11 work zones belong to (3,2) lane closure configurations, while the remaining 4 are (2,1) and (4,2) configurations, with 2 for each configuration.

#### 5.2.2.1. Comparison of Different Work Activities for (3,2) Configuration

In this study (3,2) is the most common lane closure configuration observed among the work zones. Among the seven (3,2) work zones, four were related to bridge-related work activity while the remaining three belonged to pavement-related activity. Speed-flow plots are combined by activity and illustrated in Figures 5.6.1. and 5.6.2.

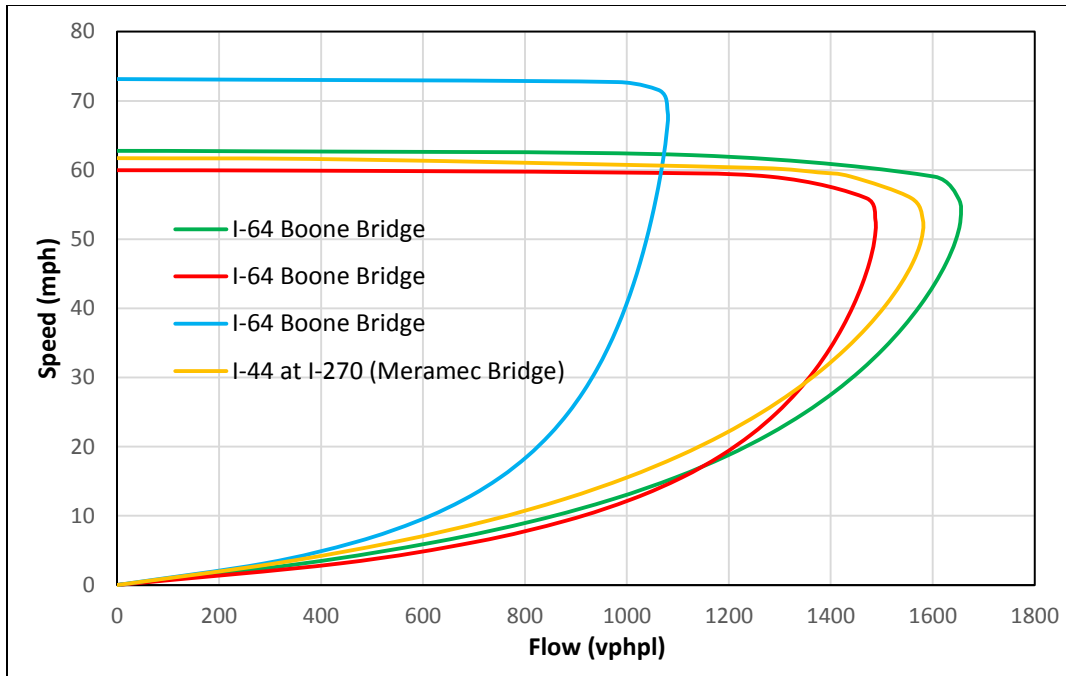


**Figure 5.6.1. Speed-flow plot for bridge-related activities for (3,2) configuration**

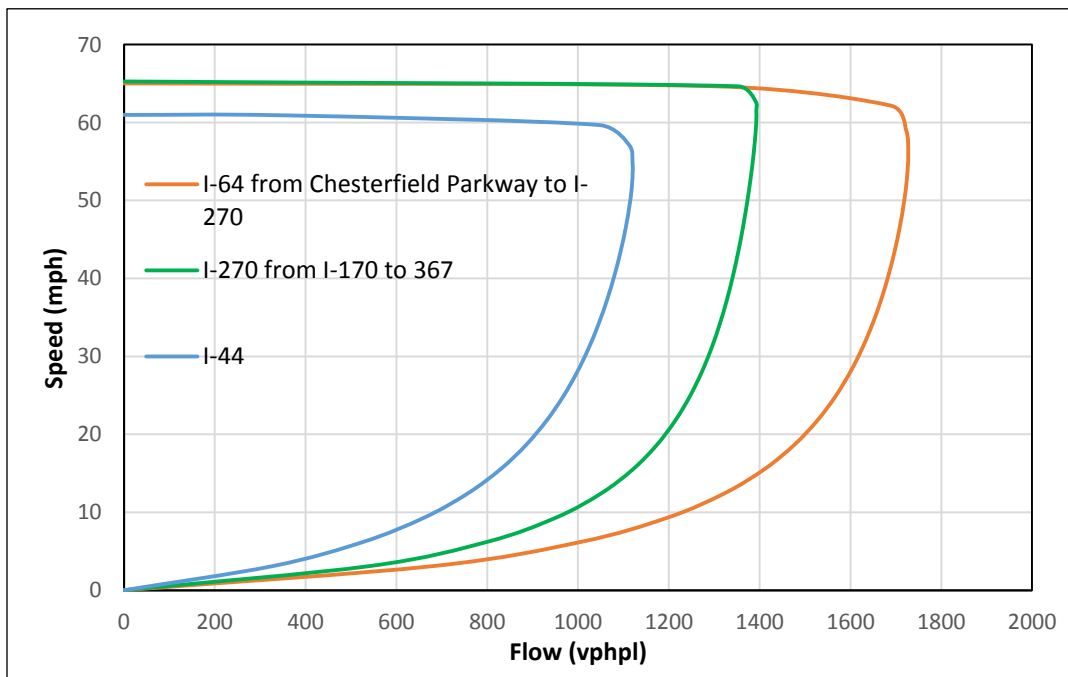


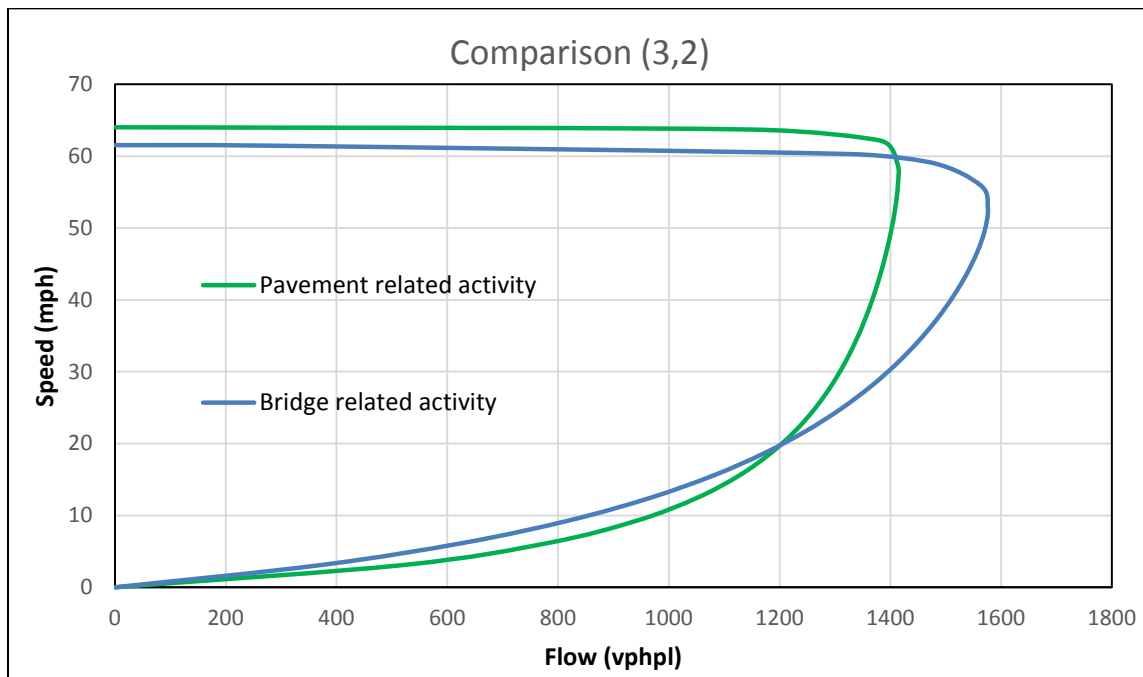
**Figure 5.6.2. Speed-flow plot for pavement-related activities for (3,2) configuration**

From Figure 5.6.1, it can be observed that one of the I-64 Boone Bridge locations (blue speed-flow curve) is dissimilar from the rest of the speed-flow curves, with unconventionally higher free-flow speed and low capacity value. The work was related to bridge demolition preparation,

which is incompatible with the bridge- and pavement-related work activities described above. Because of this incompatibility, the plot was dropped from further analysis.

From Figures 5.6.1 and 5.6.2, it can be seen that the variation in capacity value is much lower for bridge-related work than pavement-related work. There are only a few types of activities for bridge-related work (from Table 5.3), and this may be the reason for the low variance in capacity values (1,488 to 1,656 vphpl). In contrast, the pavement-related work includes a wide range of activities (from Table 5.3), and that may be the reason for higher variation in capacity values (1,120 to 1,728 vphpl).

To compare speed-flow plots of bridge- and pavement-related activities for the (3,2) configuration, representative curves for both work activity groups were developed. To develop a representative curve for a group, the Van Aerde model was recalibrated for the four parameters (free-flow speed, capacity, speed at capacity, and jam density) by using the average values of each parameter for all sites within a group. The comparison is illustrated in Figure 5.7.



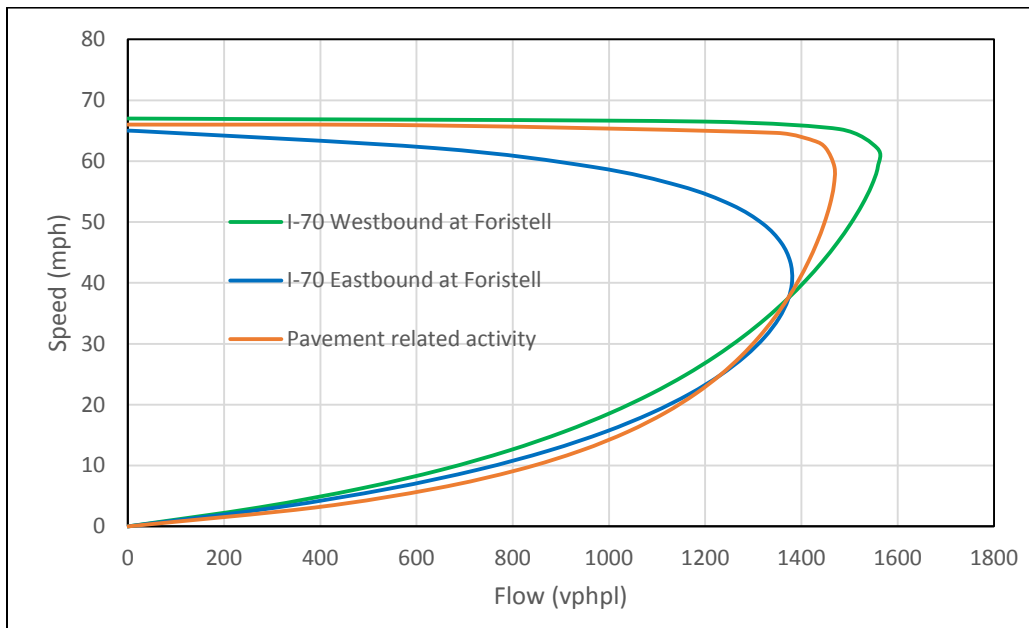
**Figure 5.7. Comparison of speed-flow plots for bridge- and pavement-related activities for (3,2) configuration**

Figure 5.7 shows a few distinctive differences in the speed-flow curves between bridge- and pavement-related activities. The free-flow speed of pavement-related activities is higher compared to bridge-related work activities. For pavement activities, the traffic stream can maintain higher speeds even at capacity, with a negligible difference between free-flow speed and speed at capacity, whereas in the case of bridge-related activity, the decline in speed is negligible until 1,300 vphpl. As the flow continues to increase, the speed decreases significantly before capacity is reached. The drop in speed after capacity is rapid in pavement-related

activities, while the drop in speed is gradual in the case of bridge-related activities. There is a significant difference in capacity value (160 vphpl) that can be observed between bridge and pavement work. Although pavement activities have a higher free-flow speed than bridge activities, the capacity for pavement activities is lower.

#### 5.2.2.2. Comparison of Different Work Activities for (2,1) and (4,2) Configurations

In this study, two of the study locations consisted of (2,1) configurations with pavement-related work activities, while there were no data for bridge-related activities. Additionally, the (4,2) configuration was observed in two study locations with bridge-related activities, while there were no data available for pavement-related activities with a (4,2) configuration. The representative speed-flow curves for (2,1) and (4,2) configurations with respective work activities were developed using the methodology explained in the previous section. The plots are illustrated in Figures 5.8 and 5.9.



**Figure 5.8. Speed-flow plot for pavement-related activities for (2,1) configuration**

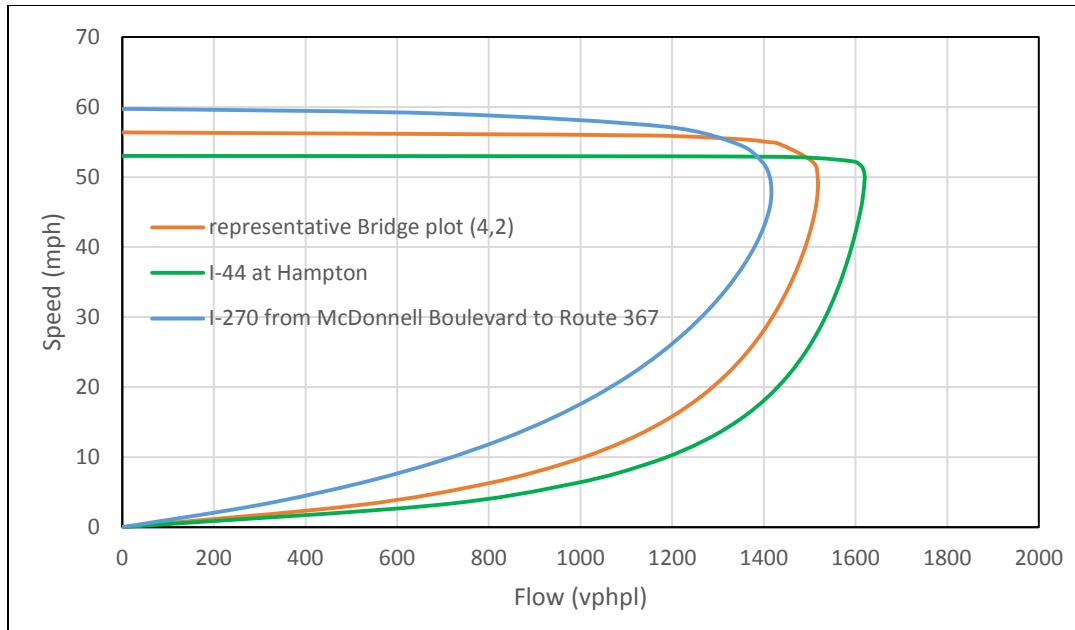


**Figure 5.9. Speed-flow plot for bridge-related activities for (4,2) configuration**

From Figures 5.8 and 5.9, it can be seen that the speed-flow plots for pavement-related activities have higher free-flow speeds than bridge-related activities. For the (2,1) configuration, the shapes of the speed-flow plots for both locations are not consistent with each other. This may be due to the wide range of pavement-related work activities. The values of capacity for the (2,1) configurations with pavement-related activities were found to be in range of 1,380 to 1,560 vphpl. The capacity values for the (3,2) configurations with bridge-related activities were found to be in range of 1,416 to 1,620 vphpl.

Bridge- and pavement-related data were not available for the (2,1) and (4,2) configurations. So, an attempt was made to develop speed-flow plots for the missing data using information available for the (3,2) configuration. As demonstrated in the previous section, both pavement- and bridge-related speed-flow plots were developed for the (3,2) configuration. Information such as percentage of increment or reduction in free-flow speed, speed at capacity, capacity, and jam density for pavement and bridge-related work were used to develop missing plots for the (2,1) and (4,2) configurations. The comparisons for the (2,1) and (4,2) configurations are illustrated in Figures 5.10. and 5.11 Dotted plots were generated for the missing data with the help of the information gathered from the (3,2) configurations.

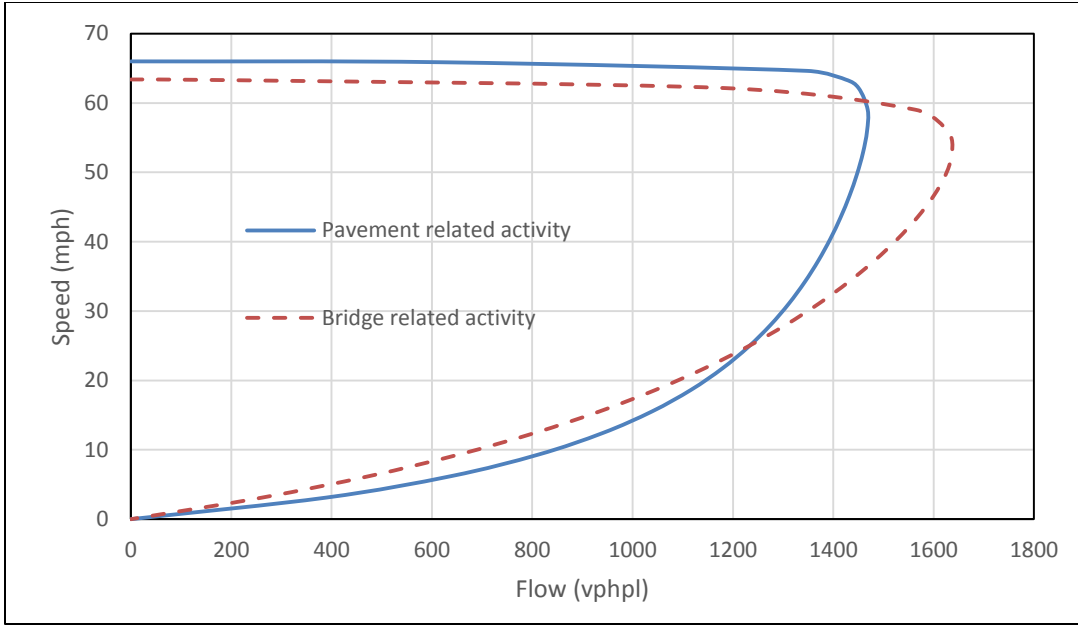


**Figure 5.10. Comparison of speed-flow plots for bridge- and pavement-related activities for (2,1) configuration**

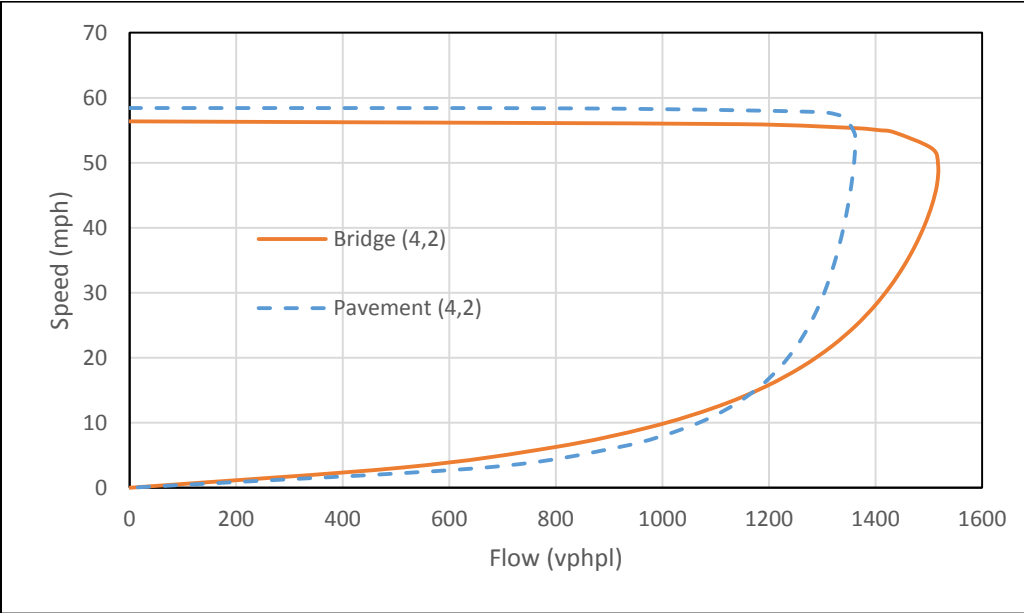


**Figure 5.11. Comparison of speed-flow plots for bridge- and pavement-related activities for (4,2) configuration**

The findings of free-flow speed and capacity by lane for both bridge- and pavement-related work activities are illustrated in Tables 5.4. and 5.5.

**Table 5.4. Work zone capacity (vphpl) by lane closure configuration and type of work**

	(2,1)	(3,2)	(4,2)
Bridge-Related (Range)	-	1,488–1,656	1,416–1,620
Bridge-Related (Representative)	1,638.0	1,575	1,518
Pavement-Related (Range)	1,380–1,560	1,120–1,728	-
Pavement-Related (Representative)	1,470	1,413	1,362

**Table 5.5. Work zone FFS (mph) by lane closure configuration and type of work**

	(2,1)	(3,2)	(4,2)
Bridge-Related (Range)	-	60–62.7	53–59
Bridge-Related (Representative)	63.4	61.5	56
Pavement-Related (Range)	65–67	61–65.3	-
Pavement-Related (Representative)	66	64	58.4

In Tables 5.4 and Table 5.5, the capacity of pavement-related work is found to be lower than bridge-related work, while free-flow speed is higher in pavement work than in bridge work. The range of capacity values is wide for pavement-related work because pavement work comprises a broad range of work activity. In the case of bridge-related activity, the range of capacity values is narrow because work activity comprises a limited number of activities. It was also found that the (4,2) configuration has the lowest capacity while the (2,1) configuration has the highest capacity among the three lane closure configurations.

### 5.2.3 Comparison for Different Lane Closure Configurations

Speed-flow plots were developed for each lane closure configuration irrespective of the type of activity (i.e., all activity types for a given lane configuration were combined). Figure 5.12. shows the plots generated for the three configurations.

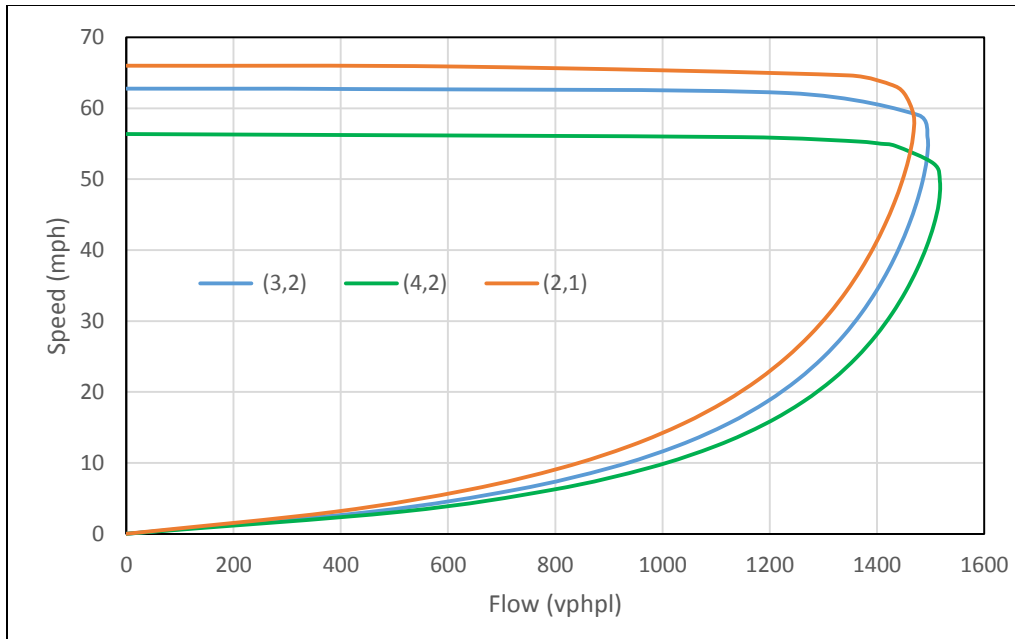


**Figure 5.12. Comparison of speed-flow plots for different lane closure configurations**

The capacity values in Figure 5.12 (values between 1,470 and 1,518 vphpl) show only a slight sensitivity to the lane closure configuration. This finding illustrates the consequences of not accounting for the activity type when generating speed-flow plots. As discussed previously, the (4,2) lane configuration did not include any pavement-related activities in the study sample. Similarly, the (2,1) lane configuration did not include any bridge-related activities.

## 6. CONCLUSIONS

The latest edition of the HCM (2016) contains a revised chapter on assessing work zone impacts. While the 2010 edition recommended using a formula to compute work zone capacity, the 2016 edition recommends a new procedure that utilizes free-flow speed and capacity adjustment factors to determine work zone capacity. However, the new procedure does not include specific guidance on how work activity effects can be incorporated. In this project, a methodology was developed to analyze traffic flow characteristics for various work activities. The methodology involves developing speed-flow curves and deriving capacity and free-flow speed adjustment factors.

The following conclusions were drawn from the study:

- Higher flows could occur either at breakdown or prior to recovery to free-flow conditions. In most cases, the breakdown flow was found to be higher than the flow prior to recovery. Therefore, to prevent underestimation, a higher value between breakdown flow and discharge flow prior to recovery should be considered as the best estimate of capacity.
- Goodness of fit statistics showed that the Van Aerde model was the best fit model for most of the study locations (MAPE < 20% for all locations). The Gipps model and Newell-Franklin model were good fits for a few locations but performed poorly (MAPE > 30%) in other locations. Thus, the Van Aerde model is recommended for developing speed-flow curves for various work activities.
- The capacity reduction factor for different work activities was found to be in the range of 0.68 to 0.95, while the free-flow speed reduction factor was found to be in the range of 0.78 to 1.0. This finding further emphasizes the need to customize the new HCM adjustment factors to different activity types. The factors shown in Table 5.2 are recommended for use by practitioners until they can develop their own adjustment factors by applying the proposed method to their jurisdictional data.
- Work activities were broadly classified into two groups: bridge-related activities and pavement-related activities. The variation in capacity values was found to be much lower in bridge-related activities, 1,488 vphpl to 1,656 vphpl, than pavement-related activities, 1,120 vphpl to 1,728 vphpl. The higher variation in the capacity values for the pavement-related activities may be due to the wider range of activities that are within the scope of pavement-related work (as classified in the MoDOT database).

Future research should apply the proposed method to analyze additional work activities from other jurisdictions. One challenge in developing the speed-flow curves is the availability of observations representing both congested and uncongested conditions. Often, work activity may occur only during one of these two periods, thus making it challenging to fit a traffic flow model for all conditions.

A second challenge is the availability of work activity data. Work zone information is typically archived in DOT planning databases. DOTs typically archive transportation data in the form of a transportation management system database. These databases also include data pertaining to work zones. However, in a majority of cases, the work zone information is obtained from the job descriptions contained in contracts. While the broad description of work and total duration mentioned in contracts may be accurate, the actual dates, types and locations of work activity, and other work zone characteristics depend on weather, construction phasing, coordination with other construction activity in the area, and other parameters. Thus, relying only on planning-level data based on contracts can lead to the use of insufficient or inaccurate data to assess work activity impacts.

State work zone coordinators and traffic management centers (TMCs) also generate a more dynamic and short-term update of work zone schedules. For example, the TMC in St. Louis generates biweekly and daily schedules of work zones that it shares with work zone personnel and the public by posting on social media such as Twitter and Facebook and distributing electronic alerts via email and text messages. Because the data are updated in real time, they tend to be more accurate. Unfortunately, these data are not always archived and are rarely in a format that can be easily retrieved (e.g., pdf, text) or queried later. Time and effort can be saved if DOTs can archive real-time data and have tools available to easily retrieve activity information, i.e., type of work, begin and end time, and lane closure information.



## REFERENCES

- Al-Kaisy, A. and F. Hall. 2003. Guidelines for estimating capacity at freeway reconstruction zones. *Journal of Transportation Engineering*, Vol. 129, No. 5, pp. 572–577.
- Al-Kaisy, A., M. Zhou, and F. Hall. 2000. New insights into freeway capacity at work zones: Empirical case study. *Transportation Research Record: Journal of the Transportation Research Board*, No. 1710, pp. 154–160.
- Benekohal, R., A. Z. Kaja-Mohideen, and M. Chitturi. 2004. Methodology for estimating operating speed and capacity in work zones. *Transportation Research Record: Journal of the Transportation Research Board*, No. 1883, pp. 103–111.
- Brilon, W. and J. Lohoff. 2011. Speed-flow models for freeways. *Procedia - Social and Behavioral Sciences*, Vol. 16, pp. 26–36.
- Burris, M. W. and S. Patil. 2008. *Measuring the Marginal Cost of Congestion*. Southwest Region University Transportation Center, Texas Transportation Institute, College Station, TX.
- Chatterjee, I., P. Edara, S. Menneni, and C. Sun. 2009. Replication of work zone capacity values in a simulation model. *Transportation Research Record: Journal of the Transportation Research Board*, No. 2130, pp. 138–148.
- Dervisoglu, G., G. Gomes, J. Kwon, R. Horowitz, and P. Varaiya. 2009. Automatic calibration of the fundamental diagram and empirical observations on capacity. 88th Annual Meeting of the Transportation Research Board, January 11–15, Washington, DC.
- Dixon, K., J. Hummer, and A. Lorscheider. 1996. Capacity for North Carolina freeway work zones. *Transportation Research Record: Journal of the Transportation Research Board*, No. 1529, pp. 27–34.
- Dong, J. and H. Mahmassani. 2009. Flow breakdown and travel time reliability. *Transportation Research Record: Journal of the Transportation Research Board*, No. 2124, pp. 203–212.
- Dudek, C. L. and S. H. Richards. 1981. *Traffic Capacity through Work Zones on Urban Freeways*. Texas Transportation Institute, Texas A&M University System, College Station, TX.
- Edara, P., J. Kianfar, and C. Sun. 2012. Analytical methods for deriving work zone capacities from field data. *Journal of Transportation Engineering*, Vol. 138, No. 6, pp. 809–818.
- Elefteriadou, L., D. Arguea, A. Kondyli, and K. Heaslip. 2007. *Impact of Trucks on Arterial LOS and Freeway Work Zone Capacity (Part B)*. Transportation Research Center, University of Florida, Gainesville, FL.
- Elefteriadou, L., M. Jain, and K. Heaslip. 2008. *Impact of Lane Closures on Roadway Capacity. Part B: Arterial Work Zone Capacity*. Transportation Research Center, University of Florida, Gainesville, FL.
- Elefteriadou, L. and P. Lertworawanich. 2003. Defining, measuring and estimating freeway capacity. 82nd Annual Meeting of the Transportation Research Board, January 12–16, Washington, DC.
- Gipps, P. G. 1981. A behavioural car-following model for computer simulation. *Transportation Research Part B: Methodological*, Vol. 15, No. 2, pp. 105–111.
- Google Maps Application Programming Interface (API). <https://developers.google.com/maps>. Access date May 2017.

- Hawkins, H., K. Kacir, and M. Ogden. 1992. *Traffic Control Guidelines for Urban Arterial Work Zones: Volume 2: Technical Report*. Texas Transportation Institute, Texas A&M University System, College Station, TX.
- Heaslip, K., A. Kondyli, D. Arguea, L. Elefteriadou, and F. Sullivan. 2009. Estimation of freeway work zone capacity through simulation and field data. *Transportation Research Record: Journal of the Transportation Research Board*, No. 2130, pp. 16–24.
- Hou, Y., P. Edara, and C. Sun. 2013. Speed limit effectiveness in short-term rural interstate work zones. *Transportation Letters: The International Journal of Transportation Research*, Vol. 5, No. 1, pp. 8–14.
- Hyndman, R. J. and A. B. Koehler. 2006. Another look at measures of forecast accuracy. *International Journal of Forecasting*, Vol. 22, No. 4, pp. 679–688.
- Jiang, Y. 1999. Traffic capacity, speed, and queue-discharge rate of Indiana's four-lane freeway work zones. *Transportation Research Record: Journal of the Transportation Research Board*, No. 1657, pp. 10–17.
- Kianfar, J. and P. Edara. 2013. A data mining approach to creating fundamental traffic flow diagram. *Procedia - Social and Behavioral Sciences*, Vol. 104, pp. 430–439.
- Kim, T., D. J. Lovell, and J. Paracha. 2001. A new methodology to estimate capacity for freeway work zones. 80th Annual Meeting of the Transportation Research Board, January 7–11, Washington, DC.
- Krammes, R. A. and G. O. Lopez. 1994. Updated capacity values for short-term freeway work zone lane closures. *Transportation Research Record: Journal of the Transportation Research Board*, No. 1442, pp. 49–56.
- Lewis, C. D. 1982. *International and business forecasting methods: A practical guide to exponential smoothing and curve fitting*. Butterworth Scientific, London, UK.
- Li, M. Z. 2008. A generic characterization of equilibrium speed-flow curves. *Transportation Science*, Vol. 42, No. 2, pp. 220–235.
- Li, P., L. Tao, D. Yang, and D. Wu. 2013. Influencing factor analysis of freeway work zone capacity and its estimation model. Fourth International Conference on Transportation Engineering, October 19–20, Chengdu, China.
- Lorenz, M. and L. Elefteriadou. 2001. Defining freeway capacity as function of breakdown probability. *Transportation Research Record: Journal of the Transportation Research Board*, No. 1776, pp. 43–51.
- Luna, R. and M. A. Mohammedi. 2014. Effects of Road Construction Intensity and Operations on Rural Freeway Work Zone Capacity. Smart Work Zone Deployment Initiative Transportation Pooled Fund, Institute for Transportation, Iowa State University, Ames, IA.
- Maze, T. H., S. D. Schrock, and A. Kamyab. 2000. Capacity of freeway work zone lane closures. In *Mid-Continent Transportation Symposium 2000 Proceedings*, pp. 178–183.
- Massachusetts Department of Transportation (MassDOT). 2006. *Project Development and Design Guide*. Boston, MA.
- Missouri Department of Transportation (MoDOT). 2004. *MoDOT Work Zone Guidelines*. Jefferson City, MO.
- Missouri Department of Transportation (MoDOT). 2015-2016. Bi-monthly Regional Mobility Reports. <http://www.modot.org/stlouis/links/traffictopics.htm>. Access date May 2017.
- Newell, G. F. 1961. Nonlinear effects in the dynamics of car following. *Operations Research*, Vol. 9, No. 2, pp. 209–229.

- Notbohm, T., A. Drakopoulos, and A. Dehman. 2009. *Freeway Work Zone Lane Capacity*. Smart Work Zone Deployment Initiative Transportation Pooled Fund, Institute for Transportation, Iowa State University, Ames, IA.
- Rakha, H. 2009. Validation of Van Aerde's simplified steady-state car-following and traffic stream model. *Transportation Letters: The International Journal of Transportation Research*. Vol. 1, No. 3, pp. 227–244.
- Rakha, H. and B. Crowther. 2002. Comparison of Greenshields, Pipes, and Van Aerde car-following and traffic stream models. *Transportation Research Record: Journal of the Transportation Research Board*, No. 1802, pp. 248–262.
- Rakha, H. and Y. Gao. 2010. *Calibration of Steady-State Car-Following Models using Macroscopic Loop Detector Data*. Virginia Tech Transportation Institute, Blacksburg, VA.
- Rakha, H., C. Pecker, and H. Cybis. 2007. Calibration procedure for Gipps car-following model. *Transportation Research Record: Journal of the Transportation Research Board*, No. 1999, pp. 115–127.
- Regional Integrated Transportation Information System (RITIS). n.d. University of Maryland Center for Advanced Transportation Technology Laboratory (CATT Lab), College Park, MD. <https://www.ritis.org>. Access date May 2017.
- Sarasua, W., W. Davis, D. Clarke, J. Kottapally, and P. Mulukutla. 2004. Evaluation of Interstate highway capacity for short-term work zone lane closures. *Transportation Research Record: Journal of the Transportation Research Board*, No. 1877, pp. 85–94.
- Shao, C. Q., and Y. Chen. 2010. Study on Urban Expressway Work Zone Capacity. Presented at the 10th International Conference of Chinese Transportation Professionals, August 4–8, Beijing, China.
- Transportation Research Board (TRB). 1985. *Highway Capacity Manual (HCM)*. Third Edition. Washington, DC.
- Transportation Research Board (TRB). 2010. *Highway Capacity Manual (HCM 2010)*. Fifth Edition. Washington, DC.
- Transportation Research Board (TRB). 2016. *Highway Capacity Manual (HCM)*. Sixth Edition. Washington, DC.
- Van Aerde, M. and H. Rakha. 1995. Multivariate calibration of single-regime speed-flow-density relationships (road traffic management). Vehicle Navigation and Information Systems Conference, in conjunction with the Pacific Rim TransTech Conference. 6th International VNIS. "A Ride into the Future." July 30–August 2, Seattle, WA.
- Venugopal, S. and A. Tarko. 2001. Investigation of factors affecting capacity at rural freeway work zones. Preprint CD-ROM. 80th Annual Meeting of the Transportation Research Board, January 7–11, Washington, DC.
- Wilson, R. E. 2001. An analysis of Gipps's car-following model of highway traffic. *Journal of Applied Mathematics*, Vol. 66, No. 5, pp. 509–537.
- Zegeer, J., J. Bonneson, R. Dowling, P. Ryus, M. Vandehey, W. Kittelson, N. Roupail, B. Schroeder, A. Hajabaie, B. Aghdashi, T. Chase, S. Sajjadi, R. Margiotta, and L. Elefteriadou. 2014. *Incorporating Travel Time Reliability into the Highway Capacity Manual*. Second Strategic Highway Research Program (SHRP 2), Washington, DC.
- Zheng, N., A. Hegyi, S. Hoogendoorn, H. Van Zuylen, and D. Peters. 2011. A comparison of freeway work zone capacity prediction models. *Procedia - Social and Behavioral Sciences*, Vol. 16, pp. 419–429.





**THE INSTITUTE FOR TRANSPORTATION IS THE FOCAL POINT FOR TRANSPORTATION  
AT IOWA STATE UNIVERSITY.**

**InTrans** centers and programs perform transportation research and provide technology transfer services for government agencies and private companies;

**InTrans** manages its own education program for transportation students and provides K-12 resources; and

**InTrans** conducts local, regional, and national transportation services and continuing education programs.



**IOWA STATE  
UNIVERSITY**

Visit [www.InTrans.iastate.edu](http://www.InTrans.iastate.edu) for color pdfs of this and other research reports.